BRNO UNIVERSITY OF TECHNOLOGY

VYSOKÉ UČENÍ TECHNICKÉ V BRNĚ

FACULTY OF MECHANICAL ENGINEERING

FAKULTA STROJNÍHO INŽENÝRSTVÍ

INSTITUTE OF SOLID MECHANICS, MECHATRONICS AND BIOMECHANICS

ÚSTAV MECHANIKY TĚLES, MECHATRONIKY A BIOMECHANIKY

ANALYSIS OF THE PROCEDURE FOR IDENTIFYING POTENTIALLY DANGEROUS LOCATIONS OF WELD JOINTS IN THIN-WALLED METAL STRUCTURES DURING LIFE ASSESSMENT

ANALÝZA POSTUPU ZJIŠTĚNÍ POTENCIÁLNĚ NEBEZPEČNÝCH MÍST SVAROVÝCH SPOJŮ TENKOSTĚNNÝCH KOVOVÝCH KONSTRUKCÍ PŘI POSOUZENÍ ŽIVOTNOSTI

MASTER'S THESIS

DIPLOMOVÁ PRÁCE

AUTHOR — **Bc. DANIEL DOLEŽEL**

AUTOR PRÁCE

SUPERVISOR — **Ing. PETR VOSYNEK, Ph.D.**

VEDOUCÍ PRÁCE

BRNO 2024

BRNO UNIVERSITY OF TECHNOLOGY FACULTY OF MECHANICAL ENGINEERING

Assignment Master's Thesis

Institut:	Institute of Solid Mechanics, Mechatronics and Biomechanics
Student:	**Bc. Daniel Doležel**
Degree programm:	Engineering Mechanics and Biomechanics
Branch:	Engineering Mechanics
Supervisor:	**Ing. Petr Vosynek, Ph.D.**
Academic year:	2023/24

As provided for by the Act No. 111/98 Coll. on higher education institutions and the BUT Study and Examination Regulations, the director of the Institute hereby assigns the following topic of Master's Thesis:

Analysis of the procedure for identifying potentially dangerous locations of weld joints in thin–walled metal structures during life assessment

Brief Description:

Assessment of the fatigue life of welds on thin–walled welded structures is one of the frequent parts of orders for inspection at the company 5M LEVIT, s. r. o. Evaluation of the fatigue life of welds is assessed here according to the procedure of the FKM standard. A key part of using this procedure is determining the critical location in the welds from the FEM calculations. However, manually searching for these places is very time–consuming and, moreover, not completely reliable. It is therefore necessary to focus primarily on this part when evaluating welds and to analyze how the critical points could be determined effectively. When processing, it is necessary to pay attention to already established procedures and available software equipment of the contracting authority. This practical topic is prepared in cooperation with 5M LEVIT, s. r. o.

Master's Thesis goals:

Development of the methodology for calculating the fatigue strength of welded joints with an emphasis on minimizing time and effort, using normative regulations ČSN EN 13749, ČSN EN 12663, and FKM Guideline. The methodology will further be practically applied to selected components.

Recommended bibliography:

Analytical Strength Assessment of Components, FKM Guideline. 7th Edition. VDMA Verlag, 2020. ISBN 978-3-8163-0745-7.

ČSN EN 13749, Železniční aplikace – Dvojkolí a podvozky - Metoda specifikování pevnostních požadavků na rámy podvozků. Praha: Česká agentura pro standardizaci, 2022, 48 s. Třídící znak 280505.

ČSN EN 12663-1+A1, Železniční aplikace – Pevnostní požadavky na konstrukce skříní kolejových vozidel – Část 1: Lokomotivy a vozidla osobní dopravy (a alternativní metoda pro nákladní vozy). Praha: Úřad pro technickou normalizaci, metrologii a státní zkušebnictví, 2015, 36 s. Třídící znak 280320.

LEE, Yung-Li; BARKEY, Mark E. a KANG, Hong-Tae. Metal fatigue analysis handbook: practical problem-solving techniques for computer-aided engineering. Waltham: Butterworth-Heinemann, c2012. ISBN 978-0-12-385204-5.

HOBBACHER, A. F. Recommendations for Fatigue Design of Welded Joints and Components. 2nd ed. Springer Cham, 2016. ISBN 978-3-319-23757-2.

Deadline for submission Master's Thesis is given by the Schedule of the Academic year 2023/24

In Brno,

L. S.

prof. Ing. Jindřich Petruška, CSc. Director of the Institute	doc. Ing. Jiří Hlinka, Ph.D. FME dean

ABSTRACT

The fatigue assessment of welds in thin-walled metal structures is vital for ensuring structural integrity in proposed designs. Despite established criteria and S-N curves, fatigue analysis of welded joints for geometrically complex structures presents inherent challenges. The primary obstacle lies in identifying the fatigue-critical locations for detailed assessment, a task that can be highly time-consuming, even with finite element modeling (FEM). This thesis thoroughly examines weld fatigue assessment, encompassing a review of the relevant literature, commercial solutions, and the practical context of railway industry standards and the FKM Guideline. A significant contribution is the development of automated FEMAP API programs for Siemens FEMAP software, aimed at streamlining the analysis process. These programs reduce time and effort by employing a simplified analysis approach based on local nominal stress assessment, in accordance with the FKM Guideline. The methodology, supported by the developed programs, is described and demonstrated in this thesis. The practical implications of this work extend to providing an efficient alternative to commercial software, ultimately enhancing the efficiency of weld fatigue analysis in structural engineering applications.

Keywords

welds, weld joints, weld fatigue, critical location identification, thin-walled structures, life assessment, FKM Guideline, local nominal stress, FEM, FEMAP, FEMAP API, automation

ABSTRAKT

Hodnocení únavy svarů u tenkostěnných kovových konstrukcích je klíčové pro zajištění integrity navrhovaných konstrukcí. Navzdory zavedeným kritériím a S-N křivkám může být analýza životnosti svařovaných spojů u geometricky komplexních součástí značně komplikovaná. Hlavní překážkou je identifikace kritických míst z hlediska únavy pro detailní výpočet, což může být časově náročné i při využití metody konečných prvků (MKP). Tato práce podrobně zkoumá hodnocení únavy svarů, zahrnuje vhled do relevantní literatury, komerčních řešení a praktický kontext norem železničního průmyslu a směrnice FKM. Významným přínosem práce je vývoj automatizovaných FEMAP API programů pro MKP software Siemens FEMAP, které usnadňují proces analýzy. Tyto programy šetří čas a úsilí tím, že umožňují zjednodušenou analýzu založenou na konceptu lokálního nominálního napětí (local nominal stress) v souladu se směrnicí FKM. Metodika, podpořená vyvinutými programy, je v této práci popsána a prakticky demonstrována. Praktické přínosy této práce spočívají v poskytnutí alternativy ke komerčním softwarům, za účelem zvýšení efektivity analýzy životnosti svarů v kontextu konstukčních návrhů.

Klíčová slova

svary, svarové spoje, únava svarů, identifikace kritického místa, tenkostěnné konstrukce, životnost, směrnice FKM, lokální nominální napětí, MKP, FEMAP, FEMAP API, automatizace

BIBLIOGRAPHIC CITATION

DOLEŽEL, Daniel. *Analysis of the procedure for identifying potentially dangerous locations of weld joints in thin-walled metal structures during life assessment*, Brno, 2024. Also available at: https://www.vut.cz/studenti/zav-prace/detail/158081. Master's thesis. Brno University of Technology, Faculty of Mechanical Engineering, Institute of Solid Mechanics, Mechatronics and Biomechanics. Thesis supervisor Petr Vosynek.

DECLARATION

I hereby declare that I wrote this master's thesis on the topic of *Analysis of the procedure for identifying potentially dangerous locations of weld joints in thin-walled metal structures during life assessment* independently using the sources stated in the reference list.

Bc. Daniel Doležel

ACKNOWLEDGEMENTS

I would like to express my thanks to Ing. Petr Vosynek, PhD. for supervising this thesis. I would also like to express my deep gratitude mainly to Ing. Ladislav Chybík and also to Ing. Luděk Krmela from the company 5M LEVIT s. r. o. for very valuable advice, discussions, and suggestions during the work on this thesis. Special thanks go to the development teams of LIMIT® and SDC Verifier for providing me trial versions of their software, and also to their technical support teams for help. Many thanks to members of my family and friends for their immense support during my studies.

Contents

1 INTRODUCTION **11**

2 PROBLEM FORMULATION **13**
2.1 Problematic situation . . . 13
2.2 Problem formulation . . . 13

3 THEORETICAL BACKGROUND **14**
3.1 Fatigue and fatigue life of welded structures . . . 14
3.1.1 Fatigue damage assessment . . . 14
3.1.2 Stress cycle . . . 15
3.1.3 Stress spectrum and cycle counting . . . 16
3.1.4 Fatigue resistance curves . . . 17
3.1.5 Mean stress effect . . . 21
3.1.6 Cumulative damage . . . 23
3.2 Weld terminology . . . 24
3.2.1 Butt and fillet welds . . . 24
3.2.2 Penetration of welds . . . 25
3.2.3 Toe and root cracking . . . 25
3.2.4 Post-weld treatment . . . 27

4 STUDIED INDUSTRIAL STANDARDS **29**
4.1 ČSN EN 12663-1 . . . 29
4.1.1 Scope . . . 29
4.1.2 Fatigue structural requirements . . . 29
4.1.3 Proof of fatigue strength . . . 30
4.1.4 Prescribed fatigue loads . . . 30
4.2 ČSN EN 13749 . . . 31
4.2.1 Scope . . . 31
4.2.2 Fatigue structural requirements . . . 32
4.2.3 Proof of fatigue strength . . . 32
4.2.4 Prescribed fatigue loads . . . 33
4.3 FKM Guideline . . . 34
4.3.1 Scope . . . 34
4.3.2 Fatigue assessment details and procedure . . . 35
4.3.3 Compliance with the studied ČSN EN standards . . . 36

5 WELD FATIGUE ACCORDING TO THE FKM GUIDELINE **37**
5.1 Nominal vs. local stresses for welds . . . 37
5.2 Nominal stresses approach . . . 38
5.3 Local stresses approach . . . 38
5.4 Local nominal stress approach . . . 39
5.5 Structural (hot-spot) stress approach . . . 42
5.6 Notch stress approach . . . 43
5.7 Effective stress approach . . . 45

6 METHODS **47**
6.1 Comparison of the FKM proposed methods . . . 47
6.1.1 Local nominal stresses . . . 48
6.1.2 Structural stresses . . . 52
6.1.3 Notch stress and effective stress . . . 55
6.1.4 Comparison and analysis of results . . . 59
6.2 Method selection and justification . . . 60
6.2.1 Currently applied work procedure in the cooperating company . . . 60
6.2.2 Choice of method for further exploration . . . 61
6.3 Research into commercially available programs employing the selected method 62
6.3.1 LIMIT® . . . 62
6.3.2 SDC Verifier . . . 66
6.3.3 Commercially available programs summary . . . 70
6.4 Original program development . . . 70
6.4.1 FEMAP API . . . 71
6.4.2 Developed methods and their integration within work procedure . . . 74
6.4.3 FE model preparation . . . 75
6.4.4 FAT groups of elements API program . . . 77
6.4.5 Fatigue analysis API program . . . 80
6.4.6 Stress parameters extraction from the element surface API program . 86

7 PRACTICAL PRESENTATION OF THE DEVELOPED METHODS **87**
7.1 Welds on the component . . . 88
7.2 Material parameters . . . 88
7.3 Model preparation . . . 89
7.4 FE model . . . 89
7.5 Boundary conditions . . . 90
7.6 Loads . . . 91
7.7 Fatigue groups of elements . . . 91
7.8 Weld fatigue analysis . . . 93
7.9 Detailed analysis of the critical location . . . 94

8 RESULTS **96**
8.1 Verification of functionality of the API programs . . . 96
8.2 Verification of results with SDC Verifier . . . 97
8.3 Perpendicular stress component effect in the area of the critical location . . . 99

9 DISCUSSION **102**

10 CONCLUSION **105**

REFERENCES **107**

LIST OF USED SYMBOLS AND ABBREVIATIONS **111**

LIST OF FIGURES **113**

LIST OF TABLES **116**

LIST OF APPENDICES **117**

1 INTRODUCTION

In the domain of structural engineering, the challenge of rapid but comprehensive fatigue evaluations has become an industry necessity. To address the recurring customer demand for thorough fatigue checks of welds in thin-walled welded metal structures, the intricacies of the process must be faced to reduce the workload and increase the reliability of the process. In a structural engineering company 5M LEVIT s. r. o., the company that proposed this thesis topic, fatigue checks of welds are a frequent part of customer orders. The topic of this thesis is therefore a direct response to the practical difficulties that have repeatedly occurred in completing customer orders.

Using today's computational power with the application of the finite element method (FEM) for evaluating the safety of structures is an industry standard. However, even when using FEM, fatigue checks of welds may become very difficult when considering all their specifics for non-trivial cases. Most of the research and publications focus on obtaining accurate results and suggesting new methods to evaluate weld fatigue and stress in welds. However, the topic of reliably and effectively identifying critical weld locations under fatigue loading in complex structures loaded in different directions is not thoroughly examined. This is where the main focus of this thesis lies: in addressing this problem.

As practical difficulties arise primarily for weld fatigue evaluation, this thesis focuses solely on weld fatigue evaluation and not on the rest of the welded structure, which is not affected by welding. The main focus is to obtain results through a reliable process in a timely manner, which would also comply with the preferences of the company proposing the thesis topic. Fatigue checks are often performed according to the respective required standard. A significant number of customer orders in the company 5M LEVIT s. r. o. are typically related to welded attachments in railway applications; therefore, in this thesis, the respective industry standards ČSN EN 12663-1 [1], ČSN EN 13749 [2] are introduced and used in this thesis for practical demonstration purposes. However, the main standard used and evaluated throughout the thesis is the 7th edition of the FKM Guideline [3], which is applicable for a wide variety of fields and not just for railway applications. This thesis strives to maintain current practices in the company while leveraging already available software programs, namely Siemens FEMAP and Microsoft Excel, without the requirement of additional financial costs due to licensing new software. Using the tools and methodologies already in place, the aim is to significantly enhance and refine existing frameworks.

This thesis follows a structured exploration of fatigue assessment, beginning with a comprehensive overview of fatigue phenomena in engineering contexts while introducing the intricacies of fatigue in welds and explaining the specific challenges and considerations in this domain. Following this, an analysis of industry standards used in fatigue assessment sets the foundation for subsequent discussions. The thesis examines an in-depth presentation of the available methodologies and models for the evaluation of welds according to the FKM Guideline [3]. To illustrate these methodologies in practice, a practical trivial example demonstrates their application, providing information on the decision-making processes to select the most viable method for automated evaluation. With the acquired knowledge, the aim is to achieve at least a certain level of automation, which serves as an essential objective of this thesis: identifying potentially dangerous locations of weld joints in large thin-walled metal structures. Subsequently, a critical evaluation of existing commercially available software programs is performed to reflect on the chosen evaluation method and to examine the state of the art in the field. Building on this assessment, the thesis navigates through the decision-making process regarding the approach to developing original and effective software tools with the goal of replicating some functionalities of these commercial solutions. It describes the practical

methodology adopted and culminates in a demonstration of the new software's functionality using a representative industry-inspired example. The thesis is hierarchically organized into chapters, sections, and subsections.

2 PROBLEM FORMULATION

2.1 Problematic situation

The fatigue checks of welds in thin-walled metal structures play a crucial role in determining the structural integrity of proposed designs. These assessments require special attention, as welding processes can locally weaken the fatigue resistance of the structure. Consequently, the welds become potential weak points where fatigue cracks could occur. To address this concern, fatigue checks of welds are conducted using specific criteria while considering the orientation of plane stress state components aligned with the weld: parallel normal stress, perpendicular normal stress, and shear stress. The fatigue resistance for each of these components is quantified on the basis of similar structural details using S-N curves with assigned numerical FAT classes, commonly defined as the stress range at $2 \cdot 10^6$ cycles.

Within the context of 5M LEVIT s. r. o., the company submitting this thesis topic for their practical application, fatigue checks of welded thin-walled metal structures are typically analyzed using FEM software. The FKM Guideline [3] and relevant industry standards serve as methodological sources for analysis. In particular, practical challenges arise during the assessment of customer orders within the railway industry, involving welded attachments to rolling stock.

An inherent difficulty arises in the analysis of the fatigue strength during the identification of the critical location among all the welds. The critical location is the location with the highest degree of utilization. Consequently, all other locations on the welds should be safer than the critical location. However, the exact degree of utilization remains unknown in each location until the complete calculation is executed, following the prescribed procedure. Unlike static checks for non-welded structures, where the critical location is relatively easily determined by the highest equivalent stress, fatigue checks require an analysis of stress states across multiple fatigue load cases. Considering the varying fatigue resistance of the welds depending on the stress orientation and the different directions of loading between the fatigue load cases, identifying potentially critical locations becomes a difficult challenge.

Given the unique complexities of the weld fatigue assessment, there is an imperative need to develop new methods integrated into the existing fatigue check procedure at the cooperating company. This aims to replace the current labor-intensive and somewhat unreliable manual search for critical locations. In particular, the focus should be on leveraging the available software within the company to minimize the financial costs associated with licensing.

2.2 Problem formulation

Refine the process of identifying potential critical locations in fatigue-loaded welded joints by developing new methods, which are consistent with the normative regulations specified in ČSN EN 12663-1 [1], ČSN EN 13749 [2], and the FKM Guideline [3]. Prioritize efficiency improvements by simplifying the critical location identification process, with particular attention to preserving integral elements of the existing procedure and leveraging the company's current software resources.

3 THEORETICAL BACKGROUND

This chapter introduces the necessary theory and terms behind fatigue, weld fatigue, and weld terminology based on established literature to help the reader understand the essentials of weld fatigue assessment that are applied later in this thesis.

3.1 Fatigue and fatigue life of welded structures

Fatigue refers to progressive damage and failure induced by cyclic loading, often resulting in structural failure at stress levels significantly below the material's yield strength as a result of accumulated damage over time. This occurs primarily due to the presence of small crack-like flaws within the material that progressively enlarge under cyclic stress, eventually leading to fatigue failure [4]. This means that assessing the safety of the structure in relation to the expected history of stress is a key aspect of evaluating the overall integrity of the structural design.

In welded structures, fatigue frequently represents a critical mode of failure due to the nature of the welds, as the welds represent significant stress-raisers, and the welding process also severely weakens the fatigue resistance of the material. Fig. 3.1 shows an example of fatigue cracks of two dominant failure modes of welded joints, originating in the weld toe in fig. 3.1a) and the weld root in fig. 3.1b). The basic terminology necessary to be understood throughout this thesis for fatigue assessment is introduced in the following subsections.

a)

b)

Fig. 3.1: Examples of weld cracks originating from a) the weld toe [5] and b) the weld root [6] of a fillet weld

3.1.1 Fatigue damage assessment

The assessment of fatigue damage can generally be performed using three different approaches:

- stress-based approach related to high cycle fatigue (HCF),
- strain-based approach related to low cycle fatigue (LCF),
- fracture mechanics.

The stress-based approach of fatigue assessment is the most widely applied because of its convenience and accuracy for the assessment of HCF. For relatively low stresses, the stress-strain relation can be assumed to remain elastic, and therefore stress can be used as the controlling variable. The strain-based approach finds applicability in scenarios involving a limited

number of cycles, typically not exceeding a few thousand, characterized by a considerable amplitude exceeding the material's yield strength, resulting in notable plastic deformation. The typical separation value between HCF and LCF for the number of cycles is 10 000. Fracture mechanics is typically applied when a detectable crack is measured using available technical equipment, and the remaining number of cycles until failure can be evaluated. [4; 7]

This thesis will be exclusively concerned with the stress-based approach; therefore, the terminology that follows is related only to the stress-based approach of fatigue evaluation. The reason for this choice is that all industry standards applied in this thesis deal exclusively with HCF.

3.1.2 Stress cycle

In the context of fatigue analysis, stress cycles represent the variations in stress levels experienced by a structure subjected to cyclic loading over time. Fig. 3.2 shows an idealized sinusoidal loading cycle with denoted parameters (σ_a – stress amplitude, σ_m – mean stress, $\Delta\sigma$ – stress range, σ_{max} – maximum stress, σ_{min} – minimum stress). However, the real time histories of stress are rarely ideal. This is why the real stress history is often described by just the parameters of the stress spectrum, which are not dependent on the exact shape of the cycle over time.

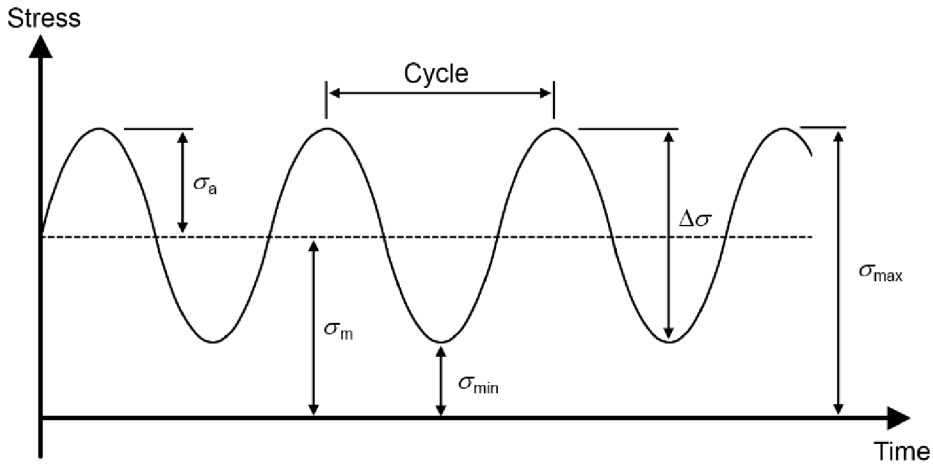

Fig. 3.2: Sinusoidal stress cycle with denoted parameters [7]

The following relations exist between the above-mentioned parameters:

$$\sigma_m = \frac{\sigma_{max} + \sigma_{min}}{2}, \tag{3.1}$$

$$\sigma_a = \frac{\sigma_{max} - \sigma_{min}}{2}, \tag{3.2}$$

$$\Delta\sigma = 2\sigma_a = \sigma_{max} - \sigma_{min}. \tag{3.3}$$

In addition, the parameter of stress ratio R is often used during fatigue analysis. It is defined as

$$R = \frac{\sigma_{min}}{\sigma_{max}} = \frac{\sigma_m - \sigma_a}{\sigma_m + \sigma_a}. \tag{3.4}$$

3.1.3 Stress spectrum and cycle counting

The idealized sinusoidal stress representation with constant amplitude and mean stress level, often used in theoretical fatigue assessments and fatigue tests, is rarely observed in the real world. In practical scenarios, structural components experience complex and varying stress patterns and irregularities in both stress magnitude and cycle period, influenced by diverse operational conditions, load variations, and environmental factors [8]. These real-world stress profiles deviate significantly from idealized cyclic loading conditions and create a stress history.

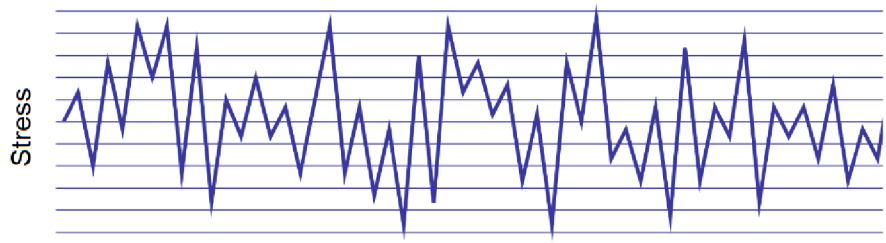

Fig. 3.3: Example of complex stress history as successive maxima and minima [8]

The stress history is a record, which can also be visually represented, of the successful stress maxima and minima (example in fig. 3.3) caused by fatigue actions during its expected service time. If there is a limited-time record, it should be representative of the whole lifetime stress history, as an unrepresentative sample might not cover the potentially more damaging part of the history. It should aim to cover all loading events and the corresponding dynamic response in a conservative way. [8]

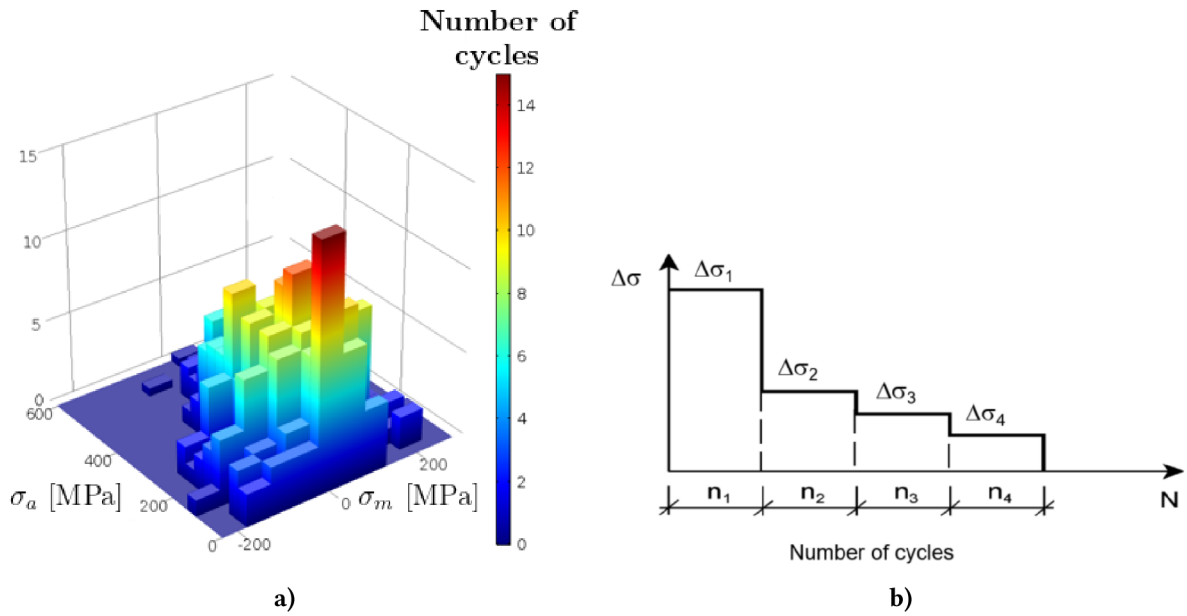

Fig. 3.4: Examples of visual representations of the stress history as a) histogram of stress parameters based on the rainflow counting algorithm [7] and b) stress range spectrum [9]

The stress history may be given as [8]:

a) a record of successive maxima and minima of stress (as shown in fig. 3.3) measured in a comparable structure for comparable loading and service life, or a typical sequence of load events,

b) a transition matrix of the stress history derived from a),

c) a stress range histogram (stress range occurrences) obtained from a) by a specified counting method (example in fig. 3.4a)),

d) a stress range histogram (stress range exceedances, stress range spectrum) specified by a design code (example in fig. 3.4b)).

Representations a) and b) may be used for component testing, while c) and d) are most useful for fatigue assessment by calculation [8].

The process of extracting specific stress history parameters, often grouped into bins for histograms for a larger number of cycles, involves employing specific cycle counting methods. Cycle counting converts a variable-amplitude stress sequence into a series of constant-amplitude cycles, ensuring equivalence in terms of damage to the original sequence. There are various methods, including zero-crossing counting, peak counting, range pair counting, and specifically for welded components, "rainflow" or similar "reservoir" methods are recommended to accurately count the cycles [8]. The rainflow counting method is also the most popular in practical applications. It derives its analogy from the rain flowing down the edges of a pagoda roof. This method, deemed significantly important, has led to the introduction of several of its algorithmic variations [4]. In its most basic principle, the rainflow algorithm can be described in the following steps:

1. **Peak and valley identification:** The algorithm starts by identifying the peaks and valleys within the stress history. These represent the maximum and minimum stress values encountered during loading.

2. **Cycle pairing:** Rainflow counting pairs peaks and valleys to form closed stress cycles. It identifies closed cycles by tracing the path from a peak to the next valley and then back to the subsequent peak.

3. **Stress parameters calculation:** For each closed cycle, the algorithm calculates stress parameters, such as the stress amplitude or range and mean stress.

4. **Bin grouping:** Optionally, for a larger number of identified stress cycles with only slightly different parameters, it might be beneficial to group them into bins with similar stress parameters.

Given that rainflow cycle counting is an algorithmic process, it can be implemented as an automated program in various programming environments or platforms, which largely simplifies the extraction and analysis of stress cycles from complex stress histories. More information on the details of the algorithm and its multiple variations can be found in [11].

3.1.4 Fatigue resistance curves

Fatigue testing involves establishing the relationship between stress and life by cyclic uniaxial stress loading of a specimen or a real component. In practice, the mean stress is often related to the stress amplitude in a way where increasing amplitude also increases the mean stress. This is actually a condition of a constant stress ratio R. Therefore, fatigue testing commonly involves maintaining a constant stress ratio. The most commonly used ratios are $R = 0$ (fully reversed loading) and $R = -1$ (pulsating tension). [10]

The resulting S-N curve relates the number of cycles until failure (also lifetime, denoted N) to the stress amplitude or the stress range. The amplitude is usually used for machined

components, while the stress range is used for welded components [10]. Generally, longer lifetimes correspond to lower stress amplitudes, displaying a strong dependence where a 10 % reduction in stress amplitude may result in a 50 % increase in lifetime [7]. Therefore, the S-N curve, also known as the Wöhler curve, is frequently portrayed as a straight line on log-log coordinates, specifically illustrating fatigue data in the HCF range. A linear axis for stress is also often used.

Some materials exhibit a stress threshold on the S-N curve known as the endurance limit, below which no fatigue damage is observed, allowing components to operate indefinitely. This non-failure stress amplitude is also often referred to as the fatigue limit. In the context of this thesis, the applied railway industry standards [1; 2] use the term endurance limit, while the FKM Guideline uses the term fatigue limit [3]. However, not all materials exhibit this threshold (such as aluminum alloys and austenitic steel); there is therefore no endurance limit, and fatigue testing must be terminated at a specified large number of cycles, which differs between standards [11]. A general term used to assign a stress-based value of the amplitude or range to a specific number of cycles to failure is known as fatigue strength [10]. An example of two S-N curves for different materials can be seen in fig. 3.5, in which the curve A shows the presence of an endurance limit denoted as σ_e while the curve B does not and therefore it is described a fatigue strength value for a specific number of cycles N_f.

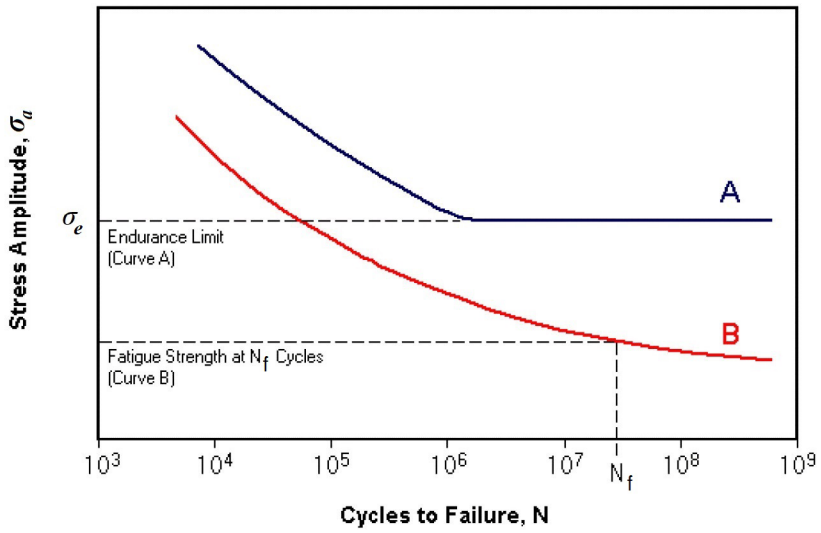

Fig. 3.5: Examples of S-N curves with (curve A) and without (curve B) endurance limit [12]

The results obtained from the fatigue tests for the S-N curves typically exhibit considerable scatter, leading to significant variance in the data. Simply regressing the measured data points with the least squares method implies a mean S-N curve with a probability of failure of 50 % for the regression curve. This is a value that is unacceptable from an engineering perspective. This is why a statistical analysis of the data is necessary. For design purposes, the design S–N curve is normally based on the mean-minus-two standard deviations (e.g., for civil engineering applications) or mean-minus-three standard deviations (e.g., for the application in the aircraft industry) of the mean curve of the relevant experimental test [4]. An example of the S-N curve determined from the experimental data can be seen in fig. 3.6, where the scatter of the experimental data is clearly visible. The plotted survival probabilities are 50 % and 97.7 %, which is equal to mean-minus-two standard deviations [8].

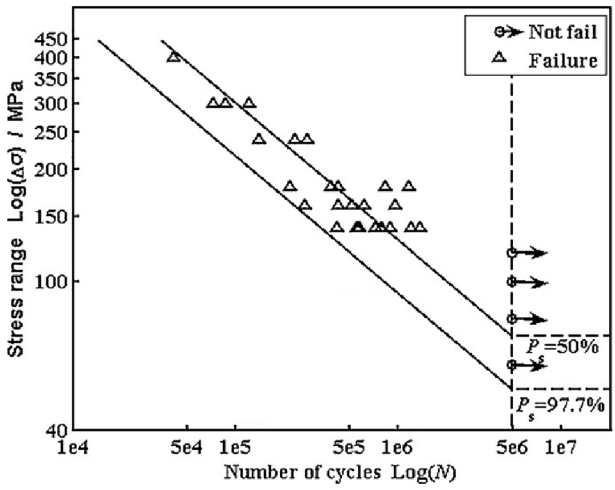

Fig. 3.6: S-N curve based on experimental data points with probability of survival P_s of 50 and 97.7 % [13]

In conventional testing of non-welded components/specimens, the state of failure is defined differently depending on the applied standards. However, welds have different criteria for failure assessment. Typically, smaller welded specimens undergo testing until complete rupture, which is often close to cracking through thickness. For larger components or vessels, failure is typically identified when the vessel is observed to have a larger crack or a crack that propagates through the wall. [8]

The fatigue strength of the welds is frequently characterized by unique S-N curves, with the corresponding assigned FAT classes determined for steel and aluminum alloys. These FAT classes are associated with standardized designations denoted by the term "FAT" followed by a numerical identifier. This number signifies the stress range $\Delta\sigma$ at $N = 2 \cdot 10^6$ expressed in megapascals (MPa) considering the probability of survival at least 95 % or 97.7 % (depending on definition). These two definitions are practically equal for engineering applications according to Hobbacher [8]. The graphical visualization of the definition can be seen in fig. 3.7. It may be important to note that, even though the number that is part of the classification has a physical dimension (MPa), it is most of the time omitted in practice and literature. This is why the term FAT value is also often used.

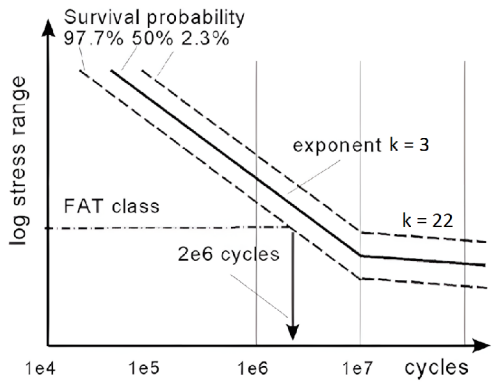

Fig. 3.7: FAT class definition marked in the S-N graph [8]

According to Pedersen [10], *"welded joints are very prone to fatigue failure. As opposed to machined elements, welded joints spend most of their lives in the crack propagation phase because of the existence of small crack-like features inherent with the welding process."* Fatigue strength

in the crack propagation phase is mostly dependent on the type of material (specifically its Young's modulus) and not on the strength characteristics of the specific material, such as the yield strength or the tensile strength [10]. This is why FAT data are universal, despite the strength characteristics of a specific steel or aluminum alloy.

The sloped part of the S-N curves of FAT classes can be described by an equation

$$N \cdot \Delta\sigma^k = C, \tag{3.5}$$

where k is the exponent of the slope and C is the empirical constant for that curve. The fatigue testing is based on categorized structural details of actual geometry, usually depicted as figures together with the measured FAT value (example in fig. 3.8).

No.	Structural Detail	Description (St. = steel; Al. = aluminium)	FAT St.	FAT Al.	Requirements and remarks
412	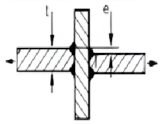	Cruciform joint or T-joint, K-butt welds, full penetration, potential failure from weld toe	71	25	Advisable to ensure that intermediate plate was checked against susceptibility to lamellar tearing
		Single sided T-joints	80	28	Misalignment < 15 % of primary plate thickness in cruciform joints

Fig. 3.8: Example of FAT class from the table of structural details from [8]

The values of FAT are given for a stress ratio $R = 0.5$ by International Institute of Welding (IIW) [8], which is at a high mean stress, with the assumption of high residual tensile stresses in the weld. They can be established based on considering different levels of stress while including or excluding various stress-raising factors (more on this in chapter 5). The most common FAT classes are based on the range of nominal stresses. For these in normal stresses, according to IIW [8], the slope $k = 3.0$, if not explicitly stated otherwise, and it is assumed that the knee point corresponds to $N_D = 1 \cdot 10^7$ cycles (S-N curves for steel shown in 3.9). For shear stresses, $k = 5.0$, and the knee point is assumed to correspond to $N_D = 1 \cdot 10^8$ cycles. It is universally assumed that the N_D values of the knee points also mark the location of the endurance limit, and the slope is flat afterward. However, it was shown that for very high-cycle applications the infinite life line no longer exists in the horizontal direction, but instead shows a slight slope of $k = 22$ (visualized in fig. 3.7). However, this is applicable only to very high-cycle operations and is still subject to research [8].

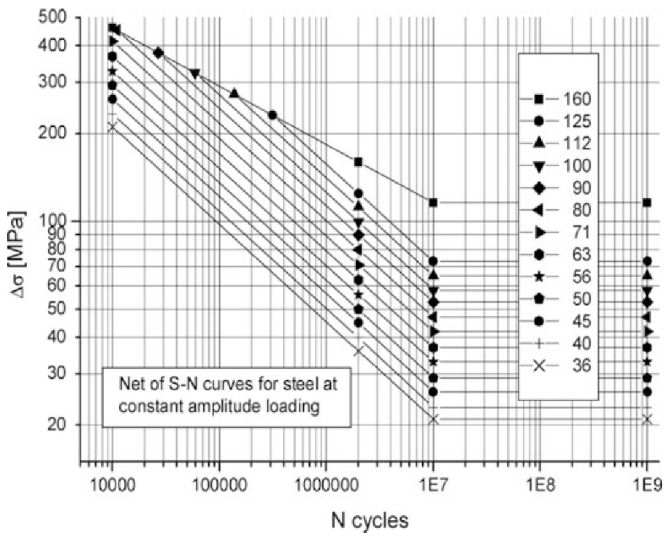

Fig. 3.9: FAT classes S-N curves for steel loaded in normal stress, standard applications [8]

In the FKM Guideline, the definitions of S-N curves slightly deviate from IIW. Firstly, the slope is set differently depending on the thickness of the welded plates. For thickness $t \geq 7$ mm, the slope is defined as $k = 3.0$ for normal stress and $k = 5.0$ for shear stress. For thickness $t < 7$ mm, the slopes are $k = 5.0$ and $k = 7.0$ for normal and shear stresses, respectively. Secondly, the knee point is defined for $N_D = 5 \cdot 10^6$ cycles for normal stress and $N_D = 1 \cdot 10^8$ cycles for shear stress, and the curve is considered flat for the number of cycles beyond the knee point. [3]

Because S-N curves for welds are derived for representative standardized structural details, many of the factors influencing fatigue resistance are already factored in during testing. For the nominal stress FAT classes, these include the following [8]:

- *"structural hot-spot stress concentrations due to the detail shown,*
- *local stress concentrations due to the weld geometry,*
- *weld imperfections consistent with normal fabrication standards,*
- *direction of loading,*
- *high residual stresses,*
- *metallurgical conditions,*
- *welding process (fusion welding, unless otherwise stated),*
- *inspection procedure (NDT – non-destructive testing), if specified,*
- *post weld treatment, if specified."*

It should also be noted that the FAT data refers to a standard quality, as given in codes and standard welding procedures, which can be expected in automated welding done in the industry. All S-N curves for weld details are limited by the S-N curve for the base material. Additionally, these S-N curves corresponding to weld details are specific to particular failure modes, commonly involving fatigue crack propagation. This propagation of fatigue cracks may originate from different weld locations. When evaluating a specific weld detail, it becomes essential to consider all possible failure modes related to the loading direction. For example, in cruciform joints with fillet welds, a comprehensive assessment requires consideration of potential failure modes, such as toe cracking through the plate and root cracking through the weld throat. [8]

3.1.5 Mean stress effect

Considering the cyclic stresses imposed, fatigue life has a strong correlation with the applied stress amplitude or range, represented by an S-N curve. However, as mentioned above, these S-N curves are usually constructed for a specific constant stress ratio R, with the most frequent values of $R = 0$ and $R = -1$. The values of the stress ratio also directly imply the position of the mean stress of the cycles. For non-welded components, the influence of mean stress is a crucial factor that should be seriously addressed in fatigue analysis. The mean normal stresses directly influence the state of the present microcracks, as a higher mean stress shifts the cycle into higher, more dangerous, tension values. Such stresses accelerate the rate of crack propagation. Consequently, normal tensile stresses have an unfavorable effect, which is detrimental to fatigue strength, while normal compressive stresses are advantageous and positively contribute to fatigue strength. This described behavior is often visualized in terms of a Haigh diagram in axes σ_a and σ_m. Specifics of the Haigh diagram with its different definitions can be found in [11].

However, for welds, the situation is different. According to Jia [4] or Pedersen [10], the mean stress effect may not be considered for welds due to its insignificant influence compared to the presence of residual stress, as demonstrated in fig. 3.10, where the high residual stress in the weld locally shifts the maxima of the stress cycle up to the yield strength σ_y.

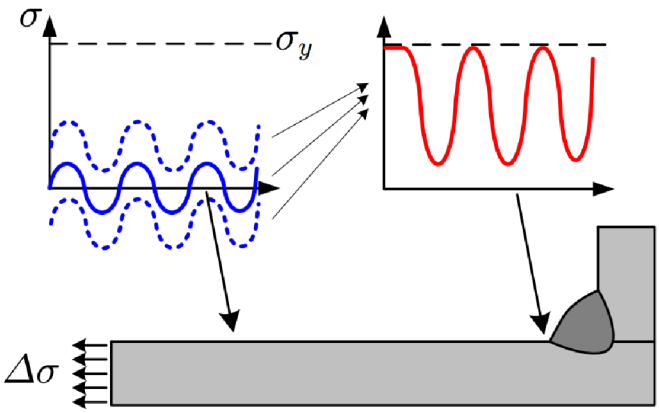

Fig. 3.10: Influence of tensile residual stress on the actual mean stress in the weld toe [20]

This is also supported in the IIW Recommendations by Hobbacher [8], which mention that the modification of the S-N curve represented by the FAT class is only applicable in cases where the stress ratio is $R < 0.5$ considering the effects of both applied and residual stress. In this case, the modification bonus factor $f(R)$ can be considered by multiplying the FAT class of the structural detail by $f(R)$ according to fig. 3.11. If there is no reliable information on residual stress, which is often the case, an enhancement factor $f(R) = 1.0$ is recommended.

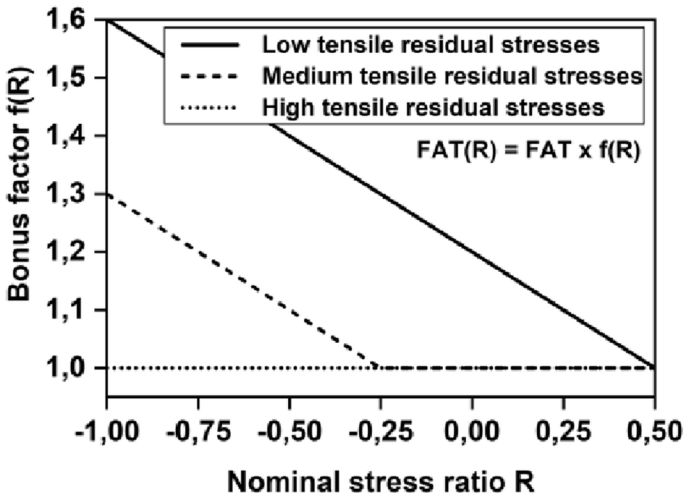

Fig. 3.11: Bonus factor $f(R)$ applicable for modification of FAT in certain cases [8]

The FKM Guideline applies slightly different modifications of the mean stress effect depending on the residual stress level. This is caused by the fact that the universal calculation procedure in the FKM Guideline is based on the stress ratio $R = -1$ [3], while the IIW procedure assumes $R = 0.5$ [8]. The different modification compensates for this difference, since the FKM Guideline uses the same set of FAT classes from the IIW Recommendations [8].

In the FKM Guideline, the facts mentioned above about not modifying the FAT S-N curve without reliable information about residual stresses are applied in the calculation only for the category of "high residual stresses," which can be assumed in the case of *"complex thick-walled components subjected to strong multiaxial stresses or in the presence of known design-related global residual stresses."* Therefore, most practical applications fall into the category of "moderate residual stresses." The category of "low residual stresses" can only be assumed in the case of subsequent stress relief or in the possibility of ruling out residual stresses completely. [3]

The consideration of the influence of residual stress for welds in the FKM Guideline is handled via two variables, namely the residual stress factor $K_{E,\sigma}$ ($K_{E,\tau}$) and the mean stress sensitivity M_σ (M_τ). In cases of "high residual stress," their values according to the FKM Guideline are $K_{E,\sigma} = K_{E,\tau} = 1.00$ and $M_\sigma = M_\tau = 0$. This means that the values of the S-N curve do not get modified with consideration of the mean stress state. For the other two categories (moderate and low), the residual stress factor values are greater than 1.00 and the mean stress sensitivity is greater than 0. This means that the S-N curves are shifted into greater stress values by considering the residual stress factor, but subsequently decreased for unfavorable mean stress levels by considering the non-zero mean stress sensitivity. [3]

3.1.6 Cumulative damage

As mentioned in subsection 3.1.3, a rainflow cycle counting technique is typically used to convert a complicated time-varying stress history to p number of blocks, with each i-th block having a corresponding number of cycles n_i with constant amplitude $\sigma_{a,i}$ and mean stress $\sigma_{m,i}$.

For each such block, the number of cycles to failure N_i can be estimated using the constant-amplitude S-N curve of the component. In this case, fatigue damage is defined as the ratio $\frac{n_i}{N_i}$. The commonly used Palmgren–Miner linear damage rule can be adopted to calculate the total accumulated damage, which assumes that fatigue damage occurs when the sum of the cycle ratios $\frac{n_i}{N_i}$ of constant amplitude reaches a critical damage value D. In a mathematical sense, this can be expressed as

$$\sum_{i=1}^{p} \frac{n_i}{N_i} \geq D. \tag{3.6}$$

The value of D varies depending on the specific publication or code. Although the original publications of Palmgren and Miner found the critical damage value of 1.0 in their studies, some suggest values significantly lower for different specific cases [11]. IIW Recommendations [8] suggest that the value of $D = 1.0$ could be non-conservative for welded components and should be reduced to $D = 0.5$ for weld and in the cases of high-fluctuating mean stress spectra to even $D = 0.2$. FKM Guideline applies a value of $D = 0.5$ as the lower limit of the effective damage sum for welded components, with emphasized caution for cases such as high-fluctuating mean stress [3].

As the constant-amplitude S-N curve is used for estimating the number of cycles to failure, it might be suggestive to assume that cycles with amplitude lower than the fatigue limit should not contribute to the overall damage sum; this approach is sometimes called the "Original Miner." However, under variable-amplitude loading, stress cycles with amplitudes below the fatigue limit could induce damage if subsequent stress amplitudes exceed the initial fatigue limit. This is based on the belief that periodic overloads contribute to an increase in crack-driving force, surpassing the initial strength of the grain barrier and facilitating crack propagation to failure. [11]

Therefore, it becomes important to adjust the fatigue limit for a component that experiences a history of variable-amplitude loading, as the fatigue limit derived from a constant-amplitude load may be negatively affected by periodic overloads. To address this, special calculation methods were introduced. Two of them are presented here, namely the Miner rule, also called the "Elementary Miner" in the FKM Guideline [3] and the Miner–Haibach rule, also sometimes called the "Modified Miner." These different hypotheses are outlined in fig. 3.12. They aim to incorporate the influence of periodic overloads on stress cycle behavior below the original fatigue limit. The "Elementary Miner" rule extends the S-N curve with the identi-

cal slope factor k. The "Modified Miner" rule extends the original S-N curve below the fatigue limit with a flatter slope factor of $2k - 1$. [11]

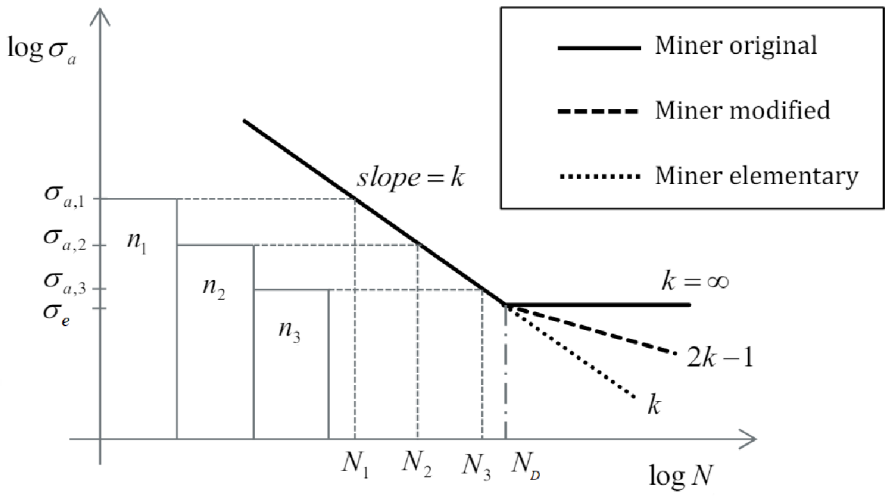

Fig. 3.12: Constant-amplitude S-N curve with graphical representation of the different damage hypotheses [14]

3.2 Weld terminology

This section provides a basic overview of terms related to actual welds, their geometry, and their relationship to fatigue resistance.

3.2.1 Butt and fillet welds

Welds can be broadly classified into two main groups: butt welds and fillet welds. Butt welds are formed in the gap between connected parts and are often used as strong load-bearing welds. Typically, it is necessary to modify the surfaces of the connected parts prior to welding. The specific treatment method for the welded surfaces depends on factors such as the type of connection, the thickness of the welded parts, the welding technique applied, and the accessibility of the weld spot. [15]

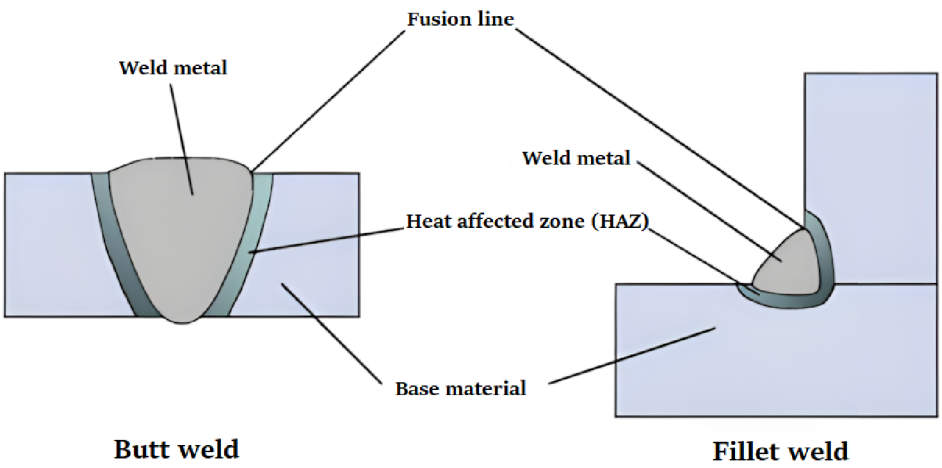

Fig. 3.13: Typical examples of butt weld and fillet weld with basic terminology [16]

Fillet welds are placed along the edge where connected parts meet, creating a triangular cross-section that resembles an isosceles right-angle triangle. This edge has a wedge type shape. Fillet welds are commonly used in T-shaped connections, cross-butt connections, angle connections, and lap joints for load bearing purposes. Unlike butt welds, fillet welds do not require adjustment of the shape of the welded parts. For statically loaded connections, a flat weld is usually employed, while a concave weld is more suitable for dynamically loaded connections due to its lower notch effects. Figure 3.13 provides examples of a butt weld and a fillet weld, together with an overview of basic terms. [15]

3.2.2 Penetration of welds

Weld penetration refers to the depth to which a weld extends into the base material. Together with the dimensions of the weld itself and the thickness of the base material, it is the most important aspect of the fatigue resistance of the weld [17]. Although insufficient penetration can be regarded as a weld imperfection of the welding process, it is also not strictly required that all welds be fully penetrated. An example of a partially penetrated butt weld can be seen in fig. 3.14. The introduction of fully penetrated welds brings significant advantages, which are examined in the following subsection.

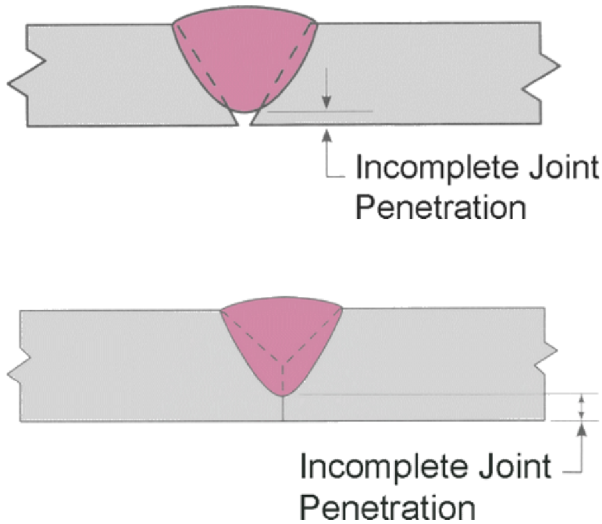

Fig. 3.14: Examples of butt welds with partial penetration [18]

3.2.3 Toe and root cracking

There are roughly five main parts that can be identified in the fillet weld: the root, toe, throat, face, and leg. The root is the deepest penetration point, located opposite the angle of the hypotenuse of the triangular cross-section. The toes are the edges or points of the hypotenuse that touch the base material. The face is the outer, visible part of the weld. The legs are the other two sides that form the triangular fillet weld, and their length is often used to designate the size of the weld. The throat is the distance from the center of the face to the root of the weld, and the throat dimension can be considered in two ways: theoretical, often prescribed in drawings, which is formed based on the idealized triangular geometry, and actual throat based on real geometry after welding. Many of the same parts found in fillet welds can be analogously described for butt welds. An overview of these terms can be found in fig. 3.15.

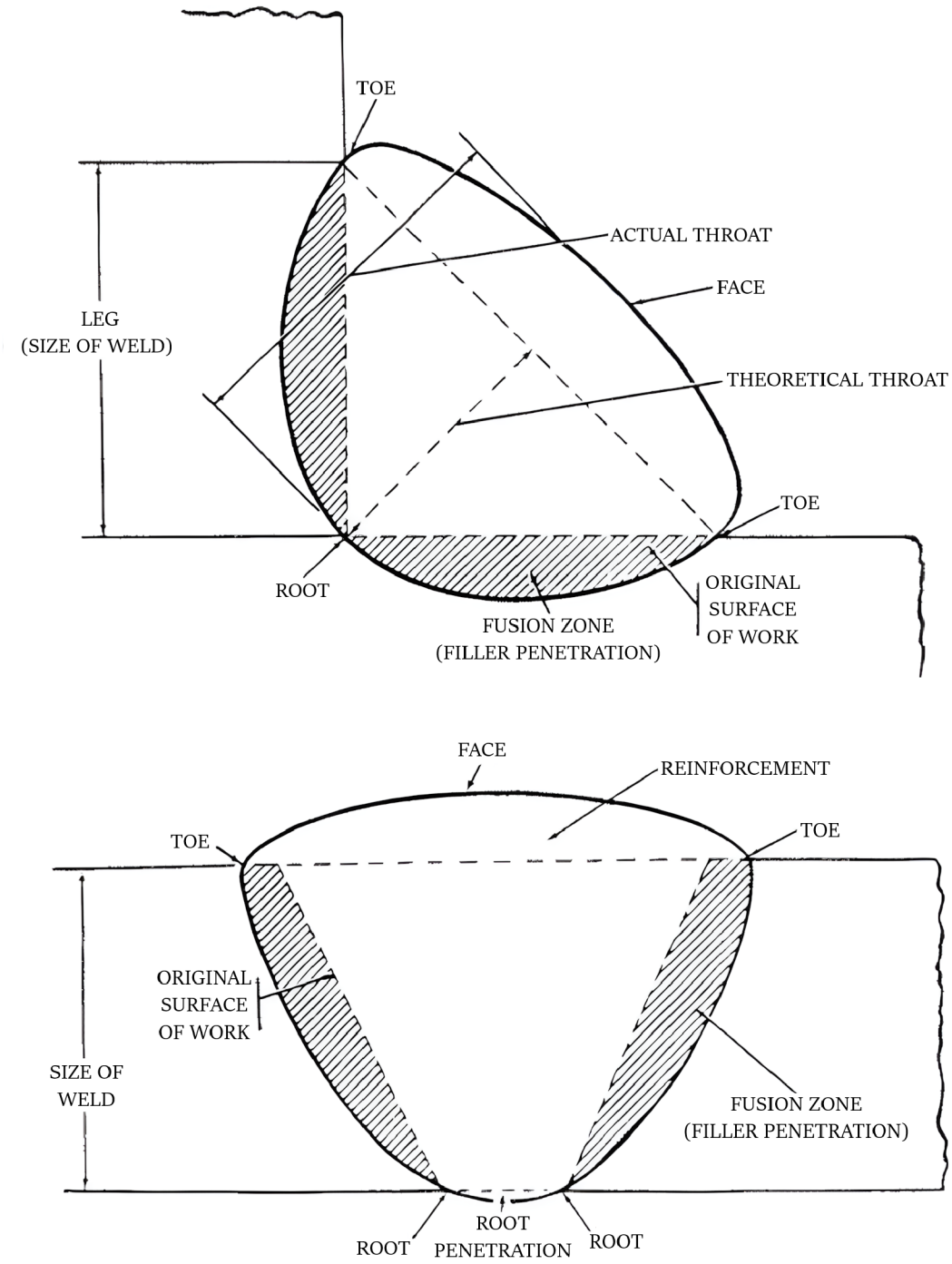

Fig. 3.15: Terms used to describe weld geometry on a fillet and butt weld [19]

When analyzing weld fatigue, there are two main critical locations where cracks can occur: the toe and the root, both presented in fig. 3.16 as both of these locations pose significant stress concentrators. Toe cracks are initiated from the toe due to the relatively sharp transition between the base and the weld metal. The crack, therefore, starts on the visible surface and grows through the base material. The root cracks, on the other hand, initiate in the weld root, which is frequently characterized by sharp slits with non-fused root faces acting like crack starters. This crack starts below the visible surface and is often not observable until it reaches the free surface, at which point it has already grown through the entire weld throat. This is why toe failure, as the expected mode of failure, is preferred, as it can be better detected and monitored. [5]

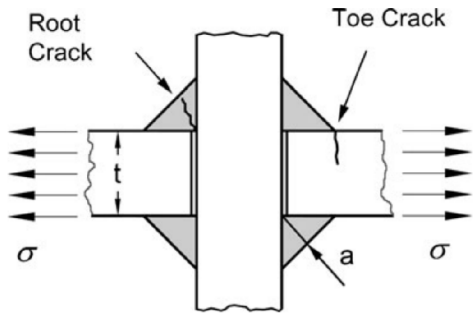

Fig. 3.16: Crack initiation locations on cruciform fillet weld joint [5]

There are several ways to increase root strength to ensure failure from the toe as the preferred failure mode. The first option is to specify a fully penetrated weld in design, in which case there will be no root face and hence no possible cracking from this location. However, this option is often expensive, so another cheaper option is to increase the throat thickness (denoted as dimension a in fig. 3.16). A combination of e.g. a partial penetration weld and large throat thickness may also be sufficient. [10]

However, the basic principles of weld design should always be kept in mind, such as ensuring that the total area of the weld throat is comparable to the thickness of the base material (denoted t in fig. 3.16), which ensures comparable geometric characteristics in terms of stress distribution.

3.2.4 Post-weld treatment

Post-weld treatment (PWT) has traditionally been used to repair or extend the life of existing welded structures. However, its application is also becoming increasingly popular for new high-strength steel structures. The as-welded condition of a weld, characterized by high tensile residual stresses and abrupt geometry changes at the weld toe, results in an elevated stress range, as depicted in fig. 3.17a). The stress ratio of the actual applied load may be largely insignificant due to these high residual tensile stresses, as previously described in subsection 3.1.5. Enhancing the geometry of the weld toe reduces stress concentration and leads to a smaller stress range, as illustrated in fig. 3.17b). This enhancement considers both the reduction of the macroscopic stress concentration resulting from geometrical changes and the improvement of the microscopic stress concentration caused by weld defects. By improving the residual stress state, the local stress ratio decreases, leading to all or part of the local stress range reaching compressive values (as shown in 3.17c)). Local compressive loading significantly reduces crack growth rates. [20]

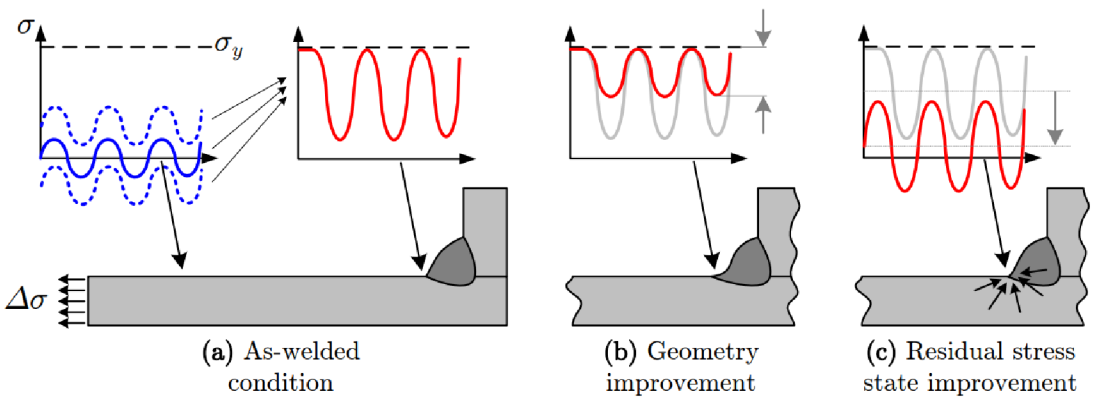

Fig. 3.17: The main types of improvement of welded joints and their effect [20]

Fig. 3.18 lists a selection of widely applied PWT techniques categorized by working principles. Various techniques exist, both generic (e.g., grinding) and proprietary (e.g., ultrasonic impact treatment - UIT). Although most peening techniques offer some degree of geometry improvement, their primary enhancement lies in improving the residual stress state. [20]

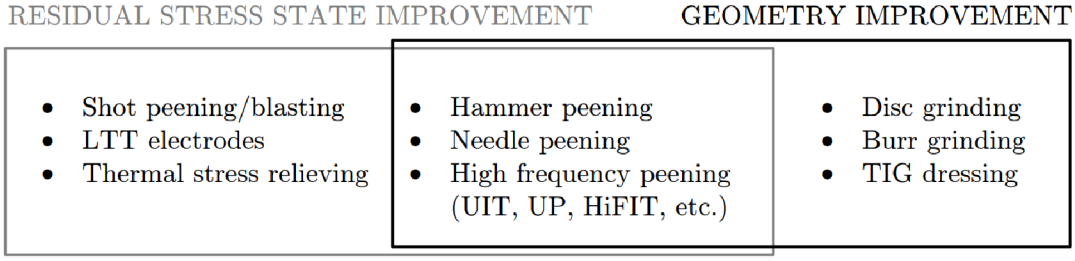

Fig. 3.18: Post-weld treatment techniques overview [20]

Although PWT is sometimes viewed as an expensive solution, it can be cost-effective when only a small part of a component experiences extreme stress, making local application preferable over increasing plate thickness to reduce stresses. The impact of PWT varies depending on specific structural details and test conditions, but generally results in an improvement in fatigue strength ranging from 30 % to 100 %. It is important to note that when the fatigue strength of the weld toe is improved, the critical location can shift to the next most critical location, such as the weld root or plate edge or surface. [10]

4 STUDIED INDUSTRIAL STANDARDS

This chapter presents a comprehensive overview of the standards and codes applied throughout the thesis. Each standard is studied in its individual section. Only relevant details on the topic of weld fatigue are mentioned here. These standards are namely ČSN EN 12663-1 [1], ČSN EN 13749 [2] and the FKM Guideline [3].

ČSN EN 12663-1 [1] and ČSN EN 13749 [2] are Czech translated versions of their respective original European standards (with the same name without the ČSN designation). Both standards are used in the design of railway vehicles. While the standard ČSN EN 12663-1 focuses on the structural requirements of vehicle bodies, ČSN EN 13749 focuses on bogie frames. These two standards were selected specifically as they are the two of the most utilized standards when completing customer requests in the company 5M LEVIT s. r. o. This is because the customer requests are mostly focused on fixing new attachments to the already existing or already designed constructions of railway vehicles. These attachments often get welded to either the vehicle body or the bogie frame, hence the choice of the mentioned standards which the construction must comply with after its modification. These standards also give a significant advantage in terms of providing the structural engineer directly with the prescribed load fatigue cases that these attachments should withstand. However, exact evaluation methods are not mentioned in these standards.

This is why the FKM Guideline [3] is used in the cooperating company, as the applicable assessment methods are presented in the FKM Guideline. As the FKM Guideline complies with the demands of fatigue assessment in accordance with the mentioned standards from the railway industry (as shown later), it is suitably applicable.

4.1 ČSN EN 12663-1

This section is entirely based on one source of the respective standard ČSN EN 12663-1 [1] and introduces the key takeaways regarding fatigue analysis using this standard. Considering this fact, citation marks will not be used in the rest of this section, as they would be largely redundant and very repetitive. The mentioned definitions are translations from the Czech version of the standard and may not absolutely correspond to definitions in the English version of the international standard.

4.1.1 Scope

The scope of this standard is the specification of the minimum structural requirements for railway vehicle bodies. It applies to locomotives, passenger rolling stock, and freight wagons. The standard defines the vehicle body as the main load-carrying structure above the suspension units, including all components that are affixed to this structure which contribute directly to the strength, stiffness, and stability.

4.1.2 Fatigue structural requirements

The assessment of structural requirements shall be done for multiple criteria. Among them, the fatigue criterion is mentioned as service or cyclic loads that should be sustained by the structure for the specified life without detriment to structural safety.

The fatigue resistance data should be based on current European, international, or national standards or alternative sources of equivalent standing. The S-N curves used should be derived for a **survival probability of at least 97.5 %** and it should be based on **classification of**

detail according to the component or joint geometry. The S-N curves should also include the following effects on material:

- rate of loading,
- time (e. g., by material aging),
- environment (moisture absorption, temperature, etc.),
- welding or other manufacturing processes.

4.1.3 Proof of fatigue strength

The fatigue strength of the structure should be demonstrated by experiment or analysis using either the endurance limit approach or the cumulative damage approach. The standard specifically mentions joints between structural members such as welds as one of the potential critical features where the effects of varying dynamic loads may be the most apparent.

The application of the endurance limit approach is possible in cases where all stress cycles remain below the endurance limit with the application of the S-N curve, where the endurance limit is defined by $1 \cdot 10^7$ cycles or fewer. For S-N curves with an endurance limit at more than $1 \cdot 10^7$ cycles or no defined endurance limit, fatigue strength at $1 \cdot 10^7$ is acceptable as the permissible stress.

The alternative is the cumulative damage approach, also generally described in subsection 3.1.6 of this thesis. The standard mentions Palmgren-Miner as one of the applicable hypotheses. It is stated that the fatigue strength is demonstrated by the provided sum of damage below 1.0. However, it also mentions that, if there is a different value in the code or standard adopted, that value should be used instead.

4.1.4 Prescribed fatigue loads

The standard defines a coordinate system shown in fig. 4.1 with respect to the orientation of the body of the railway vehicle. The positive direction of x-axis (corresponding to the longitudinal axis of the vehicle body) is in the direction of movement. The positive direction of the z-axis (corresponding to the vertical axis of the vehicle body) points upwards. The y-axis (corresponding to the vehicle body transverse axis) is in the horizontal plane, completing a right-hand coordinate system. Gravitational acceleration is defined with respect to the orientation of the z-axis as $g = -9.81$ m/s^2.

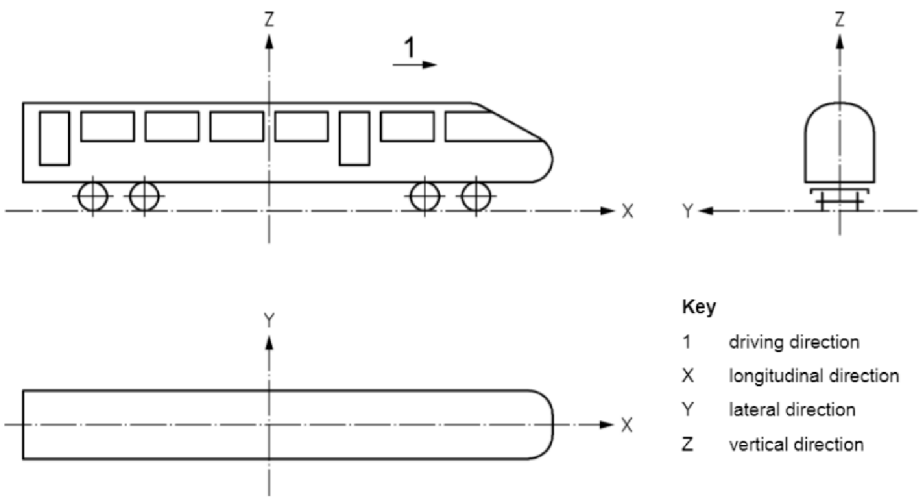

Fig. 4.1: Vehicle body coordinate system according to [1]

The standard categorizes rail vehicles, designating "L" for locomotives, "P-I" to "P-V" for passenger vehicles, and "F-I," "F-II" for freight wagons. The standard defines the different load case values for proving fatigue strength analysis for each category. The standard introduces specific tables for track-induced fatigue loads in the y- and z-axes, as well as for traction and braking loads in the x-axis. These operational loads align with normal European operations and are applicable in scenarios where no other specific source is available.

For brevity and clarity, this thesis offers a simplified version of these tables from the standard in the form of a table 4.1. For details on category divisions and exceptions outlined by * in table 4.1, it is recommended to consult the standard. The structure should withstand these loads using the endurance limit approach. They can also be used with $1 \cdot 10^7$ cycles according to the standard when applying the cumulative damage approach for each direction.

Table 4.1: Fatigue loading accelerations in x, y and z directions as multiples of gravitational acceleration, exceptions marked by * [1]

	Locomotives	**Passenger rolling stock**					**Freight wagons**	
	Category L	**Category P-I**	**Category P-II**	**Category P-III**	**Category P-IV**	**Category P-V**	**Category F-I**	**Category F-II**
x	± 0.15 g	± 0.15 g			± 0.15 g^*	± 0.2 g	± 0.3 g^*	
y	± 0.2 g	± 0.15 g					± 0.2 g ± 0.4 g^*	
z	(1 ± 0.25) g	(1 ± 0.15) g			(1 ± 0.15) g^*		(1 ± 0.3) g^*	

It is also worth mentioning that according to the standard, relevant combinations of fatigue load cases shall be identified, as combining load cases in different directions may pose a greater danger when acting together. However, in such cases, the magnitudes of the load cases may be reduced from the original values in the table 4.1.

4.2 ČSN EN 13749

This section is, in this case, entirely based on a source of the respective standard ČSN EN 13749 [2] and introduces the key takeaways related to fatigue analysis using this standard. Similarly to the previous subsection, citation marks will not be used in the rest of this subsection, as they would be largely redundant and repetitive. The mentioned definitions are translations from the Czech version of the standard and may not absolutely correspond to definitions in the English version of the international standard.

4.2.1 Scope

The scope of this standard is the specification of the requirement for satisfactory design of bogie frames. It is limited to the structural requirements of bogie frames including bolsters and axlebox housings, which are understood to include all functional attachments, e.g., damper brackets. A bogie frame is defined as the load-bearing structure generally located between the primary and secondary suspension. Suspension is a system of the resilient elements; while the primary suspension is generally located between the axlebox and the bogie frame, the secondary suspension is generally located between the bogie frame and the vehicle body or bolster. The simplified schematic of this arrangement can be seen in fig. 4.2.

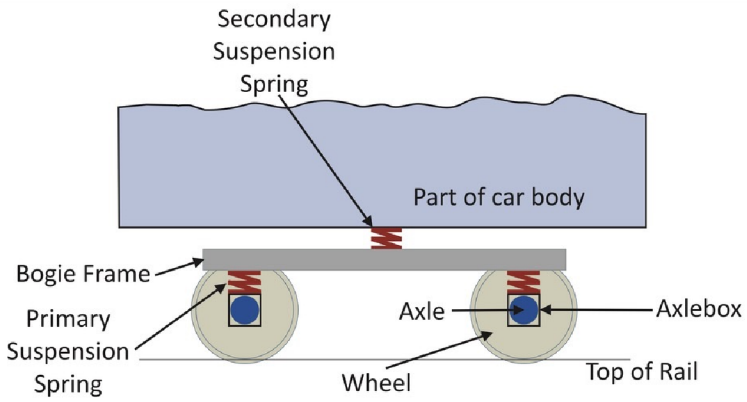

Fig. 4.2: Schematic of a suspension system showing the general arrangement with bogie frame [21]

4.2.2 Fatigue structural requirements

The bogies of the rail vehicle are required to achieve the required service life under normal operating conditions with an adequate probability of survival. This is necessary to demonstrate by analysis for prescribed load cases with a fatigue criterion, which states that the structure as a whole and its individual elements must sustain the service or cyclic loads that cause fatigue damage for a specified life without detriment to structural safety.

Fatigue resistance data should be based on current European or national standards or other alternative sources of equivalent standing. The S-N curves used in the assessment should be derived according to the **survival probability of at least 95 %** and **classification of the details according to the geometry of the components or joints**. The material performance data shall take into account residual stress in the structure, which may be a result of e.g., welding. It is possible to take into account the possible beneficial impact of techniques that reduce the influence of residual stress such as stress relief, shot blasting, and ultrasonic impact treatments where evidence of their benefit can be verified.

4.2.3 Proof of fatigue strength

It is strongly recommended by the standard that numerical methods such as finite element analysis (FEA) to be used, supplemented by hand calculations, to interpret stresses appropriate to the joint types and fatigue life assessment codes, etc. Part of the demonstration of structural integrity is fatigue life assessment using numerical analysis and/or testing. Fatigue strength must be demonstrated using the endurance limit approach, the cumulative damage approach, or other established methods.

The endurance limit approach is applicable in cases where all dynamic stress cycles remain below the endurance limit of the material, with a possible exception for very rare stress cycles exceeding the endurance limit. In cases where no endurance limit is defined, or some repetitive cycles exceed it, the cumulative damage approach shall be followed instead.

The cumulative damage approach is based on the evaluation procedure using the S-N curve and established damage accumulation hypothesis (such as Palmgren-Miner). The required fatigue strength is demonstrated in the case where the total damage for each critical detail is below 1.0 (or lower, depending on the code or standard adopted).

4.2.4 Prescribed fatigue loads

The standard defines a coordinate system of the bogie, shown in fig. 4.3. The longitudinal direction is linear in the direction of travel, the transverse direction is parallel to the plane of the track and perpendicular to the direction of travel, and the vertical direction is perpendicular to the plane of the track. These directions are also provided in the key in fig. 4.3. The standard also defines other movements and deformations; as they are not necessary here, they are omitted.

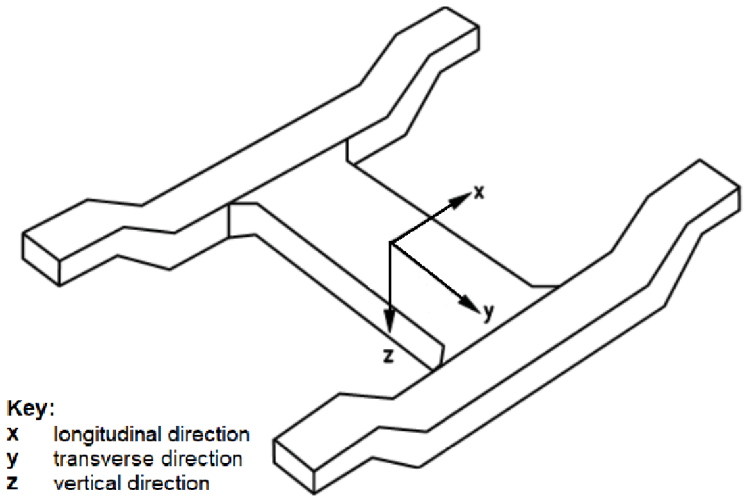

Fig. 4.3: Coordinate system of the bogie according to [2]

As mentioned previously, the attachments to the bogie frame are of main interest here. The standard specifically separates loads due to components attached to the bogie frame. For attachments that are light enough to not significantly affect the dynamic behavior of the bogie frame, the standard defines normal inertia service loads that could potentially induce fatigue damage. These are based on typical design levels applicable to rolling stock using European routes, and should be applied in cases when no other reliable data is available. For fatigue design, the levels in table 4.2 may be assumed to represent a constant amplitude load acting for $1 \cdot 10^7$ cycles that will cause the same damage as the actual dynamic excitation spectra.

Table 4.2: Fatigue loading accelerations in three perpendicular directions as multiples of gravitational acceleration for fatigue assessment [2]

Direction	Bogie frame mounted equipment acceleration	Axlebox mounted equipment acceleration
Vertical	± 6 g	± 25 g
Transverse	± 5 g	± 5 g
Longitudinal	± 2.5 g	± 5 g

The standard splits the applied loads into two groups based on the location to which equipment is attached, the bogie frame itself (antennas, lifeguards/railguards, flange lubrication equipment, sand boxes, etc.) or the axlebox (obstacle guards, braking system components, speed sensors, etc.). It should also be noted that the presented table 4.2 is a simplified version of the information in the standard itself and, for greater detail, consultation with the original standard is recommended. The gravitational acceleration is $g = 9.81$ m/s^2 according to the standard, when rounded to two decimal places.

4.3 FKM Guideline

The FKM Guideline is widely approved as the evaluation code for many fields of industry, including the railway industry. Customer orders in the cooperating company often specifically request that this specific guideline be followed, as it also complies with industrial standards.

This section deals with a brief introduction of the FKM Guideline as the main practical source for this thesis. It introduces its scope of application, basic principles, and relevant details for fatigue evaluation with a focus on welds. Finally, this section also deals with the applicability of using the FKM Guideline for the proof of fatigue strength by analysis mentioned in the elaborated ČSN EN standards.

It should be mentioned that the FKM Guideline has seen multiple editions of its release. The most recent translation in English is the 7th edition published in 2020, which is the one referenced and applied in this thesis. Various updates and improvements to the content are implemented between editions of the guideline. This is why special caution should be applied when using different editions, as details may change and the results may slightly deviate between the editions. However, the calculation procedures remain largely the same. The content of this section will be based on a singular source of the 7th edition of the FKM Guideline [3]. As such, the citation marking will not be used further in this section.

The FKM Guideline is an internationally recognized code for the analytical strength assessment of components. The main advantages of the guideline are its step-by-step approach to the calculation and the fact that practically all the necessary data for the calculation are in the guideline itself, put together from various sources, including the material data. This allows for a straightforward calculation without the necessity of breaking the workflow by accessing multiple sources and standards. The calculation procedure is uniformly structured and applies to all cases of application. The user is only required to make a few decisions. The calculation itself can therefore be to a large extent regarded as an algorithm consisting of instructions, equations, and tables.

Considering these facts, it is understandable that the guideline does not elaborate on the theory behind the calculations and usually presents figures mostly as explanatory additions. However, the original sources are usually referenced in cases where consulting the original publication is needed.

4.3.1 Scope

"The guideline is valid for components of iron and aluminum materials, including cases of elevated temperatures, produced by various industrial procedures, including welding. In detail, it applies to:

- *components with geometrical notches,*
- *components with welded joints, produced by arc welding, beam welding, resistance spot welding or resistance seam welding,*
- *static loading,*
- *fatigue loading from about* $1 \cdot 10^4$ *constant or variable amplitude cycles onwards,*
- *milled and forging steel, including stainless steel, cast iron materials as well as wrought or cast aluminum alloys,*
- *component temperatures from -40°C to 500°C for steel,*
- *from -25°C to 500°C for cast iron materials and*
- *from -25°C to 200°C for aluminum materials,*
- *non-corrosive environment."*

The use of the guideline assumes that the components analyzed have been produced professionally and technically without fault. This is particularly presupposed for welded components, where the limit values regarding weld quality have to comply with relevant welding standards.

4.3.2 Fatigue assessment details and procedure

Although the guideline provides the full evaluation procedure for both static and fatigue loading, it explicitly states that a decision must be made about which cross-section or locations of the component the evaluation shall be performed and suggests that the assessment points should be those points with the highest degree of utilization. However, the specific location of these points may not be apparent, which is the essential problem explored in this thesis, as the degree of utilization is the last step in the calculation.

The guideline states that the strength values included for both the static and fatigue strength assessment correspond to **the probability of survival 97.5 %**.

The guideline offers multiple options when it comes to evaluating weld fatigue. The two specific chapters, which also divide the evaluation methods into two different evaluation groups, are **Chapter 2 - Fatigue strength assessment with nominal stress** and **Chapter 4 - Fatigue strength assessment with local stress**. Each of these chapters provides a distinct division between evaluating non-welded and welded structures in each step of the calculation procedure, which helps the reader in navigating through it. The fatigue resistance for welded components is based on FAT classes for specific geometrical details from IIW [8]. The fatigue resistance can be modified on the basis of beneficial or negative impacts.

Although the assessment procedures are separated from each other, they are strongly similar; the calculation workflow is kept identical. What makes them distinctively different from each other are the ways in which the input of the calculation is obtained in terms of characteristic values of stresses. This also leads to different requirements for the finite element (FE) models used when calculating the stresses using FEA. More on the distinctive differences between the characteristic stresses is explained in detail in chapter 5 of this thesis.

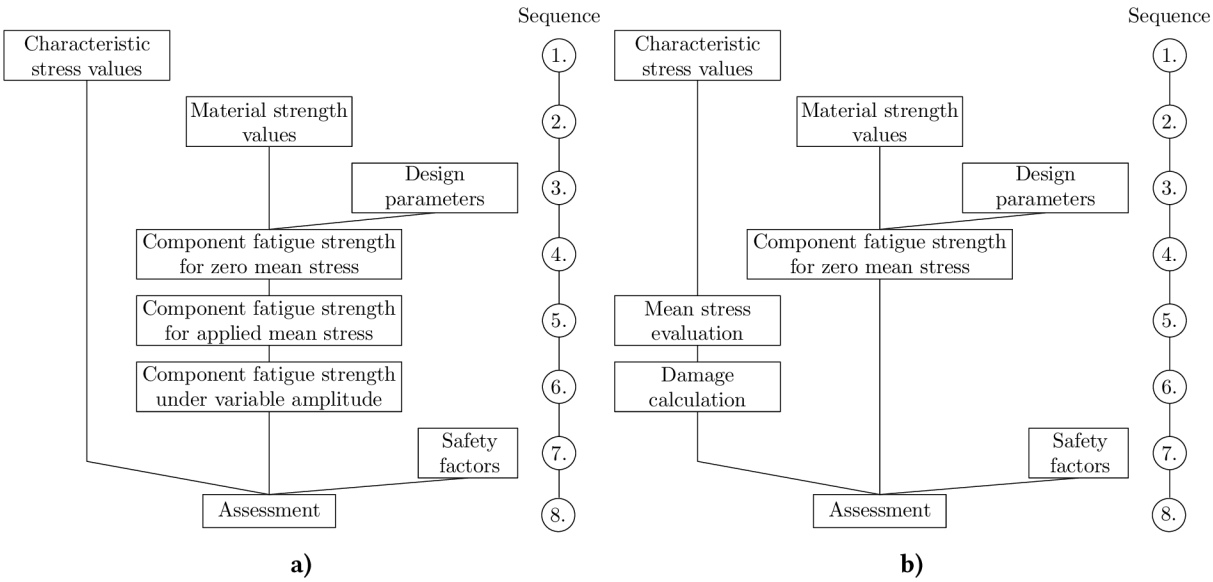

Fig. 4.4: Procedure of fatigue strength assessment using a) maximal stress amplitude b) equivalent stress amplitude, redrawn based on [3]

Regardless of the specific characteristic stress values as input, there are two possible variants of assessment: the "maximal stress amplitude" and the "equivalent stress amplitude." These

two methods eventually lead to the same results, so the choice is largely up to the user. In both variants, the component strength is calculated first. The difference is the consideration of the mean stress and the stress spectra, either on the material strength side or on the stress spectrum side. This distinctive difference can be well observed when comparing the diagrams of the calculation procedure in fig. 4.4a) for the maximal stress amplitude or in fig. 4.4b) for the equivalent stress amplitude assessment.

For maximal stress amplitude assessment, these effects are factored in on the component fatigue strength side. Therefore, the maximum survivable stress amplitude is modified. This is compared with the actual maximum stress amplitude in the spectrum $\sigma_{a,1}$.

For equivalent amplitude assessment, these effects are factored in on the stress side, as the name suggests. As S-N curves are usually measured for the stress ratio $R = -1$ (not true for FAT S-N curves), this approach modifies the spectrum into a single amplitude (with zero mean stress) with the same equivalent damage as the whole spectrum. In this way, it can be directly compared with the S-N curve.

There are two cumulative damage hypotheses as options for the user: Miner Elementary and Miner Consistent. Miner Elementary is based on the basic approach of extending the original sloped part of the S-N curve beyond the fatigue limit (as described in subsection 3.1.6 of this thesis). Miner Consistent is a much more complicated approach, with an iterative algorithm that modifies the Miner Elementary approach result.

The assessment is generally fulfilled successfully, if the applied stresses utilize the strength of the component considering all safety factors at most to 100 % (degree of utilization ≤ 1).

4.3.3 Compliance with the studied ČSN EN standards

Even though it was previously mentioned that the FKM Guideline is applied for the evaluation of the fatigue of the welded attachments as part of the current work procedure in the cooperating company, it may be worth mentioning how the calculated procedure presented aligns with the requirements of the introduced standards ČSN EN 12663-1 [1] and ČSN EN 13749 [2].

The following remarks are important to point out about the FKM Guideline that are significant for compliance with the ČSN EN standards [1; 2]:

- It is applicable for high-cycle fatigue from $1 \cdot 10^4$ cycles onwards.
- It allows for demonstration of a safe fatigue life.
- It includes fatigue resistance data for the probability of survival of at least 97.5 % (the ČSN EN standards require 97.5 % and 95 %).
- The fatigue resistance data for welded components are presented as FAT values complying with the requirement of classification of detail according to the component or joint geometry.
- The fatigue resistance data may be modified based on either negative or positive impacts.

Compliance with these points ensures a comprehensive assessment of welded structures, establishing the FKM Guideline as a methodologically correct option for the case of welded attachments to the bodies of railway vehicles as well as bogie frames.

5 WELD FATIGUE ACCORDING TO THE FKM GUIDELINE

An essential part of the fatigue calculation procedure introduced in subsection 4.3.2 are the **characteristic stress values**, which always mark the first step in the calculation procedure. As mentioned previously, the calculation procedure is largely the same between approaches, so the characteristic stresses are the most significant difference between them, together with the corresponding ultimate values. Although there are essentially only two main approaches in the FKM Guideline [3] for the weld fatigue assessment – nominal and local, the local approach includes a further selection of options. The included approaches are not specific to the FKM Guideline, as they are widely established in industry and other standards.

This chapter provides a more detailed overview of the various approaches included in the guideline, as they are introduced very broadly in the guideline itself, which may cause insufficient understanding or possible confusion of terms. Except for the FKM Guideline [3] as a reference, the other significant reference is the IIW Recommendations [8] which serves as the methodological basis for the evaluation of weld fatigue in the FKM Guideline.

5.1 Nominal vs. local stresses for welds

There are essentially three divisions marked throughout the FKM Guideline; those are between:

- static and fatigue strength assessment,
- nominal and local stresses,
- non-welded and welded components.

This subsection should clarify the difference between nominal and local stresses. However, it is also important to note that there is a difference between these terms for non-welded and welded components, which is only broadly addressed in the guideline itself.

The term "nominal stress" is universally used throughout the guideline as stress calculated using the elementary equations of technical mechanics. As such, it only makes sense for rod- and shell-shaped bodies and components because they have distinctively defined cross-sections. The stress calculated this way neglects the local stress peak that occurs because of geometrical notches or load applications.

For non-welded components, this relates to the actual local cross-section of the body, e.g., for a shaft or a thin plate in the case of a shell-shaped body. However, for welded components, the rod-shaped bodies meant for nominal calculation are the welds themselves, as butt and fillet welds can generally be regarded as rod-shaped components. As such, the stress in the weld should be calculated using the section forces acting on the weld using characteristic values for the cross-section of the actual weld. The fact that is not emphasized in the guideline is that because the stresses are analyzed in the weld itself, the respective failure mode analyzed is cracking of the weld itself.

Local stresses are calculated on the basis of the linear elastic behavior of the material. For non-welded components, these are stresses that include the influence of geometrical notches. The calculation is usually performed using FEA. The goal for non-welded components is to obtain realistic values of stresses in the critical spots of the components. However, for welds, the local stress state is generally not well-defined because the geometry is not well-defined, that is, there are small variations in the toe radius and flank angle along the weld [10]. This is why four different characteristic stress methods are included for the evaluation of welds using local stresses: local nominal stress, structural stress, notch stress, and effective stress.

It may be important to note that the FKM Guideline uses the Latin alphabet for nominal stresses (S for normal stress and T for shear), while the Greek alphabet is reserved for structural stresses (σ for normal stress and τ for shear).

5.2 Nominal stresses approach

Strength assessment of welds using the nominal stresses approach is included in Chapter 2 – Fatigue strength with nominal stresses of the FKM Guideline.

As the geometry of the weld itself can be regarded as a simple rod-shaped body, the stresses acting on the weld can be calculated by applying elementary equations of technical mechanics. From the six general section forces, the three stress components aligned with the weld should be calculated. The stress amplitudes and their respective mean stresses are denoted as:

- $S_{a,\perp,i}$, $S_{a,\|,i}$, $T_{a,i}$,
- $S_{m,\perp,i}$, $S_{m,\|,i}$, $T_{m,i}$,

where S is used for the nominal normal stress and T for the nominal shear stress. The subscript a signifies the amplitude, the subscript m the mean stress, and the symbols $\perp$ and $\|$ are used to differentiate between normal stress perpendicular and parallel to the weld orientation. The index i is the i-th block of the stress spectrum, ordered from the largest amplitude.

As may already be visible, this approach of acquiring characteristic values of stress is limited to only simple cases with a clear relation between the acting load on the welded part and the stresses in the welds. This can be done by deriving the stresses or by using tables of common weld-joint and load combinations with defined calculation formulas.

The ultimate fatigue strength values are defined by nominal FAT classes for the corresponding structural details. For certain structural details, the guideline specifically defines the stress calculation equation to be used.

5.3 Local stresses approach

Strength assessment of welds using the local stresses approach is included in Chapter 4 – Fatigue strength with local stresses of the FKM Guideline. The local stresses are split into four different assessment apporaches using:

- local nominal stresses,
- structural stresses (using hot-spot value),
- elastic notch stresses,
- effective stresses.

The methods of acquiring these stresses are different and include different structural effects. Therefore, in the end, different FAT classes are used for each stress assessment approach to compensate for the included/excluded effects on the material side. The comparison of the three main methods can be seen in fig. 5.1 (effective stress is largely just a modification of the elastic notch stress approach and therefore not displayed). In this idealized case, all three approaches lead to the same results in terms of the number of cycles to failure. In reality, this is rarely the case [10]. What essentially separates the methods from each other is which stress-raising effects are considered on the characteristic stress side and which on the material side in terms of the considered FAT value.

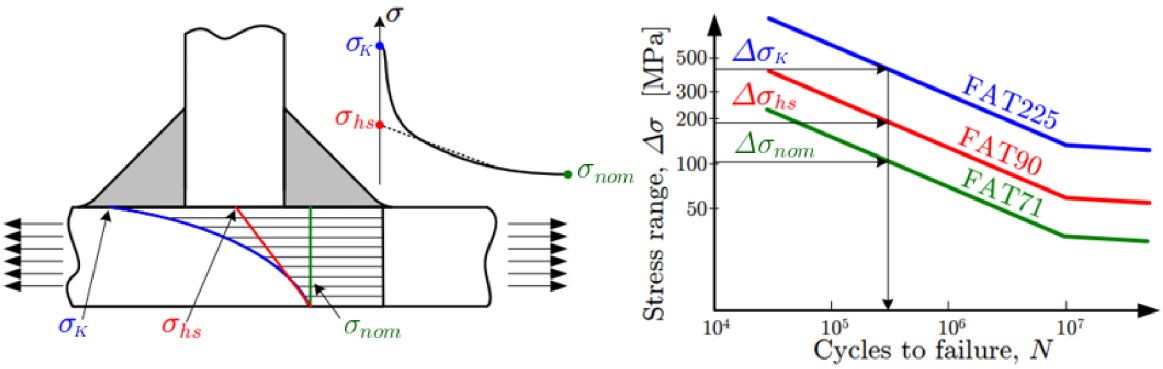

Fig. 5.1: Comparison of local nominal (green), structural (red) and notch (blue) stress approaches [10]

Otherwise, the calculation procedure is the same for all of them and local stresses aligned to the weld in terms of respective amplitudes and mean stresses are used and denoted similarly as for nominal stresses as:

- $\sigma_{a,\perp,i}$, $\sigma_{a,\|,i}$, $\tau_{a,i}$,
- $\sigma_{m,\perp,i}$, $\sigma_{m,\|,i}$, $\tau_{m,i}$,

where the subscripts have the same meaning as for nominal stresses, but σ is used for local normal stresses and τ for local shear stresses.

5.4 Local nominal stress approach

The FKM Guideline does not specifically explain the term of "local nominal stress," even though it explicitly uses it. IIW Recommendations [8] define it as nominal stresses in a component that also include macro-geometric effects (such as cut-outs), concentrated load effects, and effects of misalignment. These are stress-raising effects near the welded joint that cause significant stress redistribution, as can be seen in the example in fig. 5.2. However, the local nominal stress does not include the stress-raising effects of the welded joint itself. Overall elastic behavior is assumed. [8]

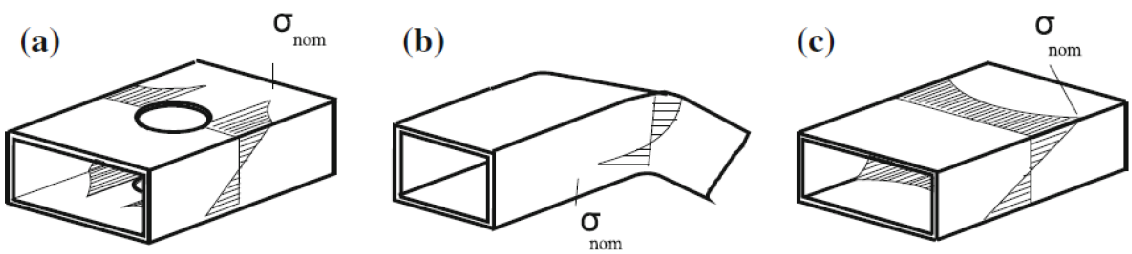

Fig. 5.2: Examples of macro-geometric effects on local nominal stress σ_{nom}, stress concentrations at a) cut-outs, b) curved beams, c) wide plates [8]

Perhaps an easier way to understand this concept is to look at it from a practical perspective. When fatigue tests are performed for the S-N curves of the FAT class, there are specific geometric details of the welds tested. The nominal stress in the cross-section is relatively easily defined, whereas the stress in the weld is not. The weld itself is subjected to much higher

stress, but the specific values are difficult to obtain. This problem is entirely avoided by using the nominal values by simply relating the S-N data and FAT value to the nominal stress. This is also the reason why there are so many nominal FAT classes to factor in all the possibilities of different weld stress concentrators. However, the additional macro-geometric effects that cause stress concentration and redistribution are not included in the FAT values. This is why modification to "local nominal stress" is necessary, as it corrects the nominal value of stress in the vicinity of the weld. However, as also specified by IIW [8], special care should be taken when calculating the local nominal stress using FEM as it is necessary to separate the stress concentration caused by the specific structural detail.

For simple components, the calculation of local nominal stress is also possible using the theories of structural mechanics, such as in the example in fig. 5.3 of a beam-like body. In special cases, the presence of certain macro-geometric effects can also be quantified using engineering textbooks.

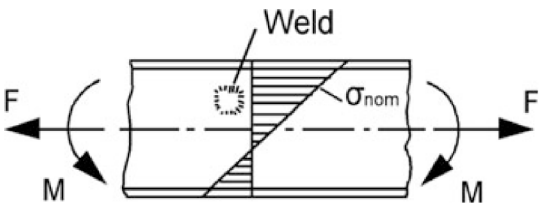

Fig. 5.3: Local nominal stress σ_{nom} distribution in a beam-like body [8]

Alternatively, the local nominal stress can be evaluated on the basis of FEA as mentioned in both [3; 8]. This is beneficial in the following cases [8]:

- complex statically over-determined structures,
- structural components including macro-geometric discontinuities, for which no analytical solutions are available.

As these are the cases in most practical applications, the use of FEA is mostly necessary for the calculation of local nominal stresses. If FEA is used, the meshing can be simple and coarse [4; 5; 8]. The use of beam-type of elements is also possible [4]. As local nominal stresses should not include the stress-raising effects of the welded joint, modeling the weld itself in the FEM model is mostly not reasonable.

It should be emphasized that the term "local nominal stress" is sometimes referred to in the context of weld fatigue as just "nominal" or "modified nominal." To address possible confusion not only with other sources but also with the term "nominal" used in the FKM Guideline, the term "nominal" will be further used exclusively for stresses in the welds, which are calculated using the basic equations of mechanics. The term "local nominal" will be used for stresses in the cross-sections of the components or the weld throats, factoring in the possible macro-geometric influences calculated mainly by FEA as defined by [8]. However, it seems that even in the FKM Guideline itself, the terms are sometimes considered universally as just "nominal," which is partly understandable as their table of structural detail containing FAT classes is just one table that is based on analytically calculated values of nominal stress.

Ultimately, the local nominal stress is defined by IIW Recommendations [8] as *"the average stress in the weld throat or in the plate at the weld toe, as indicated in the tables of structural details."* For butt welds, the weld throat can be regarded as neighboring plate thickness; for fillet welds, it is the distance from the root or deepest point of penetration to the surface of the fillet weld bead. [8]

Therefore, the stresses used in the analysis may be taken directly from the FEA results in the plane stress state. The only exception is with fillet welds, where root cracking is a possible failure mode to be checked. These should be evaluated based on stresses in the weld throat. However, as mentioned in subsection 3.2.3, this failure mode is generally avoided preemptively. However, it is also possible to recalculate the stresses of the plates to the weld throat using the methods presented in detail in [5].

Therefore, this method is primarily beneficial for evaluating fatigue details, where stress in neighboring plates is relevant for analysis and not stress in the weld throats. These characteristic stresses can be evaluated for thin-walled components using shell FEM models, where thin plates are reduced to a 2D representation with their thickness as a parameter.

Maybe not so apparent problem is acquiring the values of local nominal stress from FEA. Separation of the stress increase, which is already factored in the FAT value, may prove very difficult for complex structures. One of the solutions, which has already been mentioned, is using relatively coarse mesh. Another method is to analyze the stress at a certain distance from the weld itself [4]. This can also be observed in fig. 5.1, where the nominal tension value tension is at a certain distance already not influenced by the presence of the weld.

Specific recommendations were found for both of these methods. For the coarse mesh approach, LIMIT® developers [22] recommended an element size approximately three times the thickness of the plate, using lower-order elements and considering elemental stress values [22]. If no averaging is used, the stress distribution is constant throughout the linear-order element anyway. This approach does not eliminate the effect of the possible increase in stress, but significantly decreases its effect.

The coarse mesh with reduced integration elements gives a good representation of nominal stresses at singularities, e.g., the end of ribs. The coarse mesh is advantageous, especially when model size plays a significant role. However, this method may not be so precise in capturing stress gradients perpendicular to the weld. This is why the method of extracting stress at a certain distance is preferred, according to LIMIT® developers [22].

For the approach of stress extraction distance, the recommended value by the LIMIT® developers [22] is 1.5 times the thickness of the plate when using higher-order elements. The stresses at these extraction distances should ideally be based on the interpolation of results from the FE nodes. The choice of this distance is inspired by the German DVS 1612 [23] guideline specifically for the fatigue analysis of steel welded joints in the construction of rail vehicles using local nominal stress values. The DVS guideline specifically mentions that when determining local nominal stresses using FEM, the relevant stresses are usually at a certain distance from the weld seam and recommends a distance of 1 to 1.5 times the sheet thickness from the weld toe for perpendicularly loaded weld seams [23].

A somewhat significant general disadvantage of the local nominal stress assessment in general is that there has to exist a comparable detail in the table of structural details to acquire an accurate and representative FAT value. This may not always be the case, especially for new welds or special weld configurations. If this is the case, the use of local nominal stress is generally not possible if accurate results are needed.

Taking into account the facts of a possible difficult estimation of local nominal stresses and the possibility of missing structural details, this method is sometimes described as inferior to other approaches [10]. However, Jia [4] states that in engineering practice, for an initial screening of fatigue-critical locations in a structure, the estimated local nominal stress can be used with a rather conservative S-N curve. After the fatigue-critical locations are identified, a more dedicated stress measure can be used, if necessary, such as the structural approach (e.g., hot-spot).

5.5 Structural (hot-spot) stress approach

The brief introduction of the structural stress approach included here is based on the description of the method included in IIW Recommendations [8] as the description in the FKM Guideline itself mentions only the facts that it is usually done based on FEA with applicable extrapolation techniques or internal linearization [3]. This method, also commonly known as the hot-spot stress approach, is, as the name suggests, based on acquiring the stress at the hot-spot – the weld toe, which should include all the stress-raising effects except for the non-linear stress peak caused by the local notch in the toe.

The approach of eliminating the non-linear stress notch is based on the linearization of stress along the path leading up to the hot-spot. Fig. 5.4 shows this with two reference points for stress extraction and linearization of results between them. The resulting structural stress is significantly lower than the computed maximum.

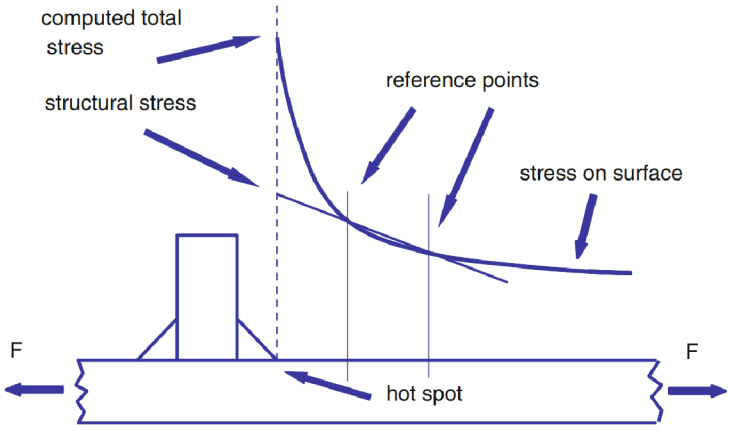

Fig. 5.4: Stress linearization with two reference points leading up to the hot-spot [8]

IIW Recommendations [8] define two types of hot-spots – "a" and "b." The definition is based solely on the path leading to the hot-spot. Toward the hot-spot of type "a" the path goes on the edge, and for the type "b" it goes on the surface. This can be observed in fig. 5.5 together with the possible levels of complexity of the FE model, since both shell and solid elements are acceptable in this approach.

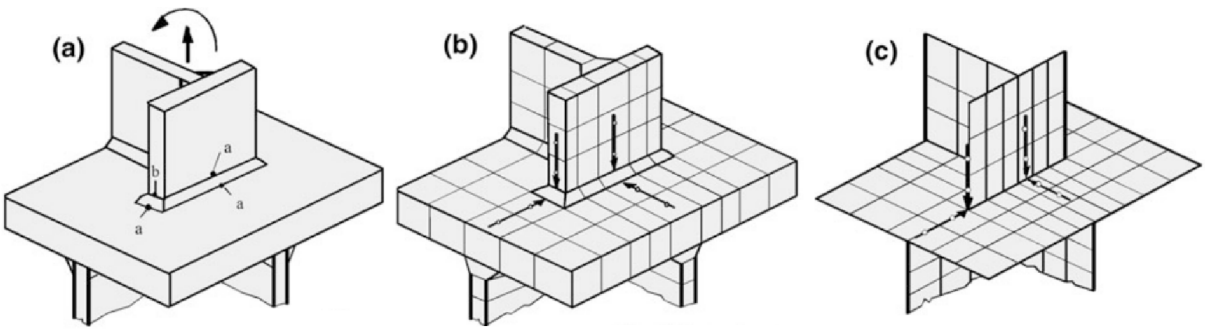

Fig. 5.5: Examples of relative coarse meshing, including stress evaluation points and extrapolation paths: a) welded component showing potential hot-spots of types "a" and "b"; b) solid element model with extrapolation points in the center points of the elements; c) shell element model with extrapolation points for the weld ends located at the mid-side nodes and for the transverse welds at the center points of the elements [24]

Based on the identified hot-spot type and density of the mesh, different linearization formulas are defined. Both the element types and the minimum size requirements are strictly prescribed by the IIW [8]. These size requirements, together with the stress extraction points, are listed in fig. 5.6. The corresponding linearization formulas can be found in [8].

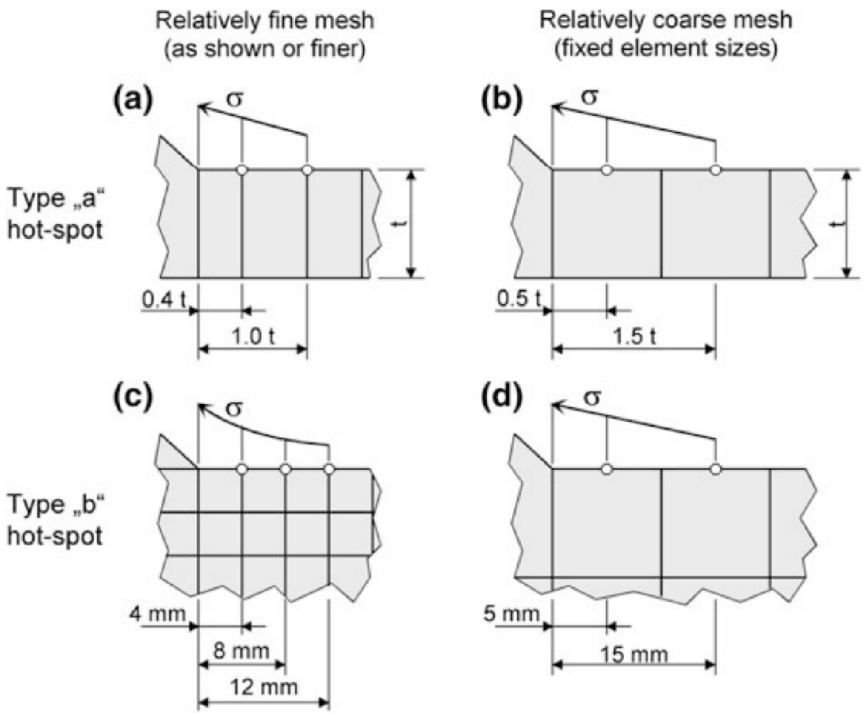

Fig. 5.6: Prescribed mesh sizes and extraction points a) and b) as options for type "a" hot-spot and c) and d) for type "b" hot-spot [8]

There are specific FAT classes and tables of structural details for hot-spot stresses. Compared to the tables of nominal stresses, the total number of details listed is significantly lower, since there is no need to describe specific stress-raising effects using specific structural details. This is also why there are only two FAT values for the "as-welded" condition (100 and 90 for steel, 40 and 36 for aluminum) in the tables listed in the FKM [3] based on table from [8].

The approach of structural hot-spot stress described here was originally developed for the assessment of the toes and ends of the welds only. However, there were several extensions of the method to assess weld roots as well; more details about this can be found in [5]. However, the FKM Guideline limits its use to toe assessment only [3].

It should also be mentioned that according to IIW Recommendations [8] the method is applicable for cases where the dominant loading is perpendicular to the weld. In cases of significant biaxial stress state, the longitudinal loading component should be analyzed using the (local) nominal stress.

5.6 Notch stress approach

The notch stress approach (also called effective notch stress in IIW Recommendations [8]) is based on the notch stress calculated for a notch with a certain assumed notch radius. Therefore, it is mostly determined using FEA with a suitable detail model. However, it is also possible to calculate it using stress concentration factors. [3]

In the basic form of this approach (included in IIW Recommendations [8]), it is assumed that the notch reference radius r_{ref} = 1 mm (the explanation of the choice of this value can be found in [10]). This is why this approach is sometimes also referred to as the R1 approach. The reference radius is applied in the FE model, including an idealized geometry (with effective throat size) of the weld with fillet radii in the weld toe and root equal to the reference radius r_{ref} as can be seen in fig. 5.7. The FE model is solved using a fine mesh in the radii to secure convergence of the stress result. Second-order elements are prescribed with side lengths of max. 0.25 mm to be used. [8]

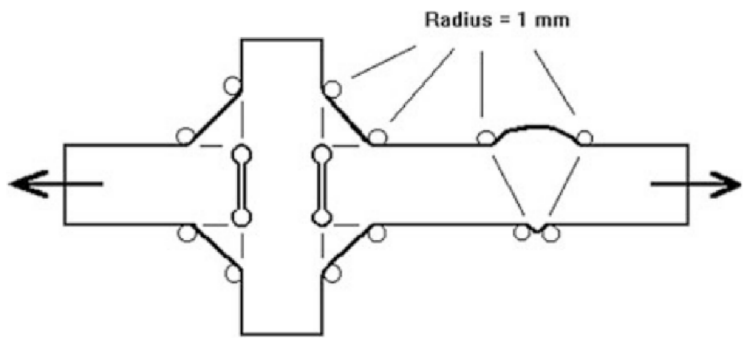

Fig. 5.7: Fictitious rounding of notches using the reference radius r_{ref} = 1 mm on weld geometry [8]

The computed stress component perpendicular to the weld $\sigma_{\perp}$ and the shear τ should be assessed based on the model with reference values of FAT. The parallel stress component $\sigma_{\parallel}$ should be assessed as a (local) nominal stress. For the notch stress approach, there is only one FAT class for $\sigma_{\perp}$ (FAT 225 for steel) and τ (FAT 160 for steel), since all stress-raising effects are factored in on the side of characteristic stress. [3]

However, these basic parameters of the described method are applicable only to plate thicknesses of $t \geq 5$ mm [8]. This is why FKM also introduces the modification of these parameters from [25] for plates with lower thickness based on fig. 5.8 by modeling smaller radii. This also means modification to the corresponding proportional smaller element size and modification of FAT values, which are larger for smaller radii and also different for toe and root (for the R1 approach, the values are the same for both).

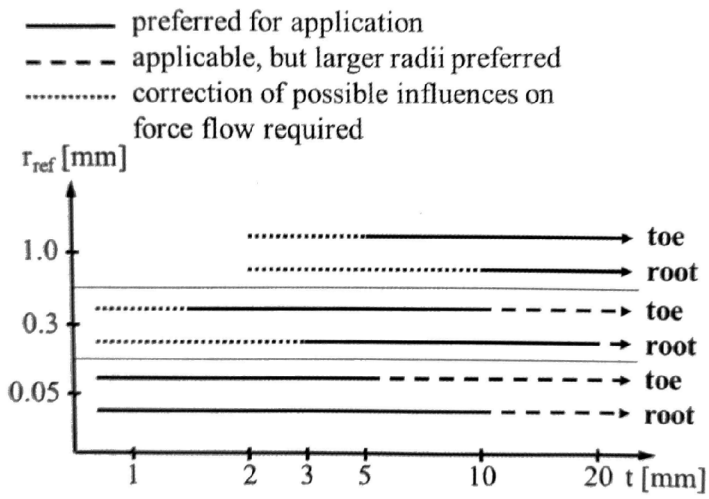

Fig. 5.8: Recommended reference radii size depending on plate thickness, originally from [25]

The FE model can be either three-dimensional or two-dimensional. The two-dimensional model is applicable if the load is primarily perpendicular to the weld and the geometry of the weld does not vary in the assessed area. [8]

The theory behind the approach has been verified for significantly notched welded joints, e.g., cruciform joints and weld roots. However, for mild notches, such as those on fully penetrated butt welds, the stress-raising effect is not significant enough for the notch stress values to be applicable. In these cases, it is necessary to check the notch factor $K_{t,\perp}$ based on the perpendicular component of the stress values, as shown in fig. 5.9 as

$$K_{t,\perp} = \frac{\sigma_{notch,max}}{\sigma_{structure}}. \tag{5.1}$$

If the notch factor $K_{t,\perp}$ is not high enough (lower than minimum for the corresponding r_{ref} the value of the notch stress should be modified to a higher value using the minimum notch factor (1.6 for r_{ref} = 1 mm, 2.2 for r_{ref} = 0.3 mm and 3.6 for r_{ref} = 0.05 mm). [3]

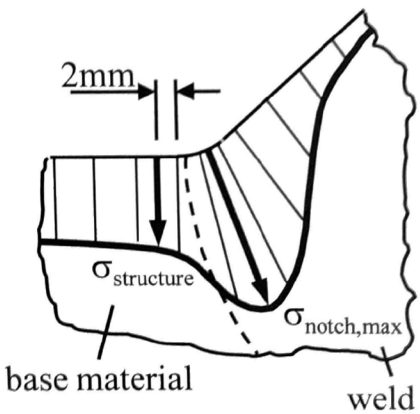

Fig. 5.9: Stress concentration factor stresses for mild notch, originally from [26]

5.7 Effective stress approach

The effective stress approach is the most thoroughly described approach in the FKM Guideline itself. Most likely because this approach does not have a background in the most recent IIW Recommendations [8]. Currently, this method is recommended for steel plates with a thickness $t < 10$ mm. It should be applied only with special caution for thicker plates and plates made of aluminum. It is largely based on the modification of the notch stress approach described in the previous section. The significant difference is that stresses are not taken directly from the notch but instead in some depth going into the material referred to as y_{eff} in the FKM Guideline as can be seen from fig. 5.10 for normal stress perpendicular to the weld; similarly, it should be done for shear stress. The value of the extraction distance y_{eff} = 0.1 mm for steel and y_{eff} = 0.03 mm for aluminum. Another modification is that the reference radius is set to r_{ref} = 0.05 mm for this method with respectively sized elements (unless the real radius of the notch is known). The FAT classes are set to 160 for steel and 50 for aluminum for both normal perpendicular and shear stress. The normal stress parallel to the weld should once again be evaluated on the basis of (local) nominal stress.

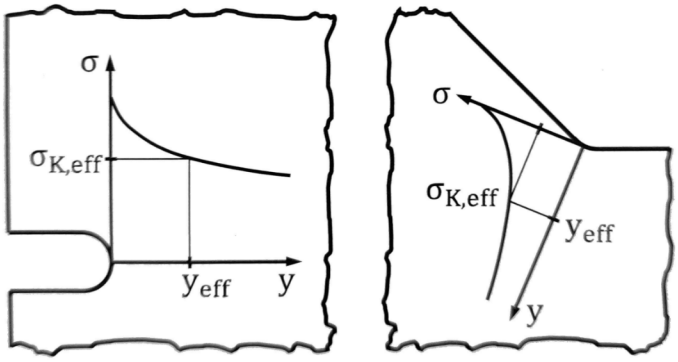

Fig. 5.10: Effective normal stress $\sigma_{K,eff}$ in the distance y_{eff} for weld root (left) and toe (right) [3]

It is not elaborated on why this approach could be in any way superior to the standard notch stress approach in the FKM Guideline itself. As can be observed in the previous subsection, for very thin plates (t $\leq$ 5 mm), the recommended value of r_{ref} = 0.05 mm. Unlike the original concept using r_{ref} = 1 mm, this approach using such a small radius does not include any kind of support effect considered in the original theory, but can be interpreted as a fracture mechanics approach [27]. Based on the results published by Bruder et al. [28], it was found that the use of this reference radius may lead to non-conservative results for very thin plates. The reason for this was explained in the research by Baumgartner et al. [27], who showed that for such thin plates with a reference radius of r_{ref} = 0.05 mm, the non-local effects of the stress gradient in the notch ligament cannot be covered by a single design value of FAT. One of the suggested non-local methods that compensates for this is the one presented in the FKM Guideline [3] as described above.

6 METHODS

This chapter describes all the content related to methods used for achieving the thesis goals and solving the formulated problem of the thesis. The chapter also includes all the steps leading up to key decisions about the solutions taken to help the reader understand why different paths were not explored further.

6.1 Comparison of the FKM proposed methods

This section provides a straightforward example that enables a comparison of the different assessment methods using characteristic stress values obtained with the methods described in the chapter 5 of this thesis. This is done together with the results obtained in terms of degree of utilization (DoU), the most essential result, at the critical location of the welds. Only local stresses methods are presented, as the nominal stresses approach has significant limitations that have already been presented.

Upon studying the different methods for the simple example, the main advantages, disadvantages, difficulties, and the required level of effort for each of the approaches should be revealed. All of this is presented considering the use of the required FEM software, Siemens FEMAP and the calculation procedure according to the FKM Guideline [3]. This comparison example should also reveal potential possibilities for automating the process. Secondly, this should lead to a comparison of the results with the different approaches to possibly reveal significant differences or to verify that all methods ultimately lead to similar results.

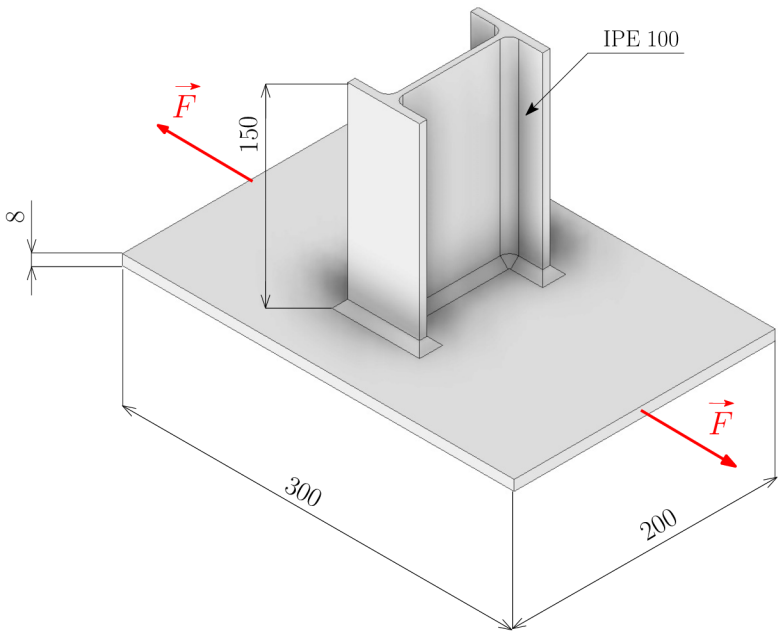

Fig. 6.1: Example configuration with marked main dimensions in millimeters

The chosen demonstration example is an industry standard steel IPE 100 profile section welded on top of an 8 mm thick flat steel plate in its center (both made of steel type S355). The main dimensions are marked in a fig. 6.1 together with the direction of applied load. The applied welds are double-sided fillet welds with a leg dimension of 6 mm. The plate is cyclically loaded in tension by a force F. To better demonstrate the abilities of the calculation procedure of the FKM Guideline [3], instead of applying a symmetric force amplitude, there is a defined load spectrum for the force F. The load spectrum is listed in table 6.1 in two blocks

already separated, with specified maximum force F_{max} and minimum force F_{min}. Since the calculation is linear using elastic material and the plate is always loaded in the same direction, it was not necessary to evaluate the stresses for each load case, that is, each force value from the table 6.1. All stress results could be proportionally recalculated based on knowledge of the loading for one of the cases; therefore, this was done for the force $F_{max,1}$ throughout the rest of the subsection. The usual material parameters of steel (Young's modulus E = 210 GPa and Poisson's ratio μ = 0.3) were used in all the following FE models presented.

Table 6.1: Parameters of the load spectrum

Load spectrum block	F_{max} [N]	F_{min} [N]	Number of cycles [-]
1	50 000	20 000	$1 \cdot 10^7$
2	40 000	30 000	$1 \cdot 10^7$

The example was chosen and set up specifically in a way that allows for comparison of all the local stress methods presented in the FKM Guideline [3]. It should be noted that such comparison is not always possible, as some conditions may prevent specific approaches from being used (such as a lack of comparable structural detail in the table of FAT classes). The example should also partially demonstrate the potential difficulty in revealing the critical location, as the welds might be situated differently with respect to the load direction and therefore have different FAT class values assigned.

6.1.1 Local nominal stresses

Based on the possibilities of recovering the local nominal stresses presented in subsection 5.4, the analytical calculation, coarse mesh approach, and offset distance are presented in this subsection.

Nominal FAT classes

The relevant nominal FAT classes are marked in the fig. 6.2 based on similar structural details from the table in the FKM Guideline [3] for nominal (normal) stresses (corresponding details mentioned in the fig. 6.2). The tables of FAT classes in the FKM Guideline are based on IIW Recommendations [8].

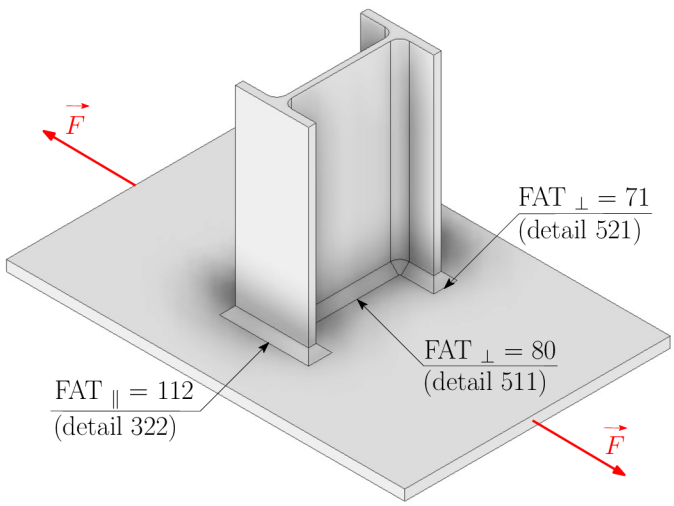

Fig. 6.2: Nominal FAT classes relevant for the direction of loading, values originally from [8]

Taking into account the approximately uniaxial stress state throughout the plate, the FAT classes were assigned considering the known direction of stress. In this case, assigning FAT classes for other stress components would be redundant. However, it should be mentioned that this is the case mainly because of the relative simplicity of the example.

Analytical solution

Considering the definition of local nominal stress presented earlier in subsection 5.4, it can be evaluated for this simple case using simple equations of mechanics. Since the plate is loaded in tension, the stress can be calculated as

$$\sigma = \frac{F}{A}, \tag{6.1}$$

where A is the cross-section area of the plate. Since the simple example does not include any significant macro-geometric stress-raising effects related to the definition of local nominal stress, the resulting stress of σ is actually the local nominal stress. For the force $F_{max,1}$ the corresponding stress is $\sigma_{\perp,\mathrm{max},1}$ is

$$\sigma_{\perp,\mathrm{max},1} = \frac{F_{max,1}}{A} = \frac{F_{max,1}}{b \cdot t} = \frac{50\ 000}{200 \cdot 8} = 31.3\ \mathrm{MPa}, \tag{6.2}$$

where b it the plate with and t is the plate thickness.

Depending on the orientation of the weld in relation to the present uniform stress, this can be locally $\sigma_\perp$ or $\sigma_\parallel$. The critical spot identification can be done on the basis of FAT classes relating to the welds present in the structure. Since the local nominal stress is approximately uniform throughout the plate, the critical spot is the one with the lowest FAT value, which is located at the ends of the flanges.

Coarse mesh approach

The first presented FEA evaluation uses lower-order shell elements (linear shell CQUAD4) with coarse mesh. These elements are called "plate" elements in FEMAP. During the creation of the FEM model, the geometry was simplified to a great extent. The plates were reduced to their respective mid-surfaces with corresponding thicknesses. The welded parts were connected at the level of the mesh. The welds themselves were not part of the model.

Based on the recommendation mentioned in section 5.4, the mesh size for this approach was set to be approximately three times the thickness of the plates. The chosen reference thickness was the thickness of the base plate (resulting element size of 24 mm), as it was the section where failure would be expected. The choice of the preferred size related to the expected critical spot could generally be difficult, since even its approximate location may not be apparent before the calculation. It may also not be easy to preserve the relation between mesh size and thickness when connecting sections of different thicknesses.

By default, FEMAP can plot the stresses in the plane stress state as stresses σ_x, σ_y and τ_{xy}. However, the axes of these stresses are not the global axes of the model. Instead, it is based on the shape of the element and its node sequence [29]. Therefore, special attention should be paid to evaluating stresses without knowing the coordinate system of the element. However, it is possible to assign each element with its "Material Coordinate System." This way the material x-axis orientation can be set. The z-axis is defined by a normal of the element, and the y-axis completes the rectangular coordinate system.

The possibility of this transformation is hugely advantageous because it practically allows for the direct plotting of the necessary stress components with respect to the weld orientation

for the elements belonging to the weld. If the material x-axis orientation is set parallel to the weld line for all the weld elements, the stress component σ_y locally becomes $\sigma_\perp$, σ_x becomes $\sigma_\parallel$ and τ_{xy} becomes τ for the entire structure at once. Transformation into the material coordinate system is done in post-processing, so no re-evaluation is necessary. However, for the demonstration example, this presented two problems related to extracting stress values.

- The nodal results are averaged between the neighboring elements when using the default plot settings.
- Corner elements have two possible coordinate system orientations because they belong to two differently oriented weld lines.

The corner elements problem can generally be solved by evaluating the element from the point of view of both weld lines and their respective coordinate systems and using the corresponding FAT classes. However, nodal averaging proved to be largely problematic. When the weld orientation changes between neighboring elements, the averaging loses much of its meaning because the orientation of the stress components is different in each element. Furthermore, when averaging is applied, the result should be based only on the elements in front of the weld and not behind the weld to be meaningful, as mentioned in [8] in the context of structural stresses evaluated similarly. When using unaveraged stress results for elements, the stresses are constant when using linear-order elements. Based on these facts, centroidal (= elemental) results were used for the evaluation, as they did not present any averaging between nodes. The plot of the transformed perpendicular stresses $\sigma_\perp$ in centroids is presented in fig. 6.3 for stresses perpendicular to the welds. The figure shows a "Criteria Plot," which is a display of the results on the respective elements. The yellow arrows correspond to the set x-axis of the material coordinate system.

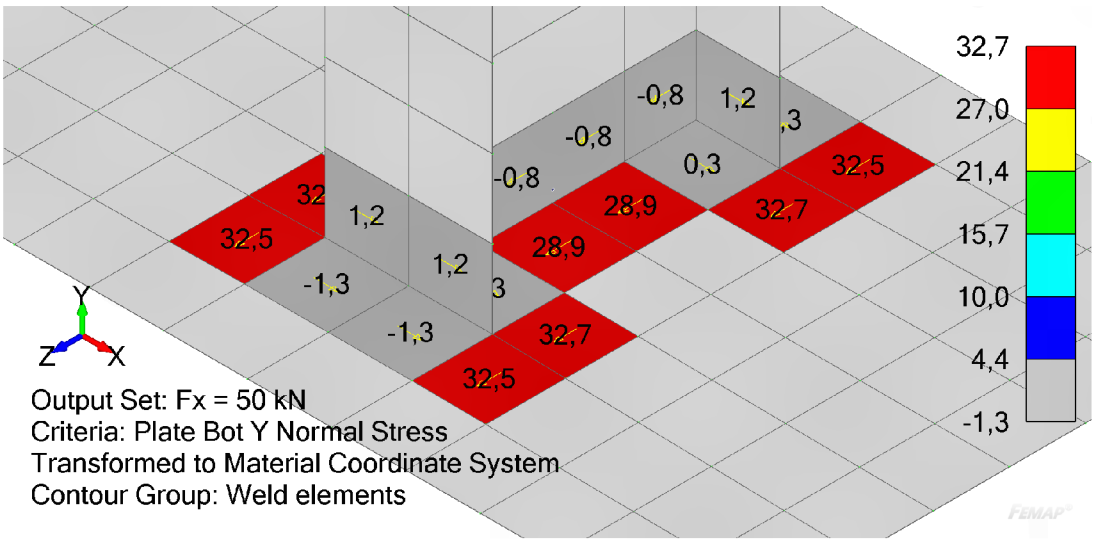

Fig. 6.3: Transformed centroidal stresses perpendicular to welds, yellow arrow marking orientation x-axis of the material coordinate system, results in MPa

Based on the known FAT classes and the extreme value of perpendicular stress $\sigma_\perp$ the critical spot could be easily identified. In principle, the value was not much higher than the perpendicular stress in the not-influenced web area of the plate. This was actually the goal of using the coarse mesh approach with lower-order elements. The denser mesh would cause a significant increase in stress at the location of the flange end due to singularity. However, this

stress-raising effect is not desirable, as the real stress increase in that area would be factored in on the side of the FAT class.

For this simple example, the critical spot was confirmed to be the end of the flange. The extracted value of stress was

$$\sigma_{\perp,\max,1} = 32.7 \textbf{ MPa}.$$

Offset distance approach

The analysis using the offset distance was largely similar to the previous analysis using the coarse mesh. It was based on the approach described in 5.4. The only major difference in modeling was the size of the mesh and the order of the elements. The size of the elements was reduced compared to the previous model to correspond to the thickness of the plate (8 mm), and quadratic QUAD8 elements were used instead of linear elements. The distance from the weld line corresponding to the recommendation mentioned in subsection 5.4 was 1.5 times the thickness, that is, 12 mm. For the quadrilateral elements, this corresponded to the mid-side node of the element or centroid, which was one row of elements away from the weld line.

The same practical principles mentioned in the previous subsection of using material coordinate system were applied to this model stress recovery approach as well. In FEMAP, stresses are not recoverable directly from a general location but only from elements (= elemental centroids) or nodes. Therefore, recovering results at a certain distance requires the presence of an actual node or element centroid in that distance.

In principle, this approach would generally require the identification of the correct nodes or elements and the evaluation of the stresses for each line at the prescribed distance. Therefore, prior knowledge of the critical location was considered during the analysis. With the denser mesh, the effect of singularity was already observable in that spot, as can be seen from the stress results of stresses perpendicular to the welds presented in figure 6.4. The results were plotted without element averaging. However, the problem of averaging did not influence the results in one row further from the weld elements.

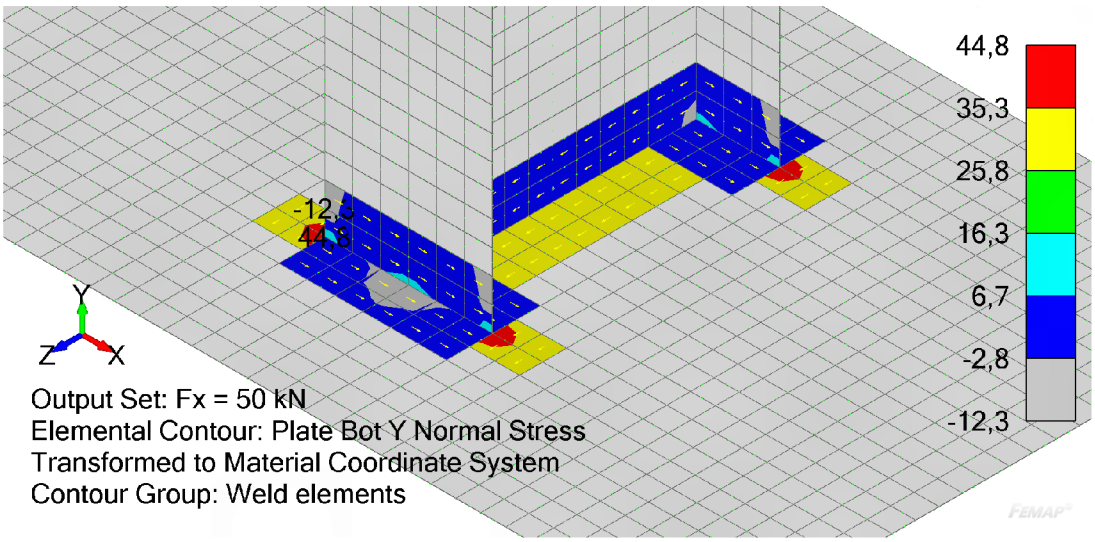

Fig. 6.4: Transformed stresses perpendicular to welds, no averaging between elements applied, results in MPa

The stress result of $\sigma_\perp$ as a function of the distance from the critical location is plotted in fig. 6.5. The perpendicular stress $\sigma_\perp$ in the prescribed distance of 1.5 times thickness based on graph was

$$\sigma_{\perp,\max,\mathbf{1}} = \mathbf{33.7\ MPa}.$$

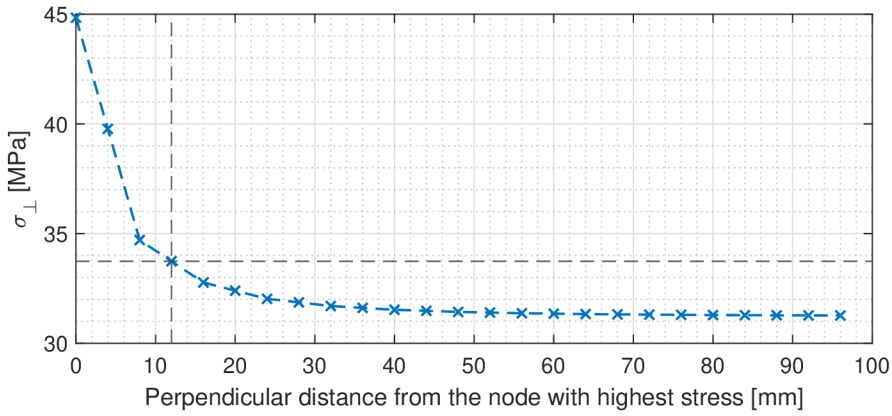

Fig. 6.5: Stress in direction perpendicular to the weld with marked value in distance of 1.5 times thickness of the plate

Local nominal stress summary

The following points from the presented approaches of recovering local nominal stress should be pointed out:

- FEMAP allows relatively easy transformation of the stress results into the weld orientation coordinate system using the material coordinate system when using the plate (= shell) elements.
- Both approaches of recovering local nominal stresses from FEA provide relatively good results comparable to the expected analytical value (filtering out the stress-raising effect already factored in the FAT value).
- Both presented approaches in principle evaluate the stress at the same distance, since the centroid of a rectangular element with a size of 3 times the thickness is also at the 1.5 times thickness distance.
- The simplicity of the example allows for relatively easy identification of critical location between welds, even when considering different orientations and FAT classes. However, for complex structures, the evaluation would require repeating the process for each element/node and considering FAT classes for different stress components.
- The coarse mesh approach requires less computational power with significantly fewer elements, is easier to carry out, and has great potential for automation.
- The coarse mesh approach is much more universal.
- There is no easy way to recognize outright the top and bottom sides of the elements, while often results only from one side are relevant for the stress evaluation, requiring additional understanding of the model by the user.

6.1.2 Structural stresses

As was mentioned in section 5.5, the approach of recovering structural stresses (hot-spot stresses) is possible using both shell and solid elements. Both will be presented for comparison.

Structural FAT classes

The relevant structural FAT classes are marked in the fig. 6.6 based on the table of structural details in the FKM Guideline [3] for structural (normal) stresses. These are again based on those of the IIW Recommendations [8]. Only FAT classes for locations of stress acting perpendicular to the weld are given here, since this is the only direction where structural (hot-spot) stress can be applied (as was mentioned in section 5.5). It is evident from the figure that the FAT classes have the same value for both sections that are loaded by perpendicular stress. The stress levels were expected to be higher near the end of the flange, which could already be observed in fig. 6.4.

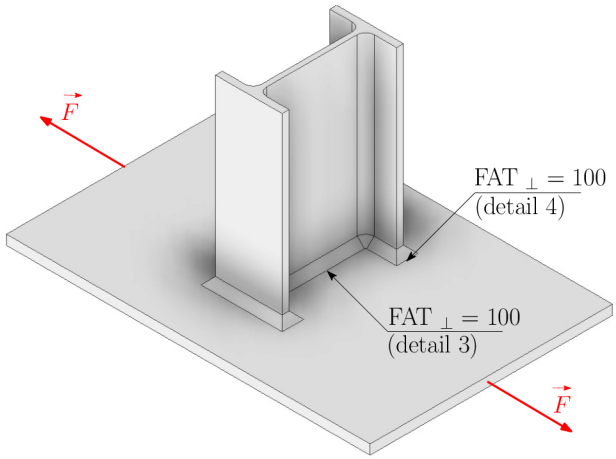

Fig. 6.6: Structural FAT classes relevant for the direction of loading, values originally from [8]

Shell elements model

Based on prior knowledge of the critical spot, an evaluation of hot-spot type "a" was carried out (see fig. 5.5 for explanation). A choice of relatively coarse mesh (fixed element sizes) was made (see fig. 5.6 for explanation). This allowed the use of the same FE model that had previously been used in the local nominal approach, using quadratic QUAD8 elements with an element size of 8 mm. Therefore, repeated displays of the same model are avoided here. See fig. 6.4, if necessary.

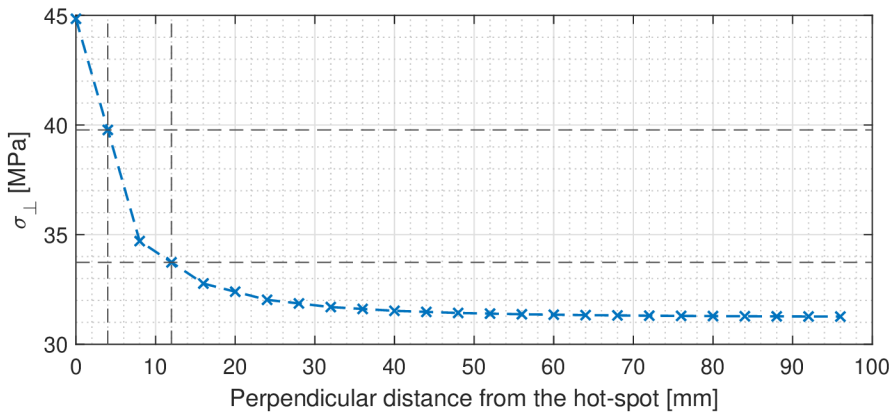

Fig. 6.7: Perpendicular stress as function of distance from the weld on the shell element model, the stress extraction distances for hot-spot stress calculation marked

The stress results were once again transformed for the relevant elements, the stress results of $\sigma_\perp$ on the nodes along the path away from the weld are presented in figure 6.7. The necessary values in distances 0.5 times and 1.5 times thickness (also marked in fig. 6.7) of $\sigma_{0.5\cdot t}$ and $\sigma_{1.5\cdot t}$ were

$$\sigma_{0.5\cdot t} = 39.77 \text{ MPa},$$

$$\sigma_{1.5\cdot t} = 33.74 \text{ MPa}.$$

Therefore, the resulting perpendicular hot-spot stress $\sigma_\perp$ according to the corresponding equation from the IIW Recommendations [8] was

$$\sigma_{\perp,\max,1} = \mathbf{1.5 \cdot \sigma_{0.5\cdot t} - 0.5 \cdot \sigma_{1.5\cdot t} = 1.5 \cdot 39.77 - 0.5 \cdot 33.74 = 42.8\ MPa}. \tag{6.3}$$

Solid elements model

The hot-spot approach is also applicable for solid elements, with a mostly similar approach to shell elements. The main difference is that, for solid elements, a simple model of the actual weld is actually present, and the extraction points are considered in the distance from the toe location. Since the example problem was double-symmetric, just a quarter was modeled and meshed. According to IIW Recommendations [8], the solid mesh should be based on prismatic elements with the recommendation of 20-node isoparametric elements with a mid-side node at the edges. Therefore, a simplified model was predominantly meshed using CHEXA quadratic solid elements, which the mesher was able to preserve for the relevant locations. In addition, the parameters related to the density of the mesh were kept identical to those of the shell element model.

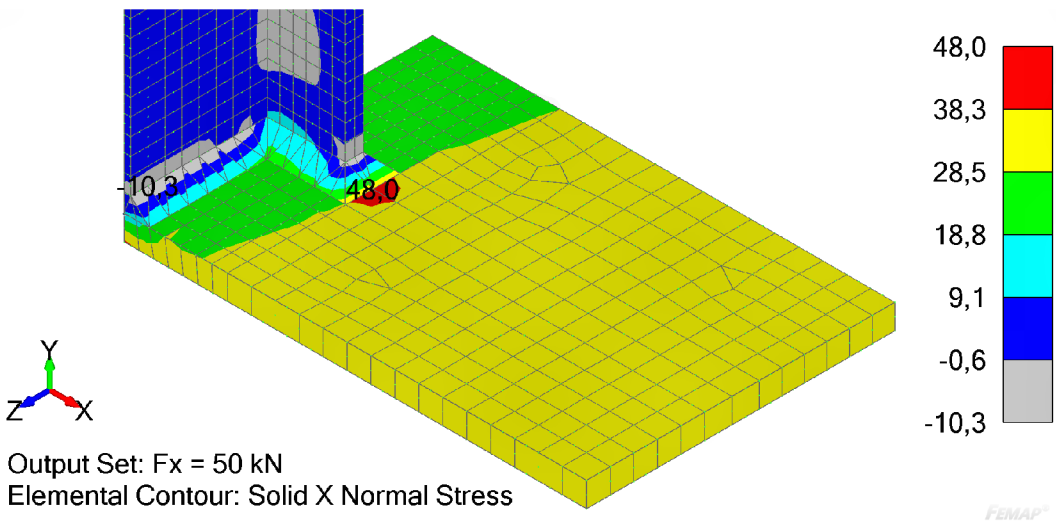

Fig. 6.8: FE model of a quarter of the example component with stresses in direction of the loading force, results in MPa

The process of stress extraction was largely similar to the shell model, this time without the necessity of differentiating the top and bottom surfaces, since both surfaces were actually modeled instead of the mid-surface. Transformation to a coordinate system aligned with welds was, however, much more difficult and time-consuming for solid elements. This is why stresses aligned to the global coordinate system were used instead (which is a default output for solid

elements in FEMAP) also considering the prior knowledge of the critical location. These results can be seen in fig. 6.8.

The necessary stress values of perpendicular stress $\sigma_\perp$ leading up to the hot-spot location (also marked in fig. 6.9) $\sigma_{0.5\cdot t}$ and $\sigma_{1.5\cdot t}$ were

$$\sigma_{0.5\cdot t} = 42.97 \text{ MPa},$$

$$\sigma_{1.5\cdot t} = 35.84 \text{ MPa}.$$

Therefore, the resulting perpendicular hot-spot stress $\sigma_\perp$ according to the corresponding equation from [8] was

$$\sigma_{\perp,\max,1} = \mathbf{1.5 \cdot \sigma_{0.5\cdot t} - 0.5 \cdot \sigma_{1.5\cdot t} = 1.5 \cdot 42.97 - 0.5 \cdot 35.84 = 46.5 \text{ MPa}}. \tag{6.4}$$

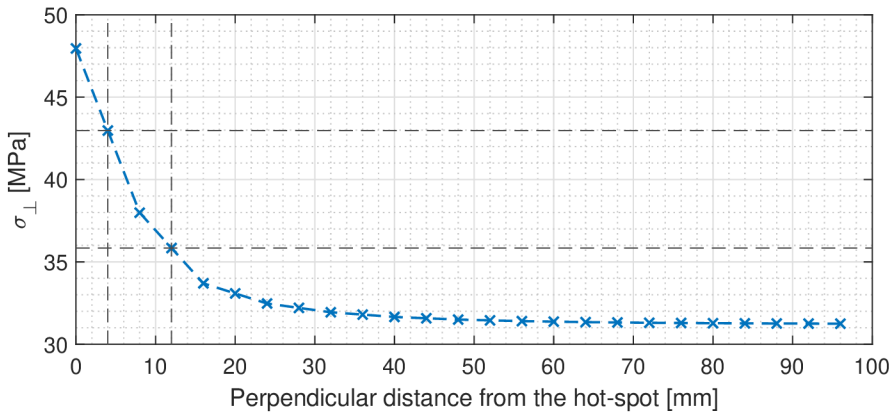

Fig. 6.9: Perpendicular stress as a function of distance from the weld on the solid element model, the stress extraction distances for hot-spot stress calculation marked

Structural stresses summary

The following remarks from the presented approaches of recovering structural stress should be pointed out:

- Using solid elements does not provide significantly different results of the hot-spot stress compared to the shell elements.
- Using structural stress requires a significantly higher level of effort compared to the presented methods of the local nominal stresses approach.
- Without prior knowledge of the critical location, the evaluation would require repeating the process for each perpendicular node or element path (considering that nodes or elements have already been prepared in prescribed distances).

6.1.3 Notch stress and effective stress

Because of similarities between the approaches of notch stresses and effective stresses, they are described here in a common subsection.

Notch stress FAT class

Since the thicknesses of the plates were in the 3 to 10 mm interval, the reference radius $r_{ref} = 0.3$ mm was chosen according to fig. 5.8. The reference radius used directly implied the FAT class, which was for normal stress $\sigma_\perp$ for weld toe FAT 300 and FAT 340 for weld root for steel according to the FKM Guideline [3].

Notch stress

The determination of the notch stress based on FEA had to be done with suitable model details (see fig. 5.6). Although the critical spot was expected to be located in the weld toe, the quarter model was modified according to the parameters required in [8] for both the weld roots and the weld toes. The purpose was to realize the level of effort required by this method when using it generally. Modifying the model, especially for the weld root location, proved to be very time-consuming since it cannot be done as easily as modeling radii at transitions. Fig. 6.10 shows the base FE model for analysis with the results of stresses aligned to the x-axis of the global coordinate system. This was the perpendicular direction for the identified critical location. The result of perpendicular stress shows the expected maximum at the previously identified critical spot of the structure.

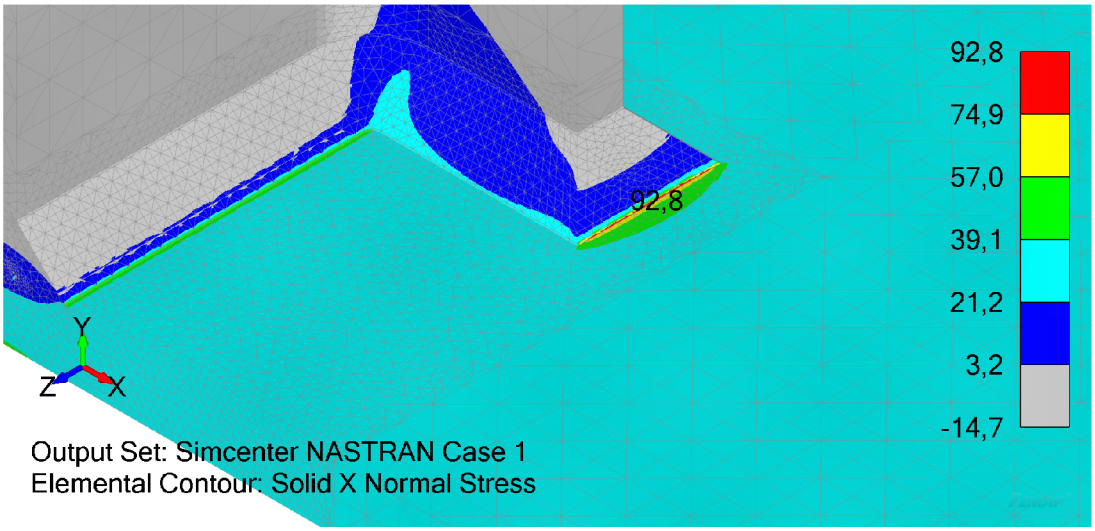

Fig. 6.10: Stress results with respect to the global x-axis of the quarter model, results in MPa

However, since the base model did not meet the criteria defined in [8], submodel analysis was performed. The original mesh had tetrahedral elements of a base size of 0.5 mm around the area of interest. However, this mesh was far from fine enough for the requirements of [8] that translated to an element size of 0.075 mm. For submodeling, a middle cut of the flange was analyzed so that the critical location would be in the cutting plane. The model was therefore analyzed as a two-dimensional plane strain model, as it matched the reduction criteria to the two-dimensional model mentioned in section 5.7. The results in the form of the first principal stress for the submodel can be seen in fig. 6.11. The maximum presented is the notch stress was

$$\sigma_{\perp,\max,1} = \mathbf{119.0\ MPa}.$$

Furthermore, in the location of the weld root, there was also a significant stress increase, reaching values around 74 MPa as can be seen in detail in fig. 6.12. This is not as apparent due to the global scale in the fig. 6.11. As the value was much lower compared to the toe and the FAT class is larger at the root, this confirms that the toe was the critical spot of the weld in this example. A mild notch check did not have to be performed, as fillet weld is not expected to have only a mild notch effect.

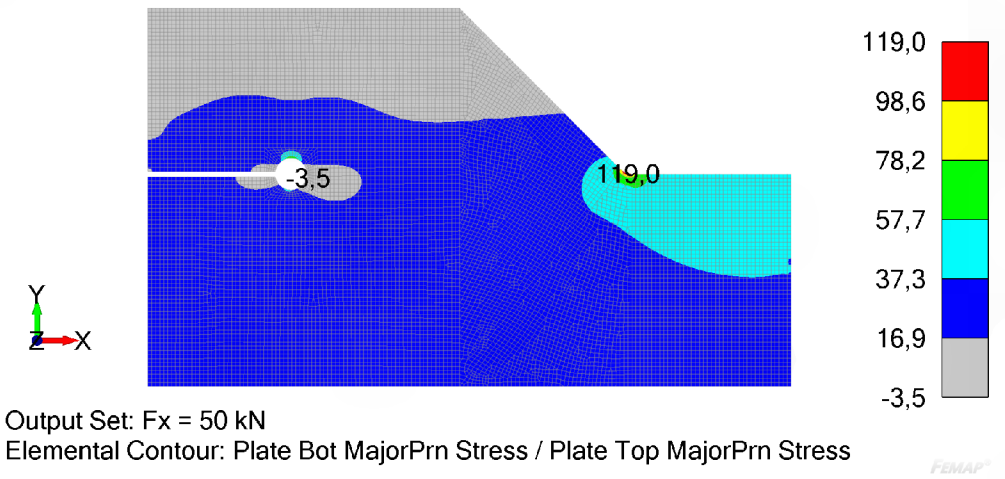

Fig. 6.11: Plane strain submodel using sufficiently dense mesh with results displaying the notch stress as maximum in the toe area, results in MPa

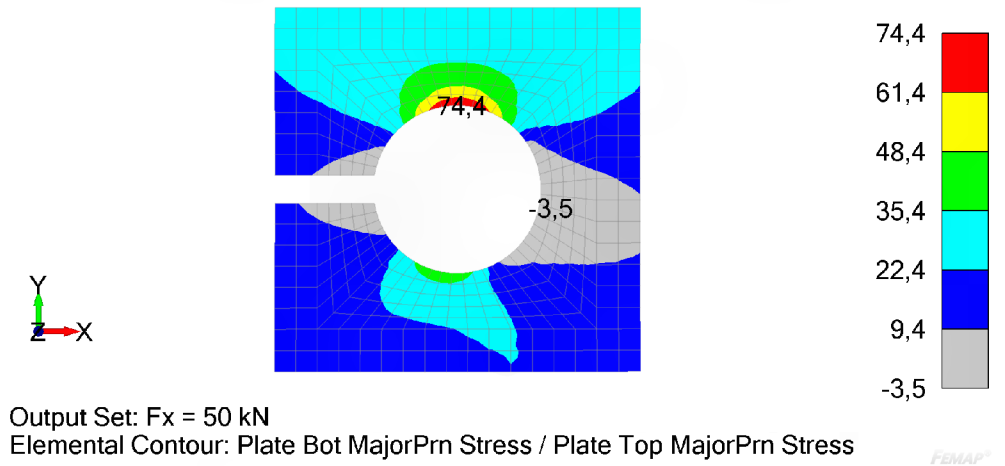

Fig. 6.12: Detail of the notch stress in the root area, results in MPa

Effective stress FAT class

Using the method of effective stress directly implies FAT class FAT 160 for steel for normal stress $\sigma_\perp$ in the FKM Guideline [3].

Effective stress

The approach of effective stress is strongly similar to notch stress; however, it has even stronger requirements on the modeled radii and, therefore, on the size of the mesh. The required radius of r_{ref} = 0.05 mm implied an element size of 0.0125 mm for analysis. To avoid repeated modeling, the previously presented submodel was reduced to accommodate only the toe and edited to meet radius and mesh requirements. Subsequent evaluation of stress along the normal path was carried out, with recovery of stress from the node approximately at the prescribed distance for steel y_{eff} = 0.1 mm for steel. The mid-section cut is presented in figure 6.13 (referenced nodes highlighted). The dependence of perpendicular stress $\sigma_\perp$ on the distance from the surface with marked reference distance y_{eff} is presented in figure 6.14.

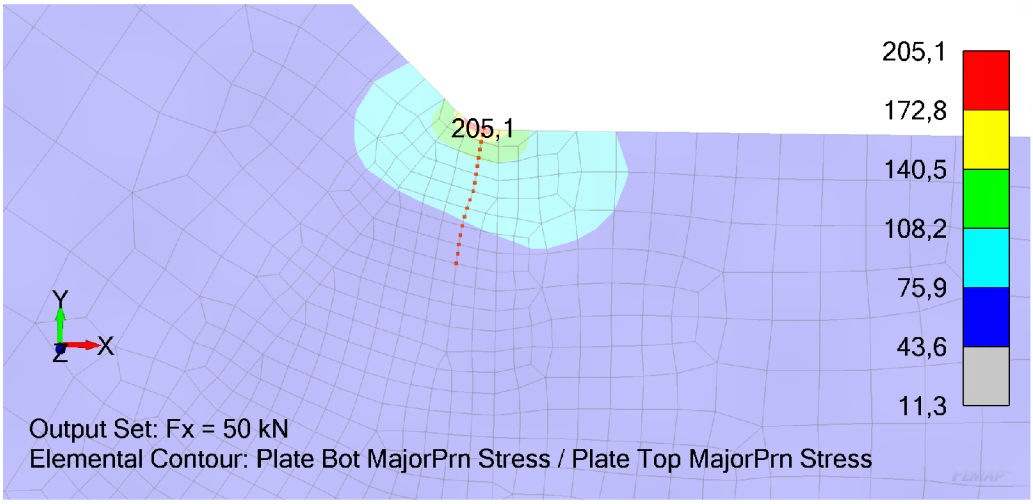

Fig. 6.13: First principal stress result in the plane strain submodel with the highlighted nodes used for results extraction as prescribed for the effective stress method

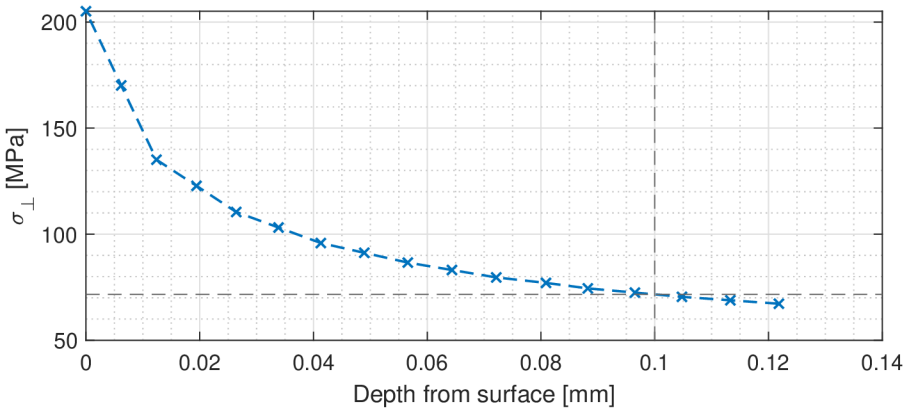

Fig. 6.14: Perpendicular stress as function of distance from the peak notch stress to the depth, with marked stress extraction distance

The value of perpendicular stress $\sigma_\perp$ in the critical spot in the distance $y_{reff} = 0.1$ mm was

$$\sigma_{\perp,\max,1} = \mathbf{71.6\ MPa}.$$

Notch and effective stress summary

The following remarks from the presented approaches of recovering the notch and effective stress should be pointed out:

- Both approaches are very time-consuming, as they require additional modifications of the model and mesh.
- The mesh requirements imply very small elements and therefore significantly more degrees of freedom. This could impose large computational demands and possibly computations that take substantially more time to solve compared to the previously presented methods.
- Both expected failures (root crack and toe crack) can be well analyzed using these methods without additional effort after the completed analysis.

6.1.4 Comparison and analysis of results

A comparison of results using the different methods of acquiring characteristic stresses is listed in table 6.2. The results in terms of cyclic DoU presented in the table were fully calculated according to the calculation procedure in Chapter 4 of the FKM Guideline [3]. However, the main focus can be on the mutual relationship between the values of $\sigma_{\perp,\max,1}$ and the corresponding FAT classes. Appendix A presents the previews of the Microsoft (MS) Excel worksheets used for all the calculations up to the result of a perpendicular cyclic DoU in the critical location. As can be seen in Appendix A, the procedure is the same for all the approaches; the only things changing are the characteristic stresses values and the corresponding values of FAT. However, there is an exception to the number of cycles at the knee point for the nominal structural detail 521 mentioned in the FKM Guideline. For this specific detail, which was applied for this example, $N_D = 1 \cdot 10^7$ cycles and not $N_D = 5 \cdot 10^6$ cycles as in the standard definition for normal stresses in [3]. The results considering the cycles of the values $N_D = 5 \cdot 10^6$ cycles are also displayed in brackets ( ) in table 6.2.

Table 6.2: Comparison of results using different stress assessment methods

Stress assessment	Element type used	Critical area element size	Extraction distance	FAT category	FAT class	$\sigma_{\perp,\max,1}$ [MPa]	DoU [-]
Analytical nominal	-	-	-	Nominal	71	31.3	0.50 (0.40)
Local nominal	CQUAD4	24 mm	Centroid (~ 12 mm)	Nominal	71	32.7	0.52 (0.41)
Local nominal	CQUAD8	8 mm	12 mm (on surface)	Nominal	71	33.7	0.54 (0.42)
Hot-spot	CQUAD8	8 mm	-	Structural	100	42.8	0.38
Hot-spot	CHEXA20	8 mm	-	Structural	100	46.5	0.42
Notch stress	CTETRA10 + CQUAD8 (Plane Strain)	0.075 mm	-	Notch stress	300	119.0	0.36
Effective stress	CTETRA10 + CQUAD8 (Plane Strain)	0.0125 mm	0.1 mm (in depth)	Effective stress	160	71.6	0.40

The figures presented in the external Appendix A are from the MS Excel semi-automated worksheets currently used as part of the work procedure in the fatigue of welds analysis in the cooperating company assigning the topic of this thesis. The company independently created these worksheets prior to the work on this thesis and provided them for application in the thesis. As the company wished not to publish the original files, only previews are provided in Appendix A. The calculation steps can be checked with the 7th edition of FKM Guideline [3].

As can be seen in the table 6.2, the results are very similar for all the various fatigue assessment methods. The only outliers are the results obtained using the local nominal stress assessment. This was caused mainly by the different definition of the S-N curve knee point. Without this consideration for that specific structural detail, the results are comparable with the others, as can be seen from the results in the brackets ( ). Note that the methods used for the local nominal stress assessment did not have the methodological sources of the FKM Guideline [3] and the IIW Recommendations [8] compared to the others. Based on the results, it can be stated that the specific approaches that were previously proposed in this thesis are relatively successful in the goal of extracting stresses without the stress concentrations already factored in the nominal FAT class values. However, the universality of these approaches remains unknown for all the specific structural details and possible gradient-related results.

Based on the provided example, it is also evident (with respect to the content of Appendix A) that the calculation algorithm utilized in the FKM Guideline, when dealing with a number of cycles exceeding the fatigue limit number of cycles N_D for the largest amplitude $\sigma_{a,1}$, reduces to just the calculation using the part of the spectrum with that amplitude $\sigma_{a,1}$ and corresponding mean stress $\sigma_{m,1}$. Consequently, if the number of cycles for the spectrum block $\sigma_{a,1}$ exceeds the cycles at the knee point N_D, the analysis becomes a straightforward comparison of just the block 1 of the spectrum with the modified fatigue limit, rendering other spectrum blocks redundant. This fact applies to all realistic values of the factor A_{ele} with respect to the total number of cycles. The algorithm uses the quantifier A_{ele} if variable-amplitude stress is applied and describes the distance between the fatigue life curve and the S-N curve. Even without explicit user knowledge by employing the calculation algorithm and treating it as variable amplitude stress, the resulting variable amplitude factor K_{BK} will be smaller than 1, in which case there is a limitation that sets the value to $K_{BK} = 1.00$. This implies that the ultimate value of the amplitude of the fatigue limit remains unchanged, contrary to possible expectations based on the calculation assessment using the maximal stress amplitude as outlined in step 6 in fig. 4.4a).

In essence, when dealing with multiple stress spectrum blocks, all characterized by cycle counts that exceed the knee point of the S-N curve, the most critical is the block of the spectrum with the highest amplitude. Consequently, safety verification should focus solely on this particular spectrum block. If the structure demonstrates safety with respect to the fatigue limit, considering the most severe spectrum block, it inherently ensures safety across all other spectrum blocks of lesser severity.

This is of special relevance considering the loads prescribed by the previously presented railway standards [1; 2], where the specified number of cycles is $1 \cdot 10^7$, while the knee point of the FAT classes S-N curves for normal stress is $N_D = 5 \cdot 10^6$ cycles [3]. However, for shear stresses, the FAT S-N curves have a knee point at $N_D = 1 \cdot 10^8$ cycles [3]. As the specified cycles in the studied railway standards have $1 \cdot 10^7$ cycles in each direction ($3 \cdot 10^7$ in total), this implies loading in the flat part of the normal stress S-N curves and in the sloped part of the shear S-N curves.

6.2 Method selection and justification

Based on the presented example of the methods available for weld fatigue analysis included in the FKM Guideline and the work procedure currently applied in the cooperating company 5M LEVIT s. r. o., a method was selected to be further explored with the aim of achieving a possible degree of automation to enhance the fatigue analysis procedure and also help identify the critical location among all welds. The following subsections include the necessary facts considered during the decision-making process.

6.2.1 Currently applied work procedure in the cooperating company

The currently applied work procedure in the cooperating company 5M LEVIT s. r. o. for the fatigue analysis of welds in thin-walled metal structures consists of five main steps:

1. The customer-provided 3D models of the structure are transformed into shell FEM model using primarily CQUAD4 elements with relatively coarse mesh in FEMAP.
2. The fatigue load cases are analyzed with defined boundary conditions and loads in FEMAP.
3. The critical location on the welds is identified from the calculated results of all load cases and the presupposed nominal FAT classes.

4. Characteristic stresses are extracted from the critical location for detailed assessment according to the FKM Guideline,
5. Calculation of degree of utilization is performed according to the FKM Guideline using the semi-automated worksheet in Microsoft Excel.

Of these steps, all, except steps 3 and 4, have been handled and perfected in the company. The analyses performed have been mainly based on the local nominal stress approach, with the analysis of only the stresses in the elements themselves. This means that an analysis of possible root cracking of fillet welds was not possible. This did not pose a problem because designs issued by customers are preemptively checked for proposed welds. In case of any fillet welds where root cracking would be a possible failure mode (e.g., not fully-penetrated fillet welds), a change of the weld design is consulted with the customer to ensure that toe cracking is the guaranteed failure mode.

So far, the identification of critical location has been based largely on a manual search between individual results from each fatigue load case in hopes of correctly identifying the critical location based primarily on the maximum stress range between all load cases while keeping in mind the corresponding FAT in that location. There was also no methodological basis for the recommended mesh size, and the stresses were usually recovered from the nodes directly on the weld line.

Based on these facts and the aim of preserving the majority of the work procedure currently applied, the following preferences were set for the method to be further explored and developed:

- utilizing shell-based FEM models with preference for quadrilateral linear CQUAD4 elements and relatively coarse mesh,
- assessing all present welds altogether, considering different assigned FAT classes for different welds,
- aim of finding potentially dangerous locations with potential of the highest DoU without direct emphasis on precise results,
- utilizing the software available and known in the company,
- emphasis on automation and relative simplicity for the user.

6.2.2 Choice of method for further exploration

Based on the presented example and the preferences mentioned for the development of an improved method, the choice was made to further explore the means of **automation for the local nominal method** of stress assessment using the shell type of elements. Apart from satisfying the mentioned preferences, this method also allows for a relatively simple way of evaluation, which appears to be possibly automatable by means already available in FEMAP itself.

This is especially true for the stress results from centroids, since FEMAP produces those as standalone result vectors. This is also true for the nodal results; there is the possibility to obtain/display the results at each node. However, the numbering of the nodes (1 to 4 for quadrilateral shell elements) does not have to be consistent. Therefore, this makes automation significantly more difficult since there is no easy way to keep track of the nodes located on the weld line or at a certain distance from it. The centroidal results also somewhat meet the demands proposed by the previously mentioned guideline DVS 1612 [23].

The choice of the local nominal method is further supported by the fact mentioned in subsection 5.4, where it was mentioned that this method is advantageous for the initial screening

of locations critical for fatigue in engineering practice. It is often the case that after the critical spot is found on the welds, the safety margin is very high (= low DoU). In such a case, the results using the local nominal method are sufficient. The application of more advanced methods would not bring significantly different results, which would crucially reduce the large margin of safety.

6.3 Research into commercially available programs employing the selected method

Based on the selected method for further development with possibilities of degree of automation, research was conducted into the software available that already implements automated evaluation methods for weld fatigue assessment. The aim was to understand the procedures implemented and the current state of the art in this field. The requirements of the software investigated were to be able to interact with FEMAP as the FEA software and to perform weld fatigue calculations according to the FKM Guideline. Not surprisingly, the programs identified to fulfill these two requirements were commercial in nature.

The two software programs investigated were LIMIT® and SDC Verifier. Time-limited trial versions of both were kindly provided by their developers for the purpose of this thesis. The following subsections provide a brief introduction of the workflow when analyzing the fatigue of welds according to the FKM Guideline using each of them. The main focus of this practical research was on the practical implementation of the local nominal method for the evaluation of weld fatigue in structures modeled by shell type of elements, since this method was selected as the method to be further explored by means of the original development. This is why the functions described in this thesis are largely narrowed down and do not cover all the capabilities of the programs, which also include a multitude of features applicable outside the narrowed scope.

6.3.1 LIMIT®

The software LIMIT® is developed by an Austrian company, CAE Simulation & Solutions GmbH. It is a commercial software tool for performing strength assessments based on stress results generated with standard commercial FEA codes. The focus of the software is on the fast calculation of degrees of utilization or safety factors against static and fatigue failure according to a wide variety of standards and regulations. [30]

The trial version 2023R001.4 provided during the writing of this thesis offered implementation of the calculation procedure only according to the 6th edition of the FKM Guideline [31]. As mentioned previously, the 7th edition is used as the main source for this thesis. As there were no significant changes between these two editions for the method analyzed, this does not pose any real concern.

The software runs as a standalone program. It does not interact directly with any FEA software, including FEMAP. Instead, it uses the files produced by the FEA programs. These files are largely a by-product of the FEA software when performing analysis. However, they include all the necessary information. For FEMAP, these files are of type .dat, which include the information about the FE model, and .op2, which include the results. Essentially, this is all the program needs as an outside input to perform a standalone analysis.

Weld identification and setup

Based on the provided FE model from the file, the program can identify possible weld locations automatically or semi-automatically based on selected method. There are various meth-

ods available, and for each weld line the program creates a "Weld Set." This set contains the respective elements and nodes belonging to that weld line. These can, of course, be created or modified by the user. The most effective method is identification based on different IDs of the shell element properties at the leading edge of the weld line. Therefore, using this method requires the user to prepare the FE model using different properties for elements even if they have the same thickness. The interface of the program with an example of identified "Weld Sets" in the FE model can be seen in fig. 6.15.

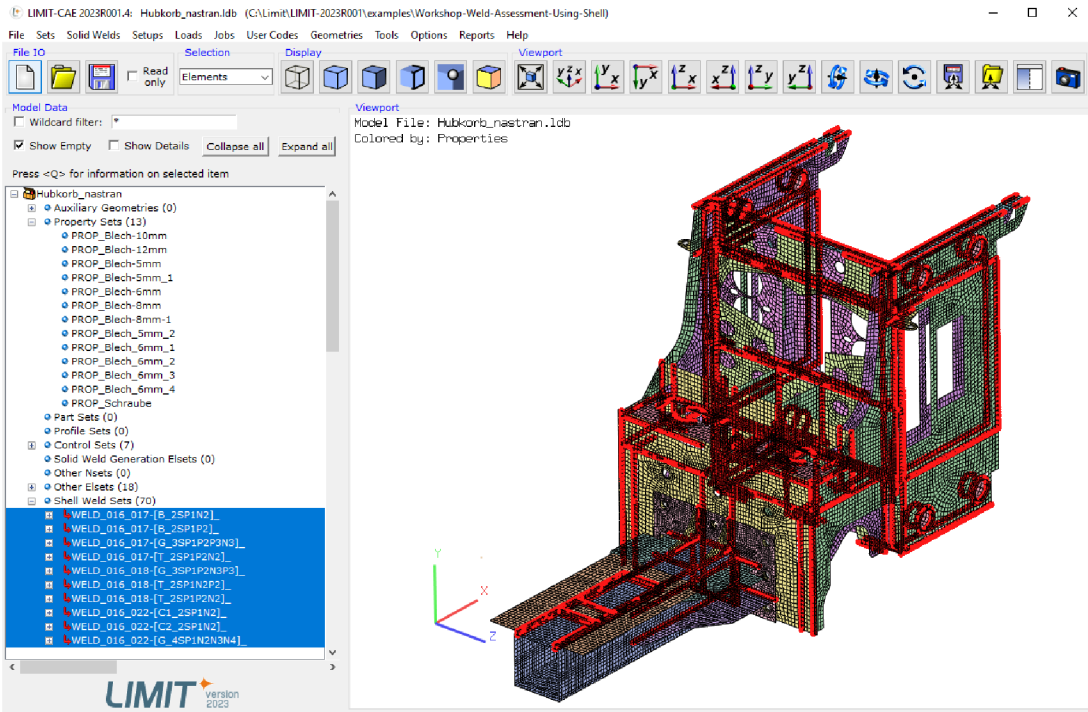

Fig. 6.15: Interface of LIMIT® with identified welds marked in red based on different property IDs in FE model containing numerous welds

What is special about LIMIT® software is the necessity to define not only the weld quality data but also the weld geometry for each "Weld Set." This is done in "Setups." The program is capable of estimating the likely weld geometry based on the topology configuration of the elements for the method of identifying "Weld Sets" based on properties. However, the user can select from a large library of prepared weld geometries, including double-sided and single-sided welds. This is also where other fatigue resistance data are entered for calculation according to the selected code for each "Weld Set." The program guides the user with the corresponding reference to the applied standard code.

It is necessary to enter a multitude of FAT values for each weld. First, there needs to be a FAT value for all three stress components of the weld – normal perpendicular, normal parallel, and shear. Second, there are also different FAT values for each location on the weld; these are marked P1 up to P6 by the program (marked depending on the selected weld geometry). For a typical example of a double-sided fillet T weld joint, these points are presented in fig. 6.16. *"The points 1 to 4 are used to calculate and assess stresses in the weld section (here the section forces and moments are used together with the relevant weld cross-section to calculate the stresses in points 1-4). Points 1 and 4 are used on the outside (toe). The points 2 and 3 are the root positions. The points 5 and 6 are toe points and use stresses with respect to the sheet material thickness (= FEM stresses)."* [22]

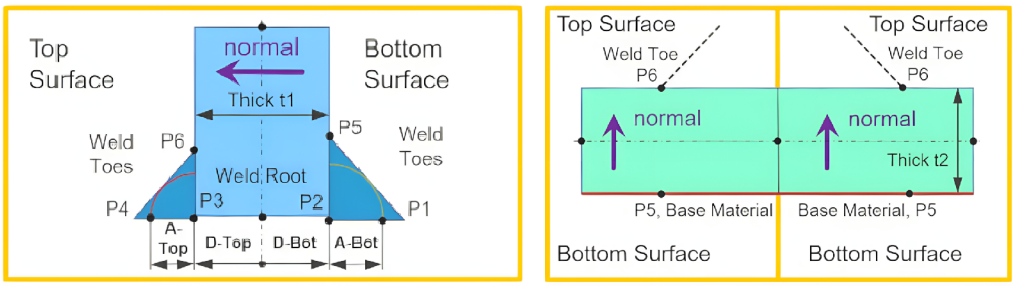

Fig. 6.16: Assessment points on the double-sided fillet T weld in LIMIT® [32]

This is how LIMIT® ultimately covers all possible failure modes using the local nominal stress assessment approach. As mentioned above, the stresses in the weld are based on the section forces and moments at the intersection of the plates. Perhaps a more interesting question is how the local nominal stresses at the weld toe are exactly recovered from the FEA results.

The solution implemented in the software is to extract the stress results in a certain distance from the weld line of the intersecting plates. The default value is set as 1.5 times the thickness of the underlying plate (as previously described in subsection 5.4). These stress results are recovered from the interpolated nodal stress results transformed into the weld coordinate system from neighboring nodes, as demonstrated in fig. 6.17 where the green points are the stress extraction points and the red points are the element nodes. This distance is set in the weld setup in terms of the "Offset" and "Endings." The "Offset" is the distance considered transverse to the weld direction, and the "Endings" lead out of the endings of the weld line. This is essentially how the evaluation differs from the approach using structural stresses in LIMIT® because another option to extract stress is from two points in prescribed distances based on IIW Recommendations [8] and perform the linearization based on the respective equation. This is just another option for the "Offset" and "Endings" implemented in LIMIT®.

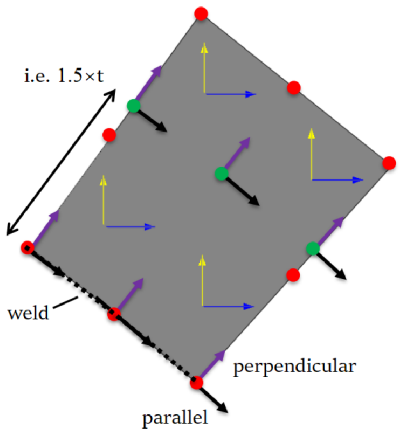

Fig. 6.17: Stress extraction points in prescribed distance on an element marked in green as applied in LIMIT®, nodes marked in red, coordinate system aligned to the weld is displayed in the points [32]

Fatigue calculation

All the calculations within LIMIT® revolve around "Jobs," which essentially represent user-defined configurations specifying the tasks to be performed and their corresponding objectives. The essential inputs for "Jobs" are "Setups" and "Loads." "Setups" have already been described. In "Loads" the user has to define which FE results are considered into analysis from

the provided results file (the file can be specified either in "Loads" or in "Jobs" in case there is only a single file including all the results in substeps). The provided FE results are transferred into "Loads," with which the user can perform operations, including creating spectra. A simple example of this procedure with two load cases from a single file is presented in fig. 6.18, other applicable options can be observed in the figure as well.

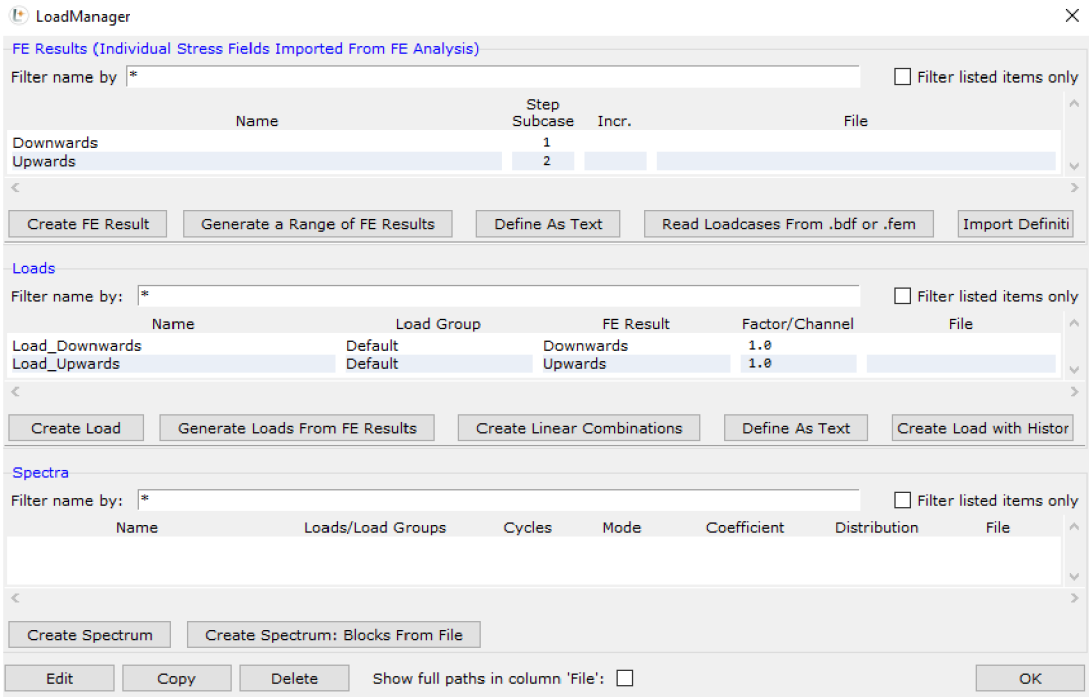

Fig. 6.18: Load Manager used for operations with FE results in LIMIT®

The "Job" setup of a fatigue analysis using "Setups," which include the identified welds and defined "Loads," can be observed in a fig. 6.19. This is where a user can select various details of the analysis (variable amplitude/fatigue limit assessment, spectrum/critical load pair, etc.). It is also where the user defines how the loaded results should be assembled and used in the calculation.

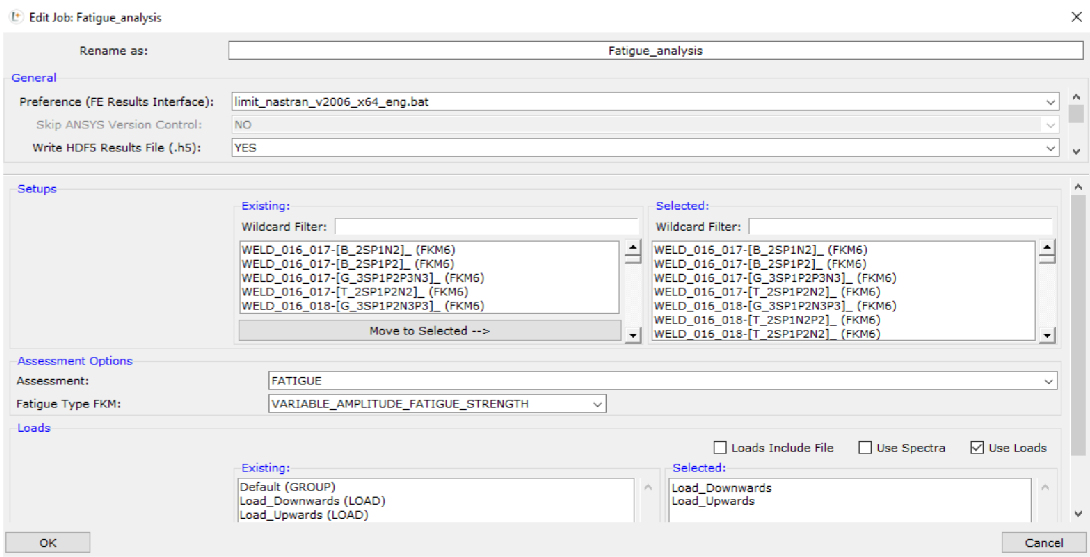

Fig. 6.19: Job setup of a fatigue analysis on defined "Setups" and "Loads" in LIMIT®

Results

The results are visually presented in a separate viewer tab of the program. When only weld elements are analyzed, the results are presented only for those elements. However, it is also possible to include the fatigue analysis of the base material elements in the same "Job" if their own "Setup" is created. The results are presented by default in terms of the maximum degree of utilization (DoU) on a colored scale. This is an understandable choice considering that the final result of the calculation using the FKM Guideline is the DoU. The DoU is presented as the maximum of all the assessment points on the weld (P1 to P6). However, it is also possible to display the results for all elements for each of the points separately. The spot with the highest DoU is the critical spot of all welds. The software also allows easy identification of spots with DoU greater than 1.0 by adjusting the color scale to a maximum of 1.0 and marking everything above in a distinctive pink color. An example of such a result of weld fatigue analysis using the program is presented in fig. 6.20. Additional analysis of results on specific elements is possible.

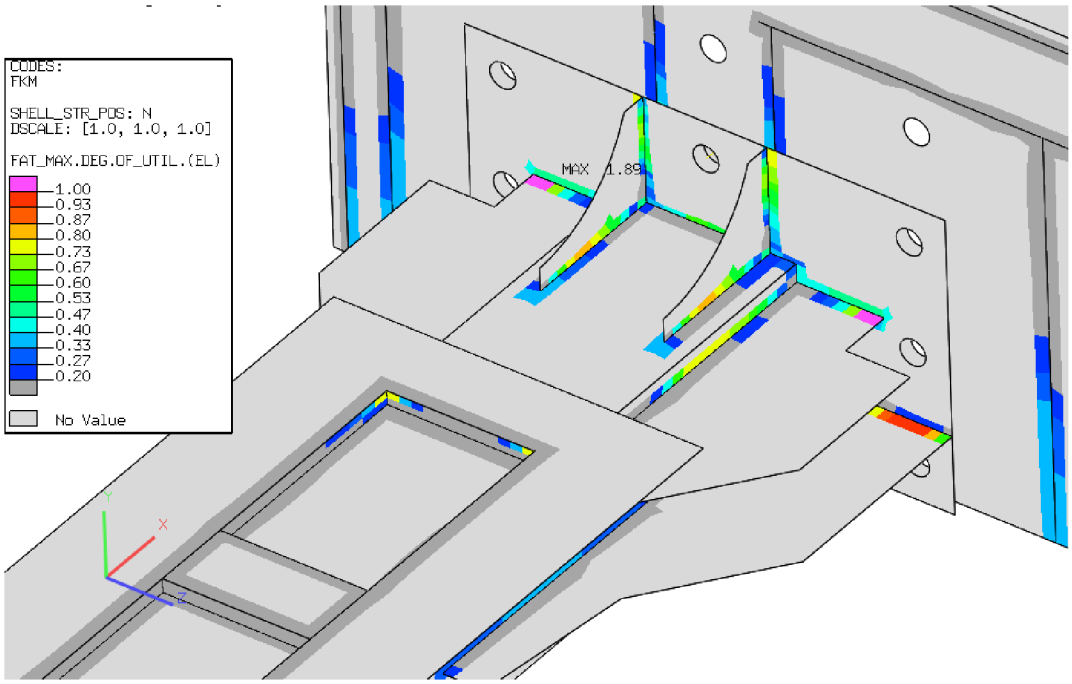

Fig. 6.20: Detail of a contour result of elemental DoU displayed on elements belonging to the welds (element edges not displayed for clarity) in LIMIT®

6.3.2 SDC Verifier

SDC Verifier is a commercial FEA and code verification software with multiple capabilities and a large library of industry standard design codes for verification. Its main goal is automating repetitive and routine tasks using the tools and features implemented. It is developed by a company with offices in the Netherlands, Ukraine, and Poland. [33]

The provided version of the program (2023 R2) did not have the 7th edition of the FKM Guideline. The 6th edition [31] was used for practical research purposes; however, the key components of the evaluation are the same between the sixth and seventh editions, as already mentioned. The version of the program 2023 R2 is described in this thesis.

The software is based on a direct interaction between the program itself and the FEM software used, in this case, FEMAP. All the outputs and data produced by the FEM software

can, therefore, be loaded by the program directly without the need to handle external files by the user. However, this also means that the corresponding FEM software must be running on the same computer during the use of the SDC Verifier. This is also why there are separate versions of the SDC Verifier for each FEM software. There is an option to run the program in a separate window or inside the FEM program itself, which allows for easier manipulation, as can be observed in fig. 6.21 with the identified welds of a component.

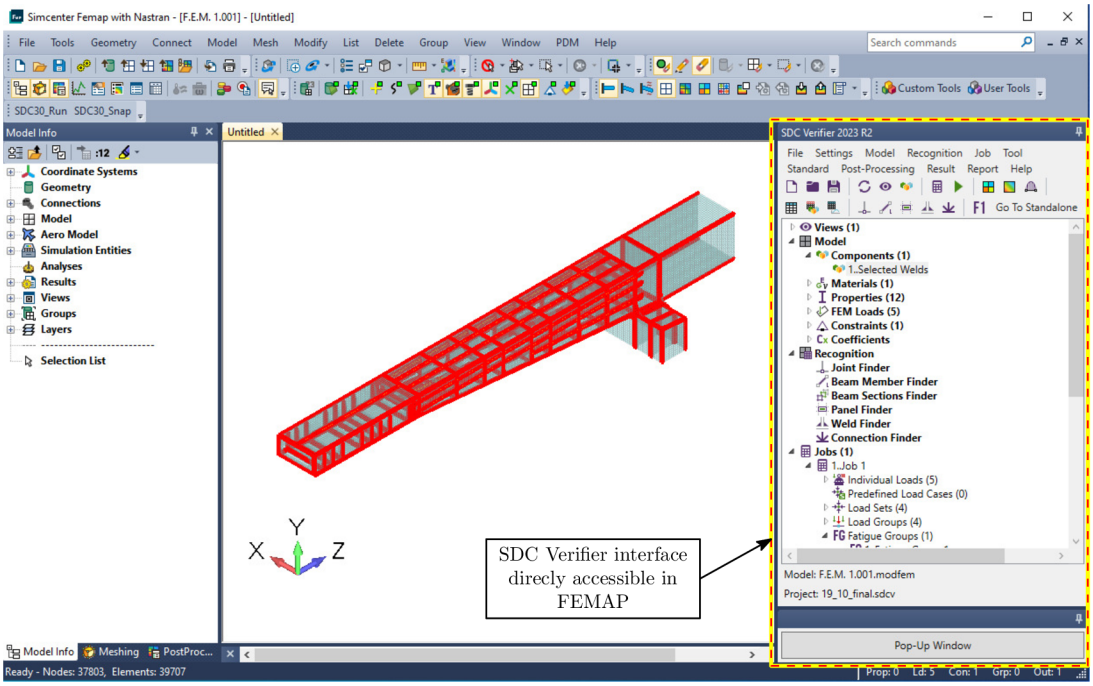

Fig. 6.21: User interface of SDC Verifier directly within the interface of FEMAP during weld analysis

Weld identification and setup

SDC Verifier utilizes a tool called "Weld Finder" for the identification of possible welds. The search of welds is performed based on different property IDs of neighboring elements or the angle between elements of the same property. The general settings for the "Weld Finder" can be observed in fig. 6.22.

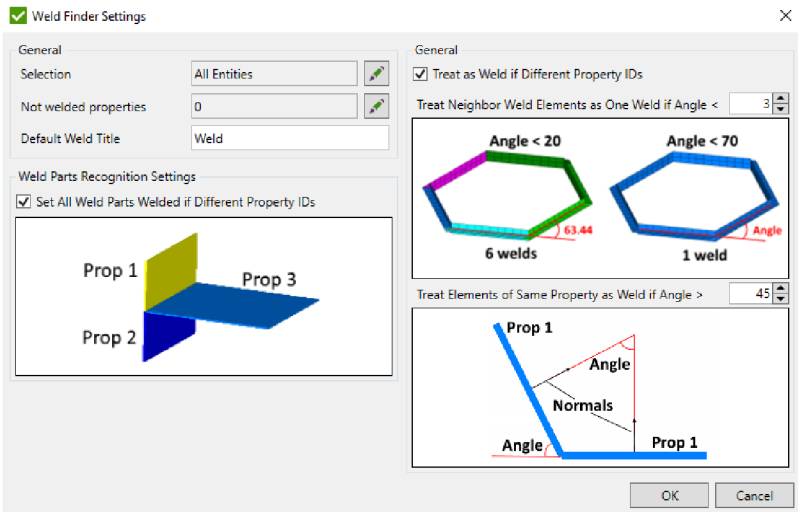

Fig. 6.22: "Weld Finder" settings in SDC Verifier

The actual geometry of the found welds can be set; however, this is used only in static calculations and omitted for fatigue calculations. In case a hot-spot stress assessment is used, the stress extraction distances can be set in this section of the calculation procedure.

Fatigue calculation

The next essential step is selecting the calculation code from available "Standards" – in this case, FKM (6th, 2012). Based on the selection, the user is prompted to fill in all the necessary details for the calculation, including all the values of the selected constants, choices from tables, and also FAT values of elements, as can be seen in fig. 6.23. The program allows the user to set FAT values for all identified welds or to select specific welds based on some selection methods. The FAT values must be set for each stress component. Different FAT values can be set specifically for elements at weld intersections. However, based on testing, it appeared that all elements of the model need to have a set FAT value, not just the weld belonging elements, but also the base material elements. It is also noteworthy that the FAT values are set specifically to elements. Another noteworthy fact is that the whole table in fig. 6.23 needs to be filled before any calculation. This means that even for a very specific task, such as just evaluating the fatigue of welds, all the other constants need to be filled, even if they do not contribute to the specific task.

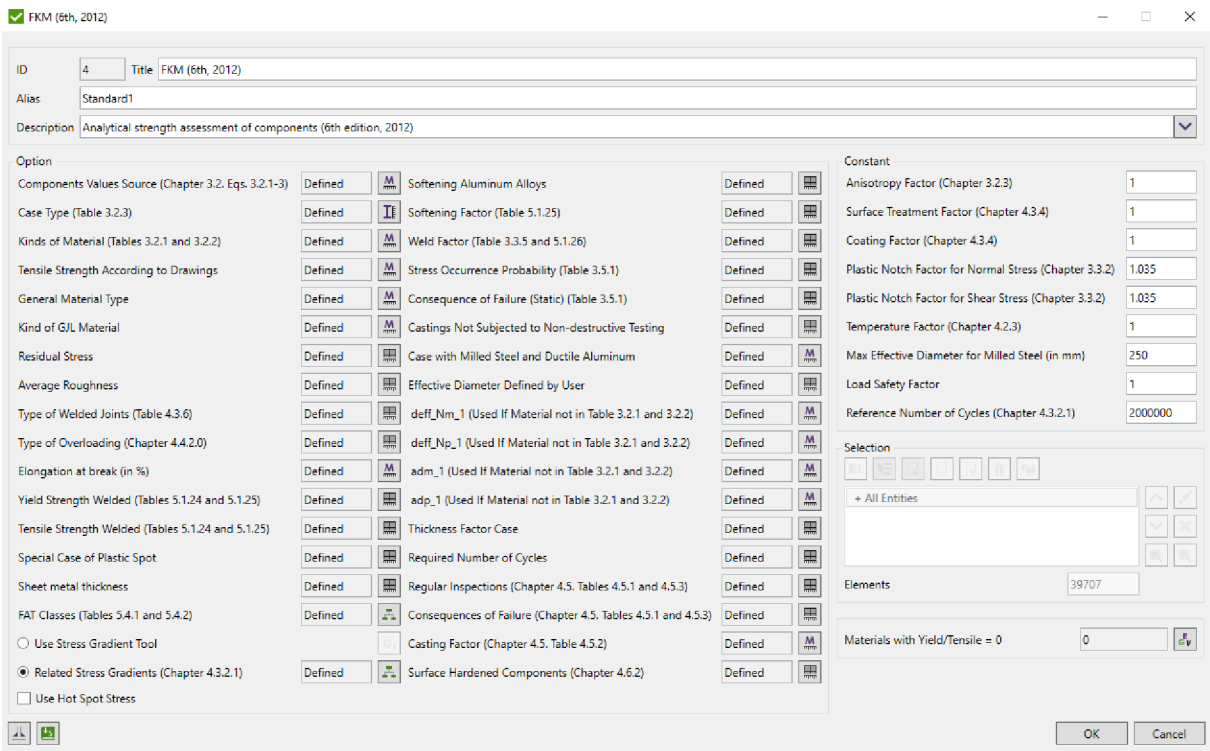

Fig. 6.23: "Standard details" to be filled in by the user in SDC Verifier

The calculations are performed in the "Checks" section of the "Standard" selected. The "Checks" can produce contour data for plotting and tables. The only other input for "Checks" not yet mentioned are loads which are included in the "Jobs" section. The loads can be based on the defined loads in the model; there is no need to actually have calculated results from an analysis. The program can run its own analyses based on the user-defined inputs. "Individual Loads" can be assembled into "Load Sets," "Load Groups" and "Fatigue Groups."

"Load Sets" are sets of "Individual Loads" acting simultaneously. "Load Group" is an en-

velope for "Individual Loads," "Load Sets," and other "Load Groups." It allows the program to determine the minimum, the maximum, and the absolute values of the stresses, the displacements, the forces, etc. [34] "Fatigue Groups" is an envelope of the "Load Groups" and their stress history (amount of cycles for stress range) which is used in fatigue standards. Their inputs are therefore "Load Groups" and their respective number of cycles [35].

This means that for evaluation using variable stress amplitude, a spectrum needs to be defined using a "Fatigue Group" consisting of multiple "Load Groups." However, only the maximum and minimum are considered from each "Load Group" even if there are more than two "Load Sets."

Fatigue "Checks" available for the FKM Standard in SDC Verifier are either constant amplitude or variable amplitude (called "Fatigue Summation").

Results

The analysis is performed based on direct user request of a contour plot, table or another output from a specific "Check," e.g., requesting plot of a utilization factor (used as an equivalent term for degree of utilization in SDC Verifier). The program runs all necessary analyses on its own while mentioning progress in the Messages window of FEMAP. It may be important to emphasize that running fatigue "Checks" with applying the FKM as the standard used, took relatively long time (order of minutes) even for not so large models compared to some other standards tested.

The standard output is the utilization factor plot. This can be done for welds separately. However, from the limited amount of testing, it seemed that the program always runs the analysis on all elements. As the program only assigns FAT values to elements, it essentially does not understand anything about weld geometry. This is why it produces a utilization factor for the top and bottom of the plates separately. An example of a result of fatigue analysis on weld elements is shown in fig. 6.24. Other outputs can also be observed by the user.

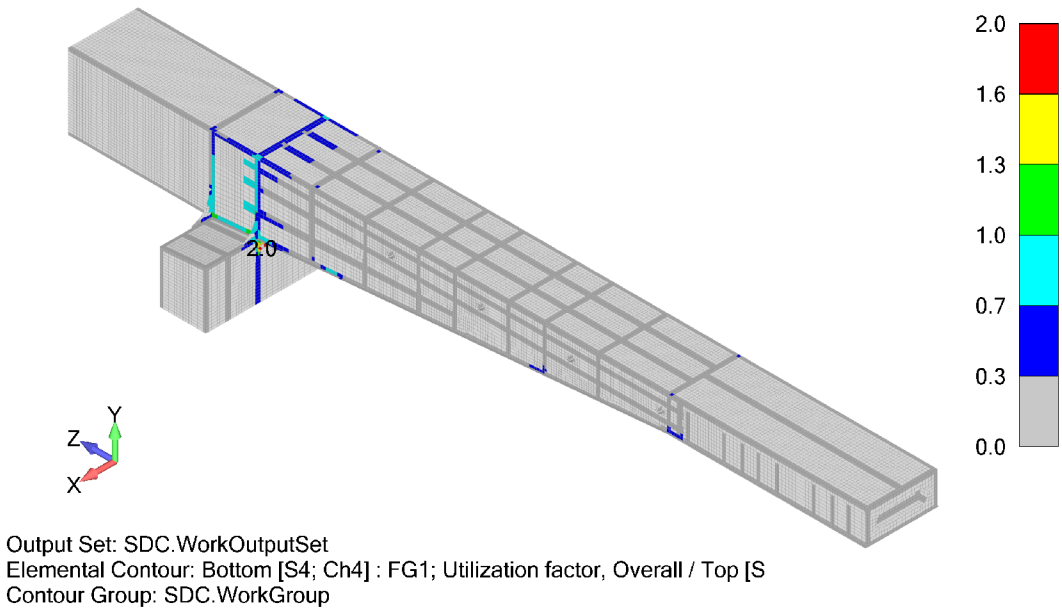

Fig. 6.24: Overall utilization factor on weld elements produced by SDC Verifier in FEMAP

6.3.3 Commercially available programs summary

Because of the commercial character of the programs presented, their direct implementation in the work procedure would not align with the requests of the cooperating company 5M LEVIT s. r. o. and the thesis goals. Implementation of these programs would not only employ entirely new software to the current work procedure, but mainly licensing of the software would bring significant financial cost to the company, which would most likely not return considering the size of the company and the limited number of customer orders that would require this newly licensed program. The licensing costs are not publicly available and, therefore, not mentioned here.

Based on research into the functionality of the programs presented, it can be said that both of them approach the analysis of potentially critical spots on the welds of the structure by running an aggregate analysis according to the algorithm of the standard used on all the weld elements. The critical location is then the one with the highest DoU. However, there are a few notable differences between the programs, mostly in terms of the complexity of the analysis.

LIMIT® analyzes all potential failure modes of welds, which is why the definition of the weld geometry is necessary and utilization at each potential failure point is calculated. Fatigue resistance data can be set for each weld separately, with different FAT classes for each point on the weld. The transformed stress at the weld toe is based on the specified offset distance approach with methodological origin in DVS 1612 [23].

On the other hand, the SDC Verifier is based on only assigning FAT values to the weld elements themselves. The stresses are only transformed into the weld coordinate system, and, therefore, the utilization is also based on transformed FEM stresses. However, for the evaluation of potentially critical locations, this may still be satisfactory. This applies especially if the focus is on failure modes that are covered by analysis using FEM stresses (not root cracking of fillet welds).

Although both programs allow the user to automatically generate reports about the completed analyzes automatically, this is not really reasonable for use in practice in the cooperating company where the reports already have a more or less standardized format. This standardized format of reports also includes the MS Excel worksheets, which have already been mentioned. By including them in the reports, customers can check the calculation parameters and variables in the critical location. Neither of the programs can convey this comprehensively for the selected critical location.

6.4 Original program development

Following an examination of commercially available software solutions, it was decided to develop custom software to emulate some of their key functionalities. Although custom-made methods may not replicate the full range of features offered by commercial options, this limitation is not overly concerning, as long as they can still serve the purpose of severely lowering the total work effort and providing reliably obtained results. Ultimately, the newly developed methods can be tailored to fit the currently employed work procedure.

After thorough evaluation of the available programming options in terms of their complexity, utility, and integration within FEMAP, as the FE software used, the decision was made to implement the new methods using the FEMAP API. Developing an entirely new external software would have significant disadvantages. First, the interaction with FEMAP would only be possible using the result files produced by FEMAP during the analysis, similarly to how LIMIT® works. Manipulation with the files can be regarded as quite bothersome. This option

would also require developing all the components of the program from the very beginning.

In contrast, programs developed using the FEMAP API integrate seamlessly with FEMAP itself. This integration allows for the utilization of existing components within the FE software. Consequently, the end user may not even realize that an externally developed tool is being used, as the user experience is essentially the same as that of using FEMAP in general. This seamless integration also streamlines the learning process as the user is already familiar with the structures, dialog windows, and options of the FEMAP user experience.

6.4.1 FEMAP API

To better understand the decision process behind the choice of FEMAP API, this subsection serves as a very brief introduction to its basic functions. For a more in-depth introduction, the original sources [36; 37] may prove useful as they go into greater detail. For even more details, the FEMAP API Guide is recommended, which is provided as part of the FEMAP installation.

FEMAP API is a Microsoft Windows OLE/COM-based programming interface and is object-oriented programming. The abbreviation API stands for "Application Programming Interface," which means that the written code is not part of FEMAP, but it is instead a program that is directly interacting with FEMAP. Essentially, every action that would be performed manually by the user by either clicking or entering data can be written as an API code. The native language of the API is Visual Basic (VB) and other commonly used languages are VBA and WinWrap. The VB code acts as traditional code, i.e., as a set of instructions, and it makes requests of the API, which acts upon those requests by either retrieving or putting things into FEMAP, which is essentially just a database holding and displaying data. It may be helpful to think of these three things as separate entities, as can be seen in the scheme in fig. 6.25. All functions based on the VB language itself are also available to the programmer, such as *for* and *while loops*, *if statements*, etc., as well as other basic programming functionalities. [36]

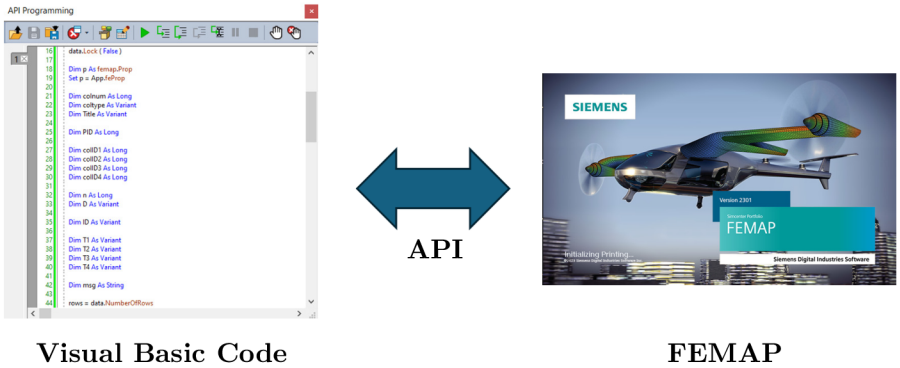

Fig. 6.25: Scheme of interaction between the VB code and FEMAP as database via the API

The main advantage of the FEMAP API is the ability to perform repetitive or tedious tasks using the code rather than manually performing them. The other option for automating a repetitive task, also integrated in FEMAP, is a "Program File," which is a recorded macro of the performed tasks. However, this option does not allow user interaction, which may be often necessary [36].

As the FEMAP API uses Visual Basic as an object-oriented language, objects are the foundation stone of the code. Objects found in FEMAP API are divided into three categories [36]:

- FEMAP Application Object,
- FEMAP Entity Objects,
- FEMAP Tool Objects.

FEMAP Application Object is essential for creating other objects; it can provide access to the FEMAP Graphical User Interface (GUI), menu options, performing operations, etc. FEMAP Entity Objects are used for manipulating entities. For every entity, there is a separate object (nodes, elements, loads, etc.). FEMAP Tool Objects are a special class of objects that provide functionality that is not stored in the model database. The most commonly used object of this category is the "Set Object." Other examples include "Data Table," "Results Browsing Object," etc. All of these objects have two types of capabilities. The first are "Properties," which describe information about the objects. The second are "Methods," which provide a way of interacting with an object. [37]

The anatomy of a basic FEMAP API program consists of:

- defining objects,
- dimensioning variables,
- performing operations using "Properties" and "Methods" on objects.

Defining objects is necessary to even be able to perform "Properties" and "Methods" on them. Dimensioning variables is necessary in VB programming in order for the program to know what data type the variable is before it is used in the program. The "Methods" have a standard syntax of **rc = object.method(inputs, outputs)** and there can be multiple inputs and outputs for each method. The left-hand side of "rc" is commonly used and stands for "Return Code." It is optional, so there is actually no need for the method operation to have a left-hand side. The left-hand side corresponds to the success in executing the method. If it was successful, -1 is returned. If it is not successful, something else is returned, depending on what went wrong. On the other hand, for "Properties," the left-hand side is the output, so the standard syntax has the form **propertyValue = object.property**. [36]

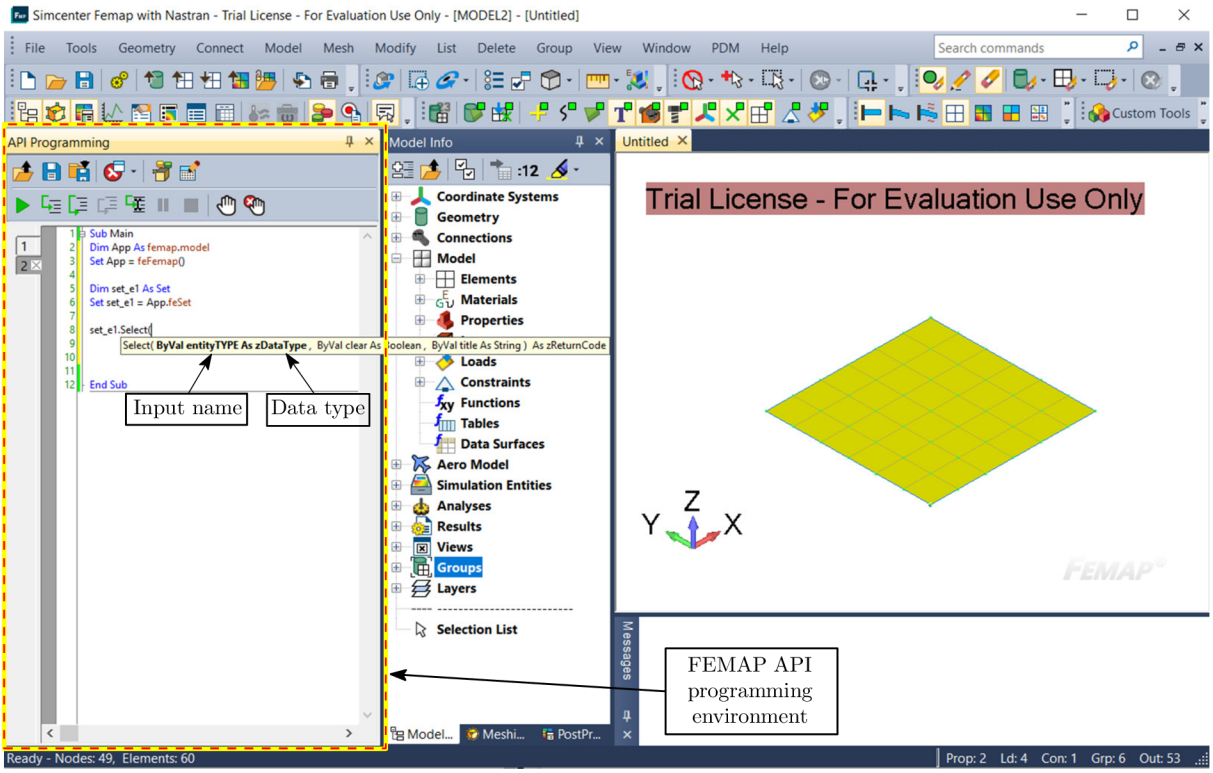

Fig. 6.26: Display of the API programming environment in a running FEMAP session

FEMAP comes with a built-in API programming environment. This environment uses a WinWrap flavor of Visual Basic, and it can be used to write and run API programs directly.

This is especially beneficial when developing new code, as it allows for straightforward interaction between currently edited code and its performed actions on the currently attached model database of FEMAP. The editor also sets out colors for different parts of the commands for easier navigation in the code. The interactive pop-up can also guide the programmer with the suggested input/output name in the command definition and the required data type. This can be seen in fig. 6.26 in the mentioned FEMAP programming environment. However, the standard procedure for learning to use the individual commands is usually accompanied by the FEMAP API Guide for the corresponding version of FEMAP used. The guide includes a description of each command, input and output names and data types, possible return codes, and, in some cases, also examples.

However, using only the examples included in the guide is often not sufficient, as most commands do not have an example. In these cases, alternative online sources may be necessary. In spite of that, since FEMAP API programming is a very specialized field of programming, the number of online discussions and sources involving specific issues is also very limited. This can often make understanding and learning new commands difficult and time-consuming.

Ultimately, the biggest source of functional API programs is included within the installation of FEMAP and it is available directly to the user without even implying that there is a code in the background. This is done via the function "Custom Tools," which is a set of API programs provided by FEMAP developers. These can be accessed, read, and even edited by the user. They can be accessed from the location of the FEMAP installation folder. This also implies an easy way to "install" new API programs, simply by copying them into the respective folder. The agreement between the groups of API programs and the corresponding folder can be seen in fig. 6.27. The API programs can be turned on directly from the "Custom Tools" menu of FEMAP, so there is no necessity to access the code whatsoever by the end user.

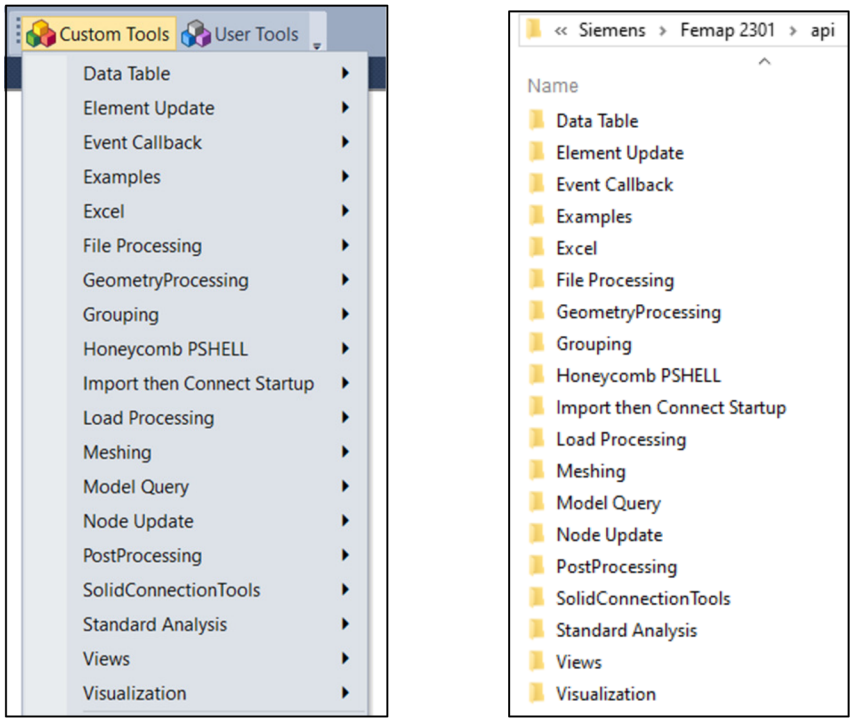

Custom Tools available in FEMAP

Folder <FEMAP install>\api

Fig. 6.27: Custom Tools menu based directly on the corresponding folder where FEMAP was installed

6.4.2 Developed methods and their integration within work procedure

Three FEMAP API programs were developed in a way that is directly aligned with the current work procedure in the cooperating company. In this way, the already functioning parts of the procedure do not have to be changed. The functionality of the API programs is inspired by the commercially available programs described previously, thus following the verified procedures. However, certain simplifications had to be applied due to the limitations of FEMAP itself and the limited available time for development. These simplifications will be mentioned in the following descriptions of the individual API programs.

The implementation of the three FEMAP API programs in the fatigue analysis procedure is visualized in the scheme in fig. 6.28. The three individual programs are colored green in the scheme. The division into three programs is intentional and logical. Running the three programs as one single program, requesting all inputs from the user in a single run, would be overly complicated and prone to repeated exits without running the full procedure of the calculation.

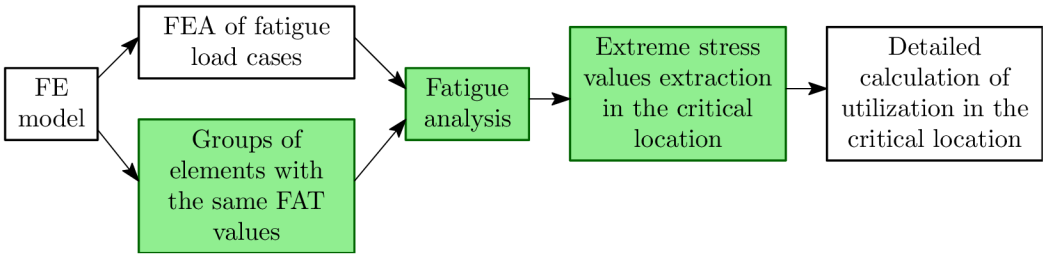

Fig. 6.28: Outlined work procedure scheme with the implemented FEMAP API programs highlighted in green

The total length of code of all three programs combined adds up to over 1 500 lines. All programs developed as part of the work on this thesis are provided in the external Appendix B of this thesis for free use and potential editing as open source. Each program is saved as .BAS file (Visual Basic Source Code). This file can be read and edited in practically any source code editor; however, the FEMAP API coding environment is recommended for the reasons mentioned previously.

The programs were coded in FEMAP version 2301 (released in 2023) and therefore follow the procedures and code syntax according to the FEMAP API Guide 2301 [38]. Backward compatibility should be guaranteed to version 2020.1. This is a version where the numbering and structure of the vector output was changed in FEMAP [38]. This also led to the implementation of Version 2 (V2) of multiple commands related to Output Vectors and post-processing. These V2 versions take as input the new ID numbers related to the Output Vectors, which are also displayed in the new versions of FEMAP starting from the mentioned version 2020.1. While the old versions of the commands, which take as input the old Output Vector numbering, are still available, they are not recommended to be used and by default produce a user warning. This was acknowledged, and V2 of these commands was used in all cases. The forward compatibility of future versions of FEMAP is not guaranteed. However, as long as the syntax of the commands used is kept identical, the programs should be functional in future versions of FEMAP as well. Possible minor changes in the command syntax can be relatively easily compensated for by modifying the codes according to the changes. Modifications to the code are also possible with the goal of achieving slightly altered functionalities. The codes were provided with comments for easier navigation and understanding of the purpose of their individual parts. This may help to make slight alterations even without a deeper understanding of the exact syntax of the code.

The programs were rigorously tested and should be functional without errors. Exception handling was implemented for expected incorrect inputs and events. Good programming practices were followed during the development of the programs to improve their processing time and make them easier to read and follow. The internal "Methods" of the FEMAP API were used, if possible, to avoid coding loops that could be solved by a single "Method" command. In some instances, repeating the same or almost the same parts of the code can be found in the programs. This was caused largely by unavoidable situations where it was necessary for the functionality of the program or when repeating the same part was more understandable and does not significantly slow down the processing time. In some instances, it may be possible to find a more elegant code solution, especially with a deeper understanding of all the available commands included in the FEMAP API Guide. However, considering the still-limited scale of the project and the limited time available for development, these possible flaws in the field of programming should be acceptable.

Installation of the developed API programs to FEMAP is very easy, as mentioned previously. The folder with the .BAS provided in Appendix B can be directly copied to the "api" folder of the FEMAP installation and immediately becomes available to the user in the "Custom Tools" menu as visualized in fig. 6.27. Alternatively, this can also be done for the "apiuser" folder, which has to be added in the same FEMAP installation folder and becomes available in the "User Tools" menu. Finally, it is also possible to add it via the "Add User Tools" in the "Custom Tools" menu or the "User Tools" in the drop-down menus directly in FEMAP.

As the fig. 6.28 suggests, the three individual API programs are interconnected in terms of functionality. In other words, the functionality of one of them depends on the output produced by the previous one. The functionality of each of the programs is described in detail in the following subsections. As the API programs ultimately utilize the functions available to the FEMAP user as well, the outputs of each of the programs can be achieved or modified manually if the function is understood correctly by the user. In some cases, this may be beneficial; however, in the majority of situations, this would bring a lot of additional tedious work.

6.4.3 FE model preparation

Due to the explicit preference for the methods to be applied, the developed programs are limited exclusively to plate elements, which is a Nastran name for elements in other FE programs known as shell elements (two-dimensional elements with assigned thickness as parameter). The preferred element type in the company is generally the linear quadrialteral shell element CQUAD4. Most of the time, meshing the whole model with just this type of element is not always possible, and a certain number of triangular elements CTRIA3 is present. The use of linear elements should also be beneficial in lowering the effects of potential singularities in FE models. However, the developed methods are not limited to linear elements and work for quadratic elements (CQUAD8, CTRIA6) as well.

The programmed fatigue calculation is based on the elemental stress results and therefore the stresses from the centroids of the elements. In this way, the stress results are taken at a certain distance from the nodes on the weld line, as described in DVS 1612 [23]. To align with the guideline DVS 1612, the recommended mesh size should be between 2 and 3 times the thickness of the base plates; this way, the centroids should be approximately at the distance 1 to 1.5 thickness of the plates. This mesh size and stresses from centroids are therefore a combination of knowledge gained and described throughout previous sections of this thesis, the combination of coarse mesh and stress extraction in a certain distance. In addition, it also fulfills the preferences of the cooperating company.

In this way, the influence of singularities is filtered out by using a coarse mesh. How-

ever, the potential flaw may be in capturing the stress gradients perpendicular to the welds, as previously mentioned in 5.4. The details of the effects of the mesh size and element type in relation to stress extraction in centroids could potentially be the subject of further studies. At this time, the mesh size recommendations are supported by the facts mentioned throughout the thesis. Additionally, the welds themselves are not expected to be in the FE models, and the connections are expected to be at the mesh level. Therefore, the location of the weld toes might very well be near the actual location of the element centroid in terms of perpendicular distance from the nodes connecting the surfaces. There are two reasons for this. First, the shell element model only considers the thickness of the plates as a parameter for computation without representing it in the model. Second, the geometry of the weld itself extends from the surface of the plate. Considering these two facts, the weld toe is actually located admittedly further from the nodes representing the weld line and nearer the element centroid for reasonable configurations of weld geometries.

For a mutual comparison of stresses between elements, the centroids used for stress extraction must be at a somewhat similar distance from the node line. This might not always be easy, especially for irregular geometries. If the location of the centroids changes significantly between elements (changing element size or geometry), it is recommended to enforce the creation of the desired element size and shape by splitting the surfaces in the distance that corresponds to the aimed mesh size. This can be relatively easily achieved in FEMAP using the "Offset Curve/Washer" tool in the "Curve – From Surface" menu and enforcing mapped meshes on the surfaces. An example of the desired mesh achieved by splitting the surface in prescribed distance can be seen in fig. 6.29.

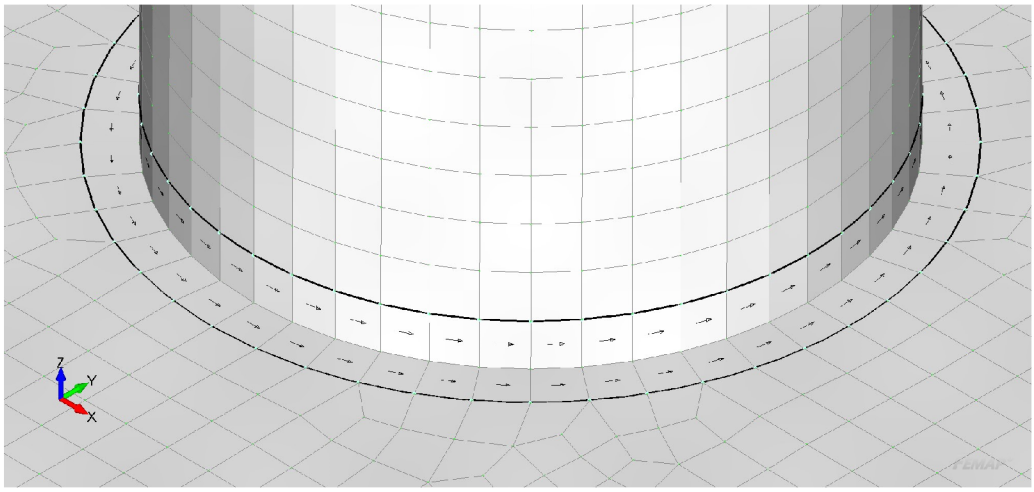

Fig. 6.29: Example of curved geometry where the black highlighted offset curves allow creation of elements with consistent elements size (centroids approximately represented by arrows of material coordinate system)

Optionally, weld lines may be meshed with rod type of elements. These elements, which are tension-compression-torsion elements (also commonly called "link" elements in other FE programs), should have an insignificant cross-sectional area compared to the thickness of shell elements. Therefore, they will not affect the relevant FEA results. When weld lines are meshed with these elements, the automatic mesher attaches them to existing nodes of the plate elements. These intentionally non-influential elements serve a purpose in the first API program for creating FAT groups of elements. Due to their one-dimensional nature, they can be used to orient the material coordinate system of the plate elements according to the adjacent rod elements. This functionality is particularly useful for cases where the underlying geometry

will eventually be deleted, which often occurs in very large models. In such scenarios, the presence of geometry may slow down operations and manipulations in FEMAP. It may also be advantageous when multiple welds of the same type are present in the structure, and the individual element properties may also be used as unique identifiers of the weld types. More detailed information on this is available in the following subsection.

6.4.4 FAT groups of elements API program

The first API program, which can be found in Appendix B as a file called **Create FAT Groups.BAS** is used to create groups of elements with three objectives:

- identifying elements with the same FAT values for the three evaluated stress components,
- assigning the residual stress level,
- orienting the material coordinate system of the elements to align with the orientation of the weld.

It takes its inspiration from commercial program procedures, where the program identifies potential weld locations, and the user has to assign the fatigue resistance data based on the standard used. The assignment of values to the actual elements is similar to the implementation in SDC Verifier. The automatic identification and classification procedure for weld locations is not implemented in the API program. Due to the limitations of API programming, the thinkable implementations would not bring significant improvement of the work procedure since they would still require a lot of user action.

Therefore, the user is directly required to identify the locations of the welds and the corresponding elements that belong to the welds. However, this process is streamlined using automated tools in the API program. After running the program, a dialog window opens, which can be seen in fig. 6.30. There are four options to choose from. When selecting one of them, a loop of the selected method is started, so the user can continue to create groups using the method until the loop is terminated.

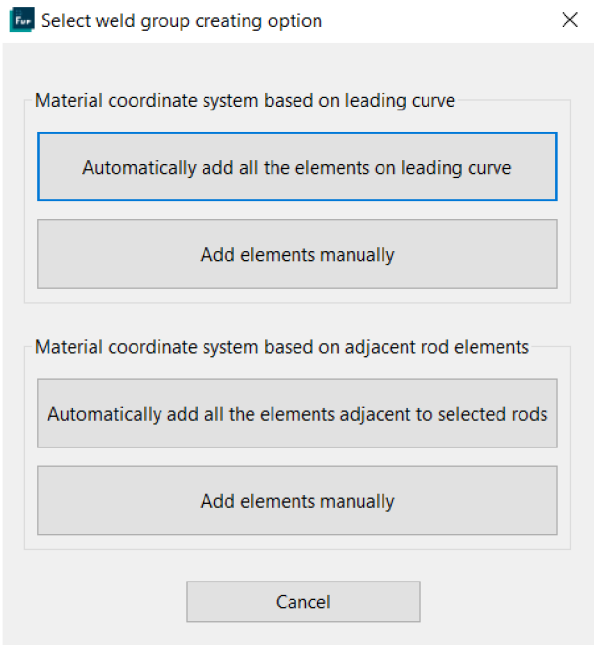

Fig. 6.30: User dialog menu for selecting the method of creating FAT groups of elements

The four methods can be split into two categories, as outlined in fig. 6.30. The first category uses the identification of elements and the orientation of the material system based on curves and, therefore, on the underlying geometry. The second category uses the identification and orientation of the coordinate system of the material based on rod elements in the model. These were mentioned in the previous subsection. For each of the categories, there are two methods – one where the selection of elements is automated and the other where the elements have to be selected manually. With this variety of methods, the user should have enough options for most configurations, where the easiest and fastest option can be chosen and used.

When the method of "Automatically add all the elements on leading curve" is selected, the user has to select only a curve in an already meshed model. The API program identifies all the nodes belonging to that curve and, based on those, all the elements on the curve. Since this identification may not result in a completely desired selection of elements, the user can see the pre-selected elements and modify the selection manually with prompted element selection menu. Based on the selected curve and the selected elements, the algorithm modifies the material coordinate system based on the orientation of the curve. The process of modifying the material coordinate system based on the orientation of the curve is based on an API program that uses this routine by Pich and Fricke [39].

After the successful modification of the material coordinate system of elements, the user is prompted with a dialog menu. This menu is used to enter the most essential fatigue resistance parameters, the FAT values for the three stress components, and the level of residual stresses, as can be seen in fig. 6.31. These should be entered using the information in the FKM Guideline. As mentioned previously, this procedure runs in a loop of curve selection, possible element selection modification, and entering FAT values until the loop is terminated in any step. It should be emphasized that the procedure is based on selecting only one curve at a time. Therefore, it is not possible to select multiple curves at once. The process of using curves with the "Add elements manually" method is the same; however, the elements have to be selected manually, and there is no automated selection based on belonging to the curve. The selection between the two methods should be based on what appears to be more beneficial and less work-intensive.

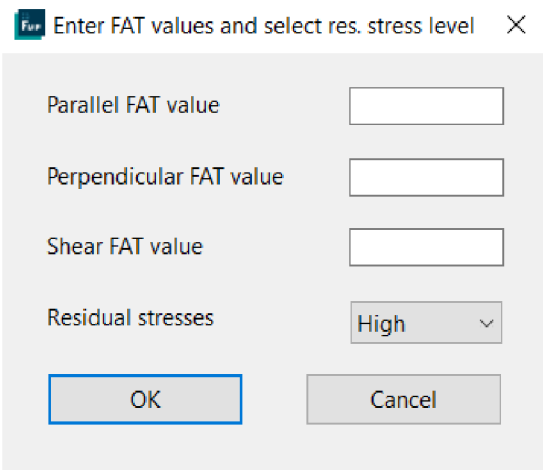

Fig. 6.31: User dialog menu for entering FAT values and residual stress for a group of elements

The method of "Automatically add all the elements adjacent to selected rods" utilizes the already mentioned rod elements of insignificant stiffness in the model. After selecting this method, the user is prompted with an element selection menu. In that menu, all the rod elements that are desired to be used for creating a new group should be chosen. For each rod

element, the algorithm finds all the plate elements that have exactly two of the same nodes in the element definition. This means that the rod element that lies on the edge of a plate element can be used to modify the material coordinate system of the plate using the orientation of that rod element in the global coordinate system. This also means that plate elements that do not have an edge on the weld line, and therefore only one shared node with the rod element, cannot be identified using this method. Fig. 6.32 shows a simple example of eight plate elements, of which only some share the edge with a rod element; consequently, only those are assigned the material coordinate system using this method. In addition, modification of the selection of the plate elements is not allowed using this method, since there should be no accidental identification of elements that do not belong to the weld line. If the user wants to handpick the specific plate elements, the method "Add elements manually" should be used instead.

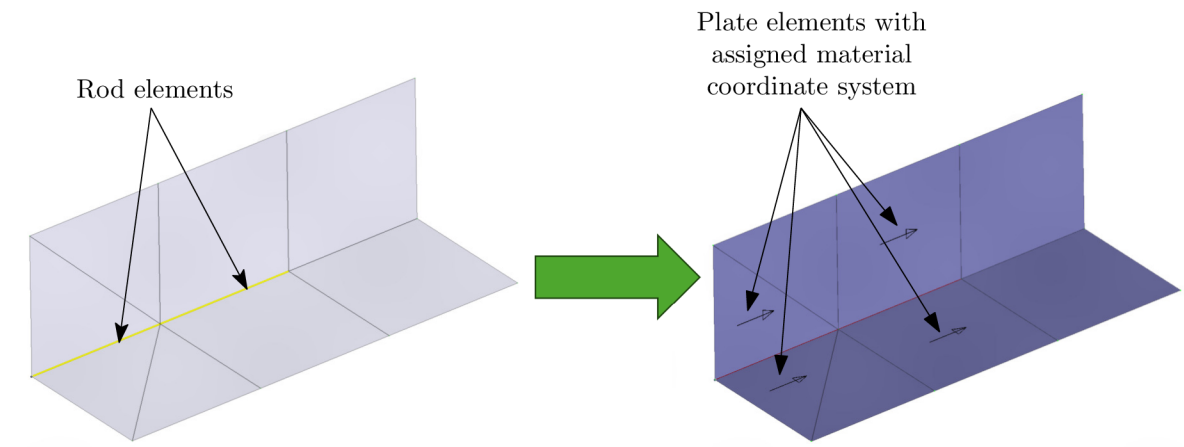

Fig. 6.32: Simple example of plate type of elements that are assigned the material coordinate system based on shared edge with the rod element

Despite the selected method, after the successful identification of the elements and subsequent modification of the material coordinate system, the dialog menu as in fig. 6.31 always follows. The method "Automatically add all the elements adjacent to selected rods" is especially beneficial if careful preparation of the model is performed beforehand by assigning different rod element properties based on the type of weld in that location. In this way, the groups can be created with really only a few clicks and with an absolute minimum number of groups.

All four methods result in the same output; therefore, they are interchangeable, and all of them can be used in this step of the procedure. The result of each run of the mentioned methods is elements with a modified material coordinate system added to a common group. The title of the group is used as a carrier of information on the FAT values and the residual stresses of the elements in it. The format of the title of the created group is "FAT parallel value, FAT perpendicular value, FAT shear value, letter indicator of the residual stresses". The example of such a formatted title is therefore "100, 71, 80, M", where M stands for "Moderate" selection of residual stresses.

Groups are an integral part of the FEMAP work procedure. This means that groups can also be modified using all available operations. Elements can be added or deleted, the title can be changed, etc. However, when performing these manual modifications, special care should be taken to comply with the rest of the calculation procedure. For example, when adding new plate elements into groups, the material coordinate system should also be assigned correctly based on the weld orientation. The titles of the groups should strictly follow the mentioned formatting. The API program that follows in the procedure will not accept any other formatting.

6.4.5 Fatigue analysis API program

The second program in a file called **Fatigue Analysis.BAS** in Appendix B is the core of the whole procedure. It uses two obligatory inputs and one optional one. These are:

- Output Sets as results from analyses of the individual fatigue load cases,
- Groups of plate elements with assigned orientation of material coordinate system and formatted titles of the group carrying the FAT values and the residual stresses level,
- number of cycles for calculation of the ultimate stress range (optional).

The API program runs through elements in each group with a properly formatted title and assigns the elements the respective FAT values for each stress component in the database. If any element is present in multiple groups, the assigned FAT value is based on the title that enters the algorithm last: the group with the highest ID (likely the last one created), and the user is notified about this. The same applies to the assigned residual stress level. The program also applies the current orientation of the material coordinate system. Therefore, if an element could belong to potentially two weld lines, special attention needs to be paid.

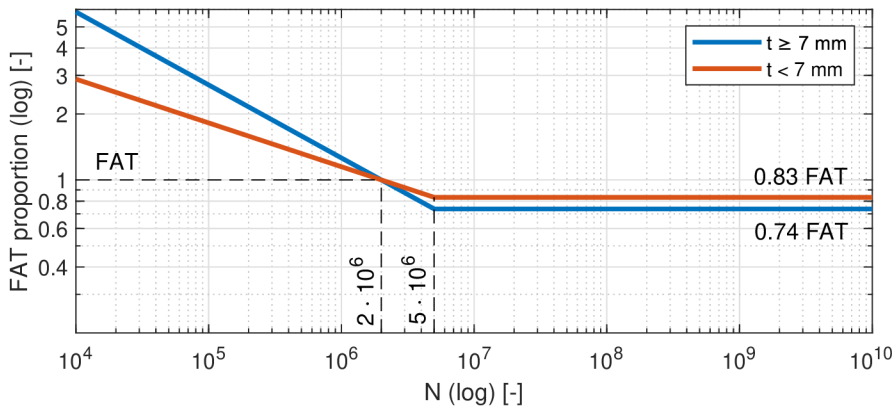

a)

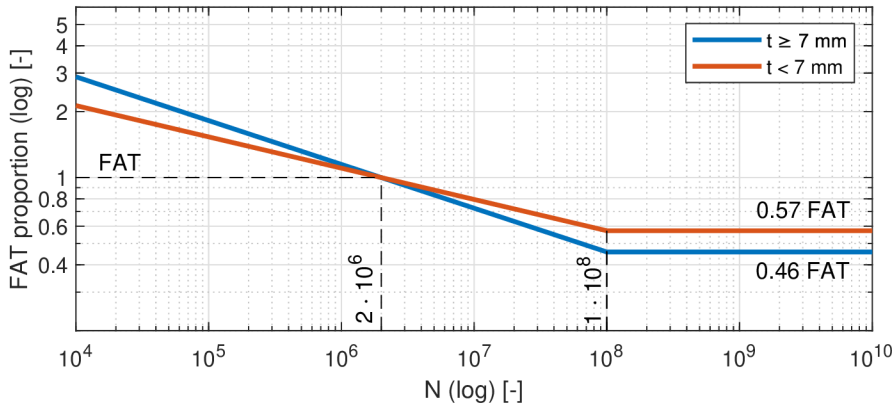

b)

Fig. 6.33: Proportion of the FAT value based on the number of cycles to failure as defined in [3] for a) normal and b) shear stress depending on plate thickness

Based on the number of cycles entered, the program calculates the ultimate stress range (fatigue strength) according to the definition of the FAT S-N curves in FKM [3]. If the user leaves the dialog window empty, the FAT values are used as the ultimate stress range, which corresponds to the stress range at $2 \cdot 10^6$ cycles. If a valid number of cycles ($\geq 1 \cdot 10^4$) is entered, the corresponding ultimate stress range is calculated according to the definition of

the FKM [3] that also considers the thickness of the plate elements, as the definition of the S-N curves is different depending on the thickness of the plate. The API program extracts the thickness from the model for each element and adjusts the calculation of the ultimate stress range accordingly. The visualization of the proportion of FAT value (ultimate stress range divided by FAT) depending on the number of cycles to failure N can be seen for the S-N curve in fig. 6.33 depending on the plate thickness.

FEMAP does not operate directly with units. Therefore, throughout the calculation procedure, the program works in a system of FEM-consistent units common to mechanical engineering by considering dimensions in millimeters and stresses in megapascals. The thickness of plates is therefore expected to be in millimeters, and the stresses are also expected to be in megapascals, since the stress ranges applied for determination of the FAT classes are in megapascals. In the case of using a different system of FEM consistent units, the work procedure needs to be adjusted accordingly, and the code also needs to be modified. Additionally, other modifications of things that would deviate from the currently coded definitions from the 7th edition of the FKM Guideline [3], such as the definition of S-N curves (e.g., number of cycles at knee point), can also be relatively easily adjusted in the code if necessary.

The actual fatigue analysis of the program runs according to the scheme provided in fig. 6.34. The figure demonstrates the analysis only for the top side of the elements for the sake of clarity. The bottom side is analogical. With respect to the FKM Guideline, the calculation is performed according to the maximal amplitude assessment with consideration of overload case F2 (consideration of the constant stress ratio R) [3] as this overload option is the most widely applied in practice.

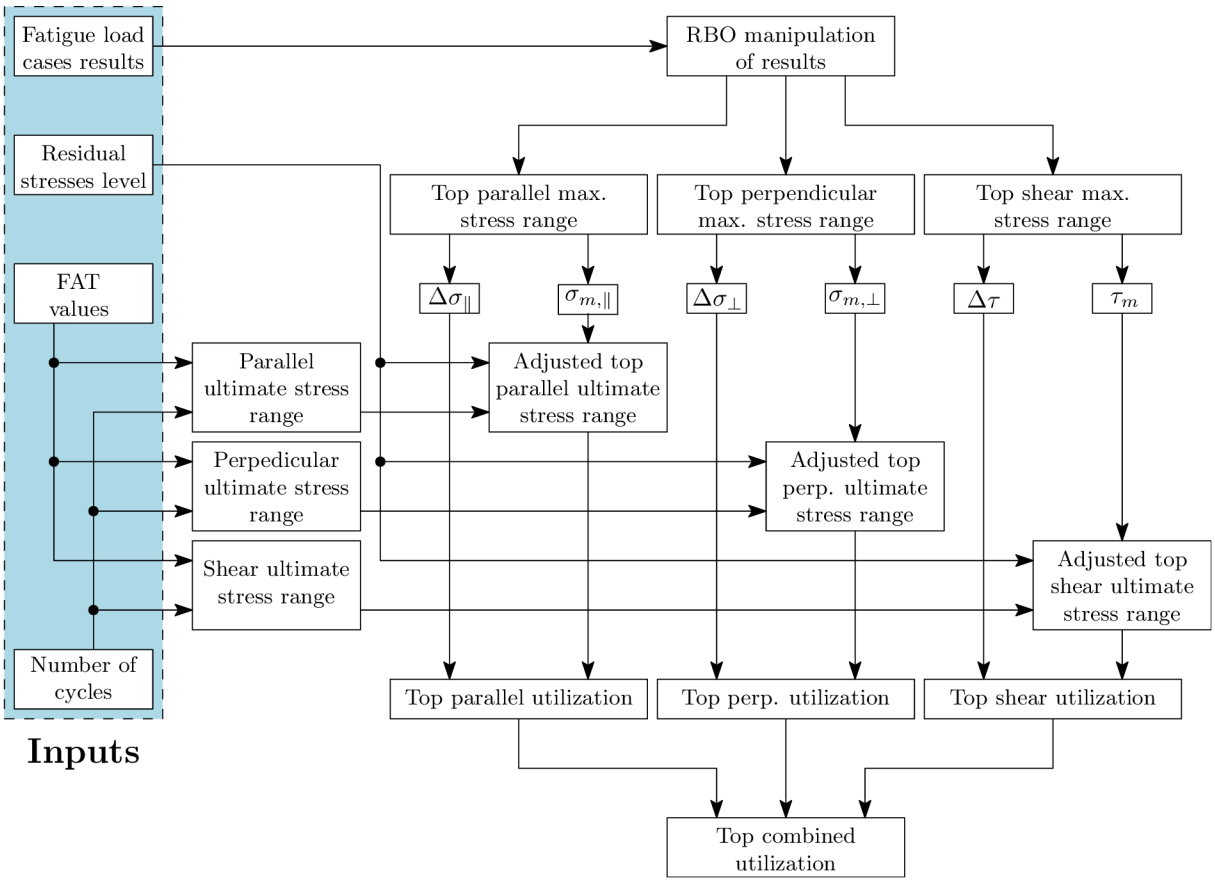

Fig. 6.34: Fatigue analysis program functional scheme running in parallel on each element, only evaluation for top shown for clarity

The key part of the analysis scheme is "RBO manipulation of results." RBO stands for "Results Browsing Object," which is a special FEMAP Tool Object used specifically for manipulation of analyses results and post-processing. In a very basic principle, RBO is just a table where columns are added by commands of the API. Multiple commands can then be used to extract the relevant data from the RBO and output it in various ways, including creating an entirely new Output Set. More details on the practical use of RBO can be found in [40]. The program utilizes RBO in the following way:

1. Add specific Output Vector (e.g., Top X Normal Stress) from all the selected Output Sets into columns of RBO.
2. Transform data in columns of RBO into the material coordinate system.
3. Create maximum envelope column.
4. Create minimum envelope column.
5. Extract and save maxima, minima, and IDs of Output Sets where they originate for each element.
6. Clear RBO.

By the process of transformation into the material coordinate system, the original stress components become the stress components in the necessary orientation with respect to the weld orientation. The list of these stress components and the stress components they become through transformation consists of:

- Top X Normal Stress → Top Parallel Normal Stress;
- Top Y Normal Stress → Top Perpendicular Normal Stress;
- Top XY Shear Stress → Top Shear Stress;
- Bot X Normal Stress → Bot Parallel Normal Stress;
- Bot Y Normal Stress → Bot Perpendicular Normal Stress;
- Bot XY Shear Stress → Bot Shear Stress.

Some solvers additionally produce Output Vectors with different IDs because they perform non-linear analysis. The program does not operate with those and always considers the Output Vectors in the list above.

The presented enumerated process of utilizing the RBO has to be performed for each of the stress components separately, this is why the RBO has to be cleared after extracting the necessary results for each stress component. This is because the commands finding envelope results approach the RBO as a whole table of numbers blindly without understanding where they originate from, and therefore adding results from different stress components would not be meaningful. The API should also not use more than one RBO at the same time unless necessary to efficiently use computer memory [40]. This is why just one RBO is recycled throughout the whole program.

The goal of finding the maxima and minima for each element is to find the largest possible stress range between all load cases. Arguably, this can result in a stress range between load cases which do not form an expected stress cycle together. However, since the standards of the railway industry presented [1; 2] do not describe the succession between the fatigue load cases, it is possible to regard them as randomly ordered with a prescribed number of occurrences. In such a case, the rainflow analysis of the stress history would result in a spectrum, where the largest stress range would be formed by the envelope maximum and minimum of the stress history. Therefore, this extracted stress range is on the conservative side of the whole calculation.

Using the maximum stress range extracted between load cases, the corresponding mean stress is calculated. Together with the residual stress factor and the mean stress effect, the

adjusted ultimate stress range is calculated for each stress component on the top and bottom of each element. As the effects of mean stress are different depending on residual stresses, knowledge of residual stresses is necessary. Based on the adjusted calculated maximum stress range and the identified maximum range, the corresponding approximate cyclic DoU for each stress component can be calculated by a simple division separately for the top and bottom of the element. Based on the calculated utilization for the three stress components, the combined cyclic DoU on top and bottom of each plate element is calculated separately. This is also visualized in fig. 6.34. The formula used to calculate the combined DoU is based on the formula provided in FKM [3] in a form

$$a_{BK,\sigma v} = \frac{1}{2}\left[\left|a_{BK,\sigma_\perp} + a_{BK,\sigma_\parallel}\right| + \sqrt{\left(a_{BK,\sigma_\perp} - a_{BK,\sigma_\parallel}\right)^2 + 4 \cdot a_{BK,\tau}^2}\right], \tag{6.5}$$

where $a_{BK,\sigma v}$ is cyclic DoU for combined loading, $a_{BK,\sigma_\perp}$ is a cyclic DoU for perpendicular stress, $a_{BK,\sigma_\parallel}$ is a cyclic DoU for parallel stress and $a_{BK,\tau}$ is cyclic DoU for shear stress. However, this formula applies only in the cases of proportional or synchronous stresses, which is the worst case possible. Generally, the maximum stress ranges extracted by the algorithm do not have to originate from the same load case couples. However, since the use of this formula is the most conservative option, the results of the combined DoU using this formula will always be equal to or higher compared to the combined DoU values of the actually possible combinations of the load cases.

In addition, the use of this formula requires the consideration of signs for the degrees of utilization of normal stresses. The sign should be considered on the basis of the actual signs of identifying load cases responsible for maxima or minima in the cycle, minus for compression and plus for tension. For example, considering a load case where $\sigma_\perp$ is in its maximum in tension and $\sigma_\parallel$ is in its minimum in compression, $a_{BK,\perp}$ would be substituted with positive sign and $a_{BK,\parallel}$ with negative sign in equation (6.5). Taking into account the absolute value and the second power in the equation, formula (6.5) takes one of two forms, depending on the situation of the signs. In the case of substituting both with the same sign, the equation takes a form

$$a_{BK,\sigma v} = \frac{1}{2}\left[a_{BK,\sigma_\perp} + a_{BK,\sigma_\parallel} + \sqrt{\left(a_{BK,\sigma_\perp} - a_{BK,\sigma_\parallel}\right)^2 + 4 \cdot a_{BK,\tau}^2}\right]. \tag{6.6}$$

On the other hand, in the case of substituting the different signs of the normal stresses, the equation takes a form

$$a_{BK,\sigma v} = \frac{1}{2}\left[\left|a_{BK,\sigma_\perp} - a_{BK,\sigma_\parallel}\right| + \sqrt{\left(a_{BK,\sigma_\perp} + a_{BK,\sigma_\parallel}\right)^2 + 4 \cdot a_{BK,\tau}^2}\right]. \tag{6.7}$$

The result of $a_{BK,\sigma v}$ from (6.6) is always larger than or equal to the result of (6.7). The results are the same for $a_{BK,\tau} = 0$. The inequality can be visualized in a 3D plot as can be seen in fig. 6.35 for a non-zero value of $a_{BK,\tau} = 0.5$ as an example. The formula implemented in the API program is, therefore, (6.6), to approach the calculation from a conservative standpoint without explicit consideration of signs.

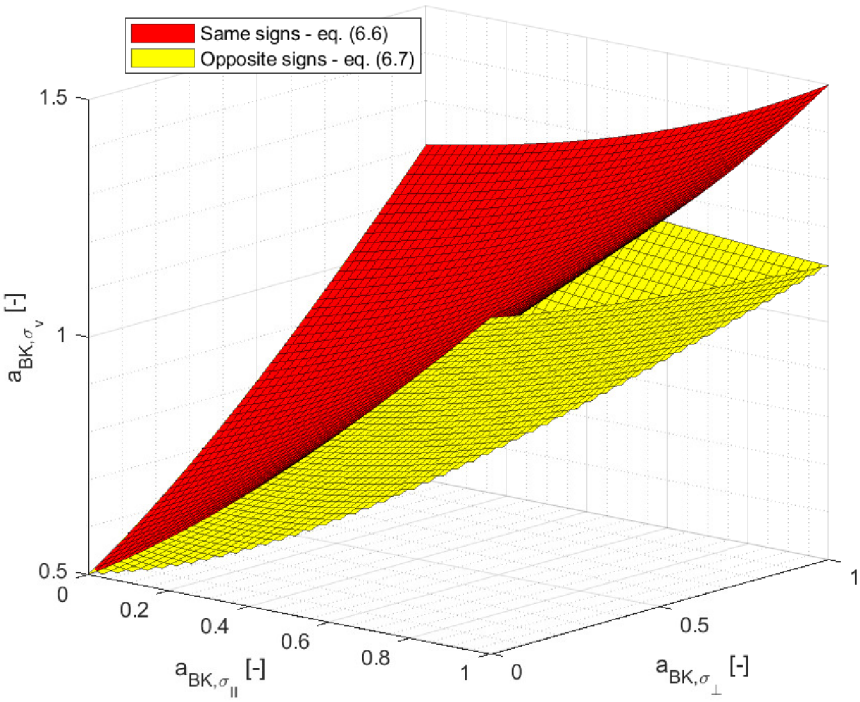

Fig. 6.35: Comparison of results of the equation for combined cyclic DoU for cases of the same signs and different signs (plotted for $a_{BK,\tau} = 0.5$)

The results of the API program are saved in the database as a new Output Set with the name "Weld Fatigue Analysis." The output of the program is, except for approximate combined DoU for the top and bottom sides of the weld elements, also other results; these can be seen in a selection list in fig. 6.36 and include all the relevant results which the user could possibly want to observe for a deeper understanding of the combined DoU results. Each of the results can be observed directly in the FE model.

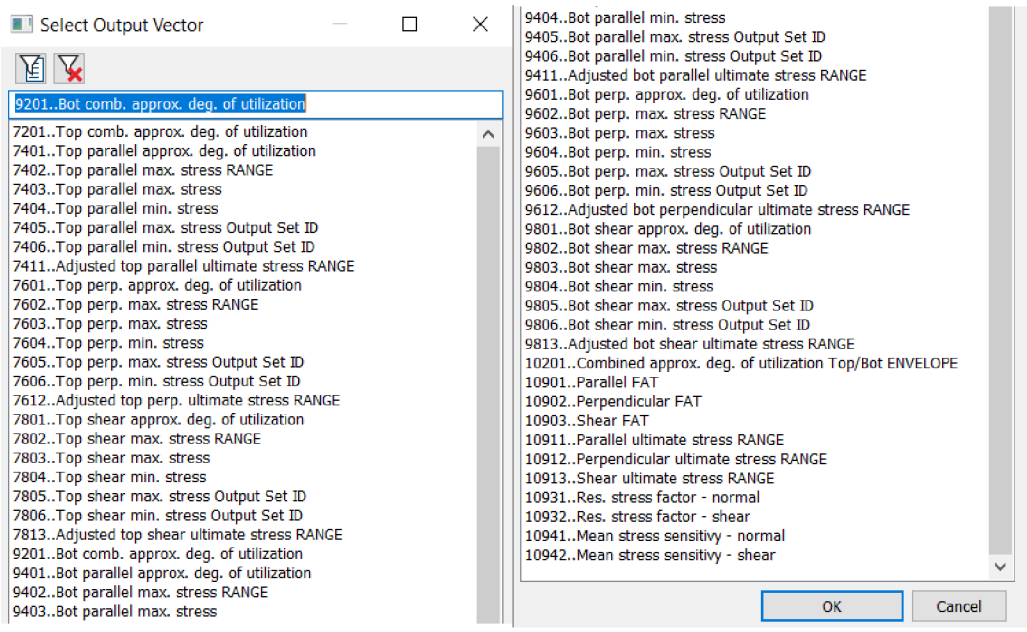

Fig. 6.36: List of Output Vectors with their IDs produced by the API program as displayable results

It is also possible to check the input of the fatigue resistance data that the program assigned based on the provided group titles. The result vectors have IDs assigned from the series 7 000, 9 000, and 10 0000. The series 7 000 and 9 000 are chosen specifically, since FEMAP allows for a display of "Double-Sided Contour" using these IDs, where the series 7 000 belongs to the top side and 9 000 to the bottom side. Therefore, the user can visualize the specific results of the analysis for both sides of the plate element without having to switch the display or having to understand which side is which. This option is turned on by default by the API program. It is up to the user to judge whether the top or bottom side of the element should be further analyzed with respect to the actual location of the welds in the structure. The default output view option is without averaging between elements. Since the whole analysis is based on results from the centroids, averaging between elements is not meaningful.

The location of the highest combined approximate cyclic DoU marks the critical location of all analyzed welds. If there are more locations with similar high values of the highest combined cyclic DoU, they mark potential candidates for the most critical location.

Since the calculations performed by the API program are largely just manipulations of vectors and the number of factors influencing the results is minimized, they take a very short amount of computational time. In addition, the analysis runs only on the elements present in the groups entered as input. Therefore, even for considerably large models with a limited number of elements entering the analysis, the remaining elements do not slow down the calculation by being redundantly analyzed.

Arguably, this whole calculation procedure takes a few shortcuts compared to the full calculation procedure described in FKM [3] and compared to the commercial programs described in section 6.3. There are multiple factors that potentially modify the values of the allowed ultimate value of the fatigue stress range in the FKM Guideline, e.g., influence of thickness, surface treatment, etc. There are two main reasons why these are not considered in the program procedure. The first reason is the limitation of the available storage of information about the welds. Since fatigue resistance data must be stored in the actual titles of the groups, there is limited space to store information. Furthermore, searching for specific values of the additional factors that modify the fatigue resistance values for all welds can be very time-delaying without significant influence on the mutual results between elements. Simply put, for most cases, it is unlikely that factoring in all the additional factors would cause such a significant influence on utilization results between elements that would entirely change the critical location compared to the presented simplified algorithm for the usual use cases.

Based on these facts, simply assigning the FAT values, residual stress level, and number of cycles reduces the procedure of assigning fatigue resistance data to an absolute necessary core that still produces fundamental results for mutual comparison of utilization between all the weld elements. Additionally, using the simple and understandable format of the title of the groups in terms of only the FAT values and the residual stress indicator allows easy checks and potential modification by simply renaming the groups.

It should be emphasized that the results of this API program should still serve mainly for the identification of the critical location. The detailed calculation using the extracted stresses is aimed at being performed by the semi-automated MS Excel worksheets that are already an established part of the work procedure in the cooperating company. The factors mentioned that are not included in the API program that still influence fatigue resistance are considered during that process, so they do not get left out completely.

As the calculation procedure utilizes the mentioned choices based on the desire to stay on the conservative side of the results, it is possible to consider these choices later. If they result in too high results of cyclic DoU, the steps taken can be additionally analyzed to possibly bring down the calculated result of combined DoU. This applies especially in cases where the

actual stress conditions might bring down the combined cyclic DoU into acceptable results compared to conservative choices taken. However, in such cases of high results of DoU the accuracy of the local nominal method should be additionally considered, as it may not be sufficiently reliable, and the found critical location should be analyzed in more detail, e.g., using the hot-spot method.

6.4.6 Stress parameters extraction from the element surface API program

The third program called **Stress Parameters Extraction.BAS**, which can also be found in Appendix B, serves as a handy tool for extracting the necessary stress parameters from the element surface, namely the maxima and minima for each stress component and the respective Output Set IDs where they originate from. The program runs as follows:

1. User selects an element.
2. User selects an element side – top or bottom.
3. Data Table of the stress extremes and their originating Output Sets IDs is displayed.

Using this API program, the process of extracting the necessary data from the element of interest is significantly streamlined. Although the program is expected to be used mainly for the extraction of stress extremes from the identified critical location or candidates for the critical location, the selection of the element is entirely up to the user. To help the user with additional identification of the desired element side – top or bottom, arrows pointing up in the direction of the element normal matching the top side are displayed during the selection. The list of Output Vector data is then displayed in a Data Table from which it can be easily exported or copied. The list of vectors is different depending on the selection of the element side. The overview of results pushed to the Data Table for the selected element is listed in table 6.3. Using this API program enables the user to extract the stress results necessary for detailed fatigue analysis using the automated MS Excel worksheets.

Table 6.3: Overview of results pushed into Data Table

Top/Bot		
Parallel max. stress	Perp. max. stress	Shear max. stress
Parallel min. stress	Perp. min. stress	Shear min. stress
Parallel max. stress Output Set ID	Perp. max. stress Output Set ID	Shear max. stress Output Set ID
Parallel min. stress Output Set ID	Perp. min. stress Output Set ID	Shear min. stress Output Set ID

7 PRACTICAL PRESENTATION OF THE DEVELOPED METHODS

The developed programs and the full enhanced fatigue analysis of welds procedure are chronologically presented in this chapter on an industry-inspired component, which is a welded bracket mounted to the train vehicle frame. The inspiration for the shape of this component was found in a similar bracket. Its purpose was attaching a functional component of significant mass to a frame of a railway vehicle of type P-II according to ČSN EN 12663-1 [1] as a passenger vehicle combined with a power unit. The bracket, which served as an inspiration, was previously problematic in terms of searching for the critical location for weld fatigue, and therefore it was a suitable example for demonstration.

The bracket analyzed was made up of three separate plates made of aluminum alloy type EN AW-5754 H24 with a thickness of 5 mm. Fig. 7.1 shows the complete welded bracket in yellow. The main dimensions are marked in millimeters. The figure also displays the position of the center of gravity (COG) of the attached functional component. The assumed component mass was 8 kg. This component would be attached to the bracket via eight bolts. The bracket itself would be connected to the vehicle frame by four bolts. The frame of the railway vehicle was considered to be made of steel, and the flange thickness was 15 mm. In the fig. 7.1, the frame is represented just by the flange of the carrying I-type profile.

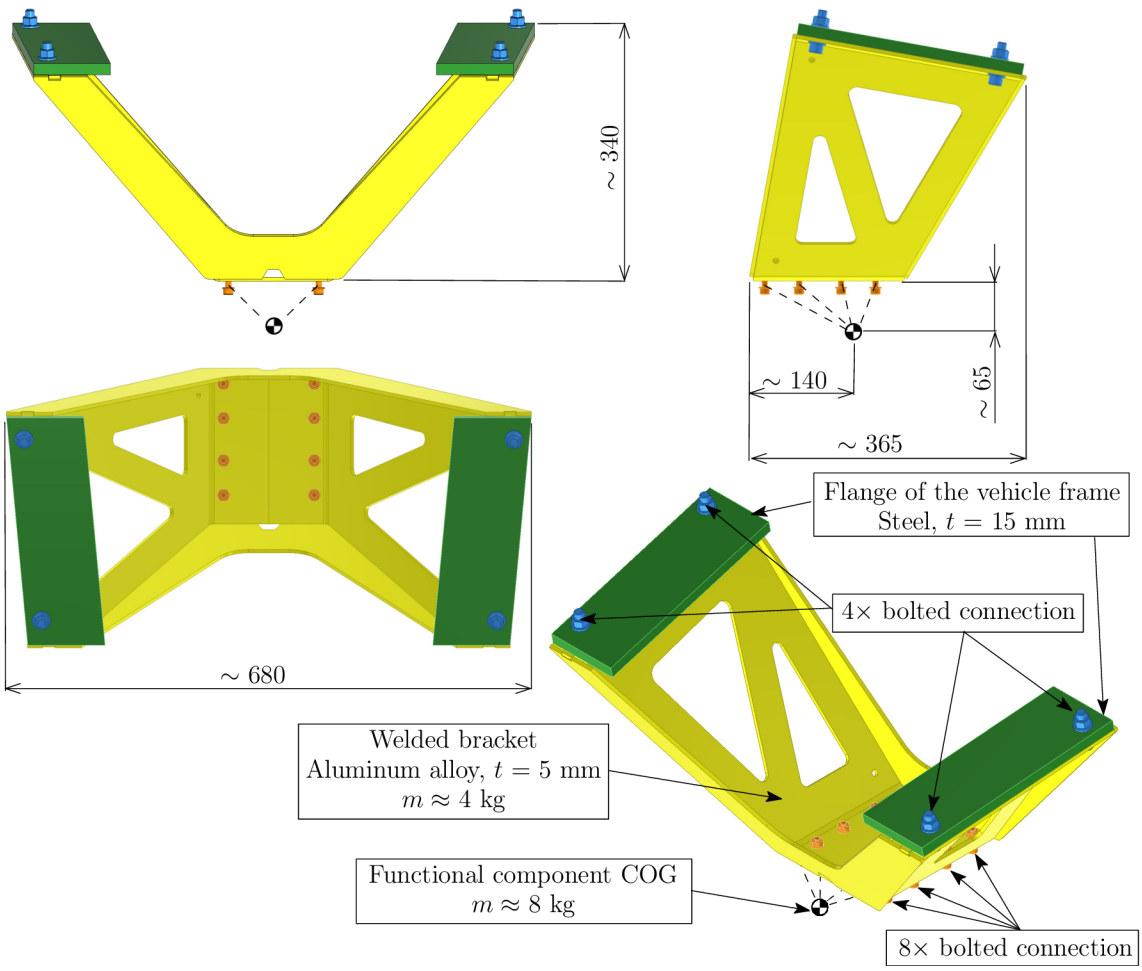

Fig. 7.1: The welded bracket and other significant parts of the assembly considered in analysis, main approximate dimensions marked in millimeters

7.1 Welds on the component

The considered types of welds were, in all cases, automatic double-sided fully penetrated T-type K-butt welds. NDT of the welds was assumed to be performed. The welds at the top and bottom of the bracket were assumed to be continuous, whereas the welds leading from the top to the bottom section of the bracket were assumed to be intermittent. The welds are marked together with their dimensions in fig. 7.2. The additional details about the welds (full penetration) would be included in the specifications of the drawing of the component. The three plates forming the welded part are separated by color and marked by numbers for clarity in the figure.

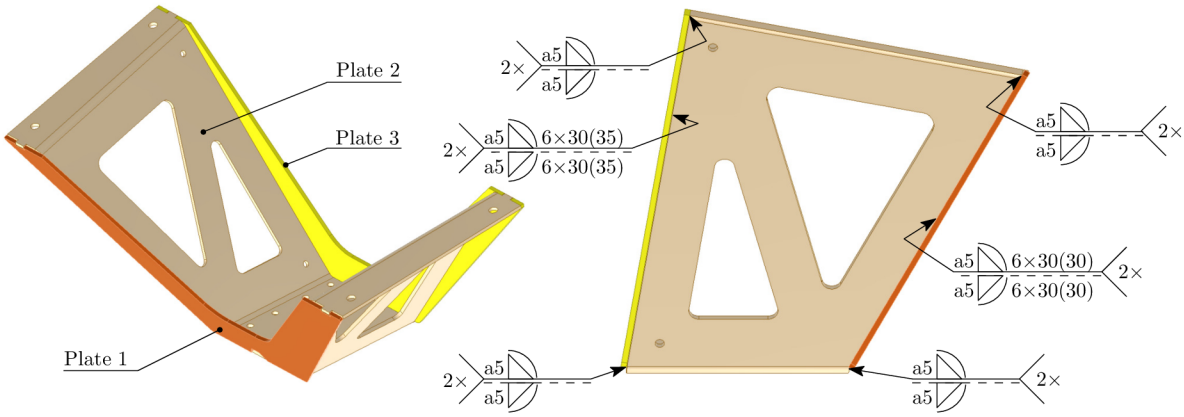

Fig. 7.2: The three welded plates separated by color and proposed welds

The welds directly implied the values of the FAT classes according to the respective similar structural details based on the table of nominal FAT classes found in FKM [3] originally taken from IIW Recommendations [8]. The overview can be seen in table 7.1. Since the analyzed bracket material was aluminum alloy, the FAT Al values were applied. The longitudinal FAT values of the intermittent weld are generally based on the mutual ratio between the normal stress at the flange and the shear stress at the weld ends. Since the exact values of this ratio could differ between locations, the most conservative ratio was assumed, implying the lowest FAT value from the available selection ($FAT_{\|} = 14$) of structural detail 324.[1]

Table 7.1: FAT parameters derived for the weld geometries; values and detail numbers originally from [8]

Weld group	FAT parallel		FAT perpendicular		FAT shear	
	Value	Detail no.	Value	Detail no.	Value	Detail no.
Continuous	50	321	25	412	28	2
Intermittent	14	324	25	412	28	2

7.2 Material parameters

Both the bracket and the frame flange were modeled using a linear elastic model of material in compliance with the FKM Guideline [3]. The only essential material parameters were therefore Young's moduli, Poisson's ratios, and mass densities. These are listed in table 7.2.

[1]This FAT class value applies to the weld ends, since this is where the failure would be expected. For simplicity, it was used for all lengths of the intermittent welds.

Table 7.2: Material parameters used for FE linear elastic models of materials [3; 41; 42; 43]

Material	Young's modulus [GPa]	Poisson's ratio [-]	Mass density [kg/m^3]
Aluminum alloy EN AW-5754 H24 [3; 41]	70	0.3	2 700
Unspecified steel [42; 43]	210	0.3	7 850

7.3 Model preparation

Since the geometry did not allow for simple mapped meshing due to shape irregularities, the surfaces were additionally split to allow quadrilateral meshing on the surfaces where elements would belong to welds. This modification can be seen in fig. 7.3.

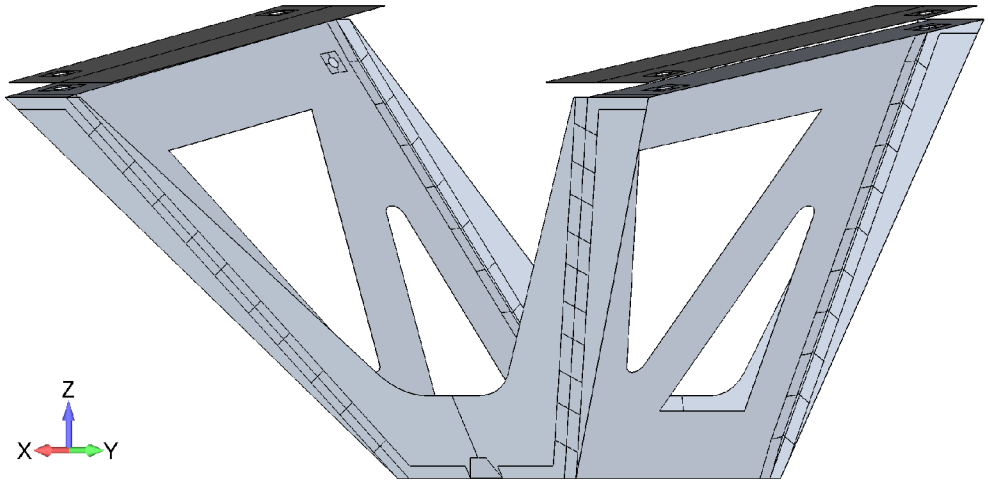

Fig. 7.3: Surface splits in locations of welds that enable the creation of quadrilateral elements

7.4 FE model

The FE model was created in Siemens FEMAP 2301. The model used these types of elements:

- CONM2 element – concentrated mass element, used for modeling the attached component as just a mass point;
- CBUSH elements – spring/damper elements, used for modeling the bolts between the bracket and the frame as highly stiff springs;
- RBE3 elements – distributing coupling elements, used for connection of CBUSH elements to the structure;
- RBE2 elements – kinematic coupling elements, used for rigid connections between elements when modeling the intermittent weld;
- CQUAD4 and CTRIA3 – linear plate (shell) elements used for modeling the bracket plates;

- CROD elements – used for easier identification and orientation of welds (explained in subsection 6.4.3).

This added up to a total of 4 813 nodes and 4 664 elements. The base mesh size was set to 10 mm (2 times the thickness of the plates), which is consistent with the mesh size recommendations mentioned in 6.4.3. The visualization of the model can be seen with details on the specific types of elements in fig. 7.4.

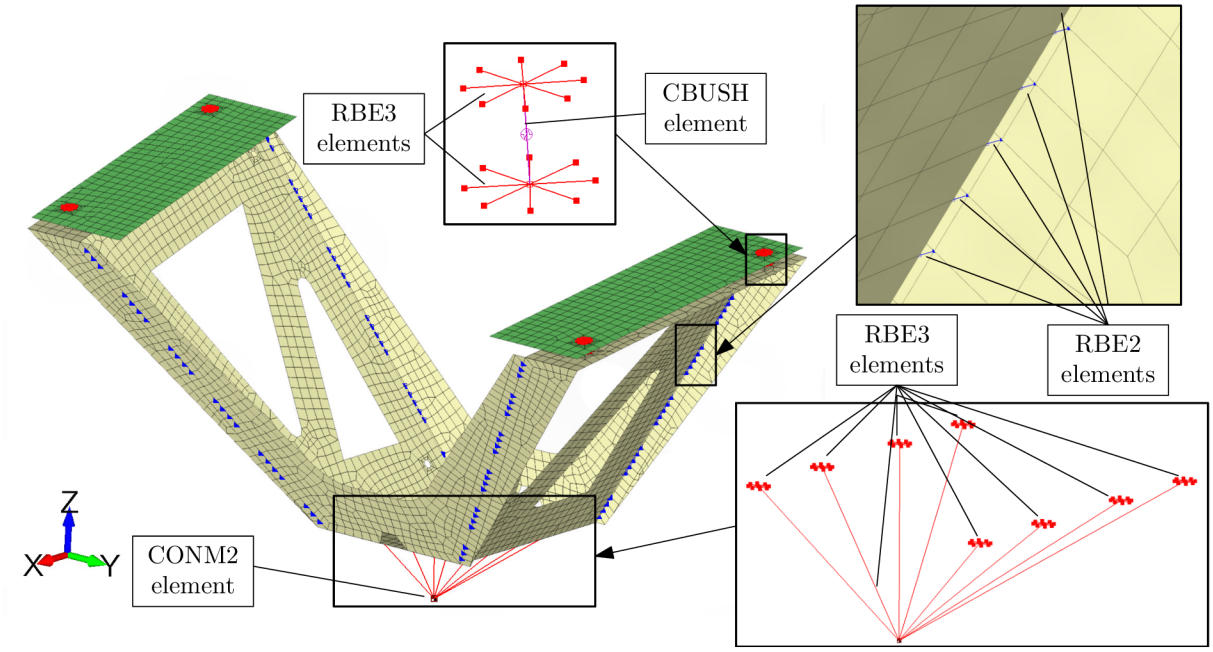

Fig. 7.4: FE model of the bracket with details on special non-shell elements

It may be important to clarify the function of the so-called "Rigid" elements – RBE2 and RBE3 which are relatively specific for FE programs working with NX Nastran. These elements serve as multi-point constraints (MPC), allowing for the coupling of degrees of freedom between multiple nodes. In the case of RBE2, the motion in one node influences the movement in all connected nodes by imposing a rigid connection between the degrees of freedom coupled [44]. In the presented model, this was useful for modeling intermittent welds, where a gap was left between surfaces and RBE2 elements were used to connect the mesh only in areas where actual welding would be performed.

On the other hand, RBE3 elements average the behavior of connected nodes to determine the response at a single node. This means that the motion of a dependent node is calculated by considering the weighted average of motion from multiple independent nodes [44]. In the model presented, RBE3 elements were used to transfer loads between bolts and holes, as well as to attach a concentrated mass element to the structure.

7.5 Boundary conditions

The webs of the I-type profiles of the vehicle frame were not included in the model. The missing webs of the profiles were replaced by boundary conditions in their respective locations. This was done by restricting all translational and rotational degrees of freedom (DOFs) of the nodes on the line corresponding to the location of the web, as can be seen in fig. 7.5.

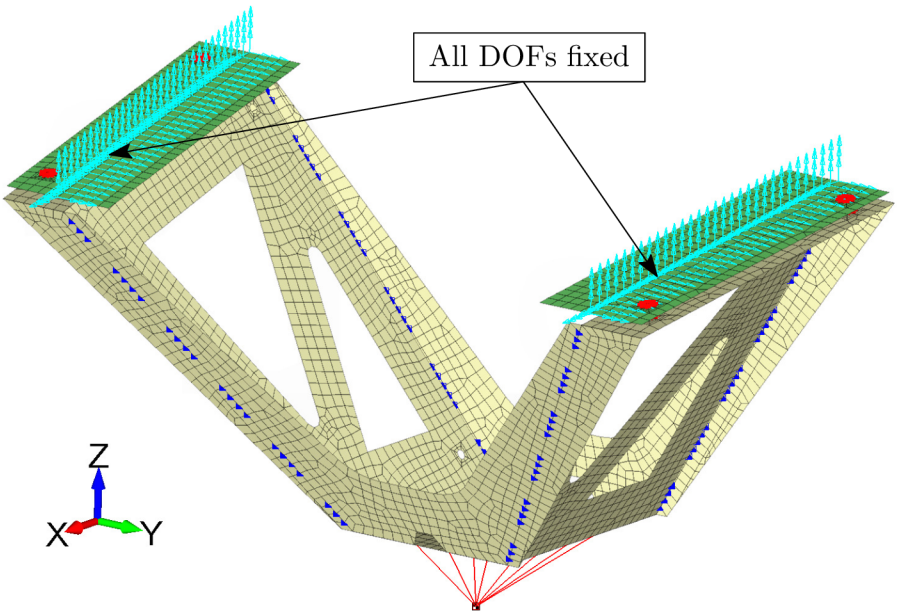

Fig. 7.5: Imposed boundary condition of fixing all DOFs on the center line of the frame flanges

7.6 Loads

Assuming the category P-II of passenger rolling stock according to ČSN EN 12663-1 [1] and the table 4.1 previously presented, the bracket should withstand the load cycles formed by the load cases presented in table 7.3. The load cases forming a cycle for the x-axis are 1 and 2. Similarly, 3 and 4 for the y-axis, and 5 and 6 for the z-axis. Each direction corresponds to $1 \cdot 10^7$ cycles. Combinations of load cases were not considered since their number of cycles would be difficult to assess. The magnitudes of accelerations in the table therefore correspond to full magnitudes according to the standard. Each load case represented a static analysis result calculated using the linear static NX Nastran SOL 101 solver. The directions in the model were set to align with the prescribed vehicle body coordinate system presented in fig. 4.1.

Table 7.3: Accelerations in fatigue load cases based on table 4.1 for P-II type of passenger rolling stock

Load Case ID	a_x $[\mathrm{m \cdot s^{-2}}]$	a_y $[\mathrm{m \cdot s^{-2}}]]$	a_z $[\mathrm{m \cdot s^{-2}}]$
1	1.47	-	−9.81
2	−1.47	-	−9.81
3	-	1.47	−9.81
4	-	−1.47	−9.81
5	-	-	−8.34
6	-	-	−11.28

7.7 Fatigue groups of elements

There were only two distinct types of welds in the structure. The location of the welds was pre-meshed with the rod elements during the FE model preparation. For each type of property, a separate property was selected. This allowed for a smooth creation of FAT element groups when selecting all elements of that individual property. The simplicity of the selection process is visualized in fig. 7.6 where the creation of the Group containing the elements belonging to the intermittent weld is demonstrated.

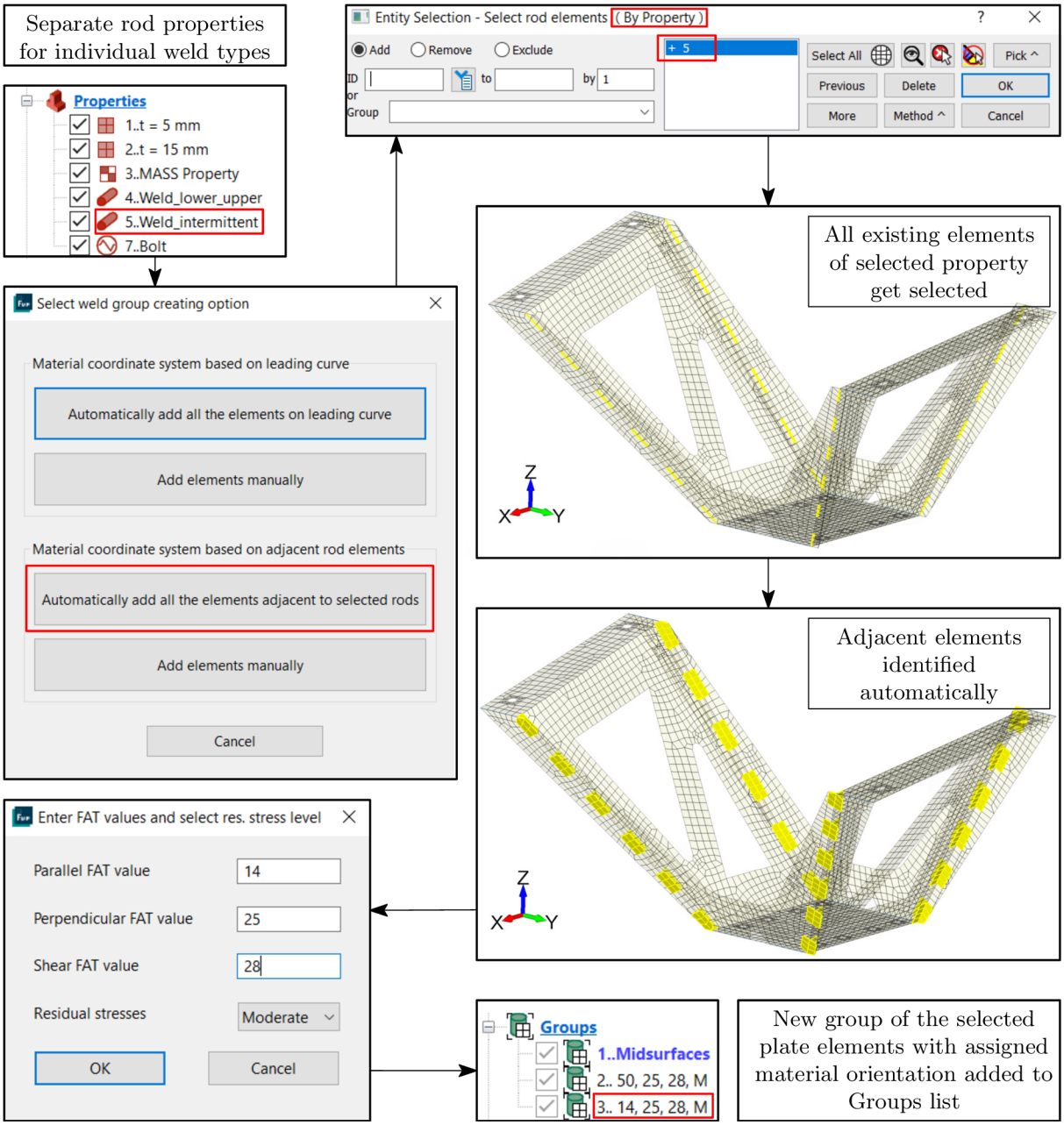

Fig. 7.6: Creation of a single weld element group using the automated method with prepared rod element property as weld type identifier

It would also be possible to use the option of manually selecting elements and orienting them based on a selected geometry curve. However, this would require repeated selections of curves and elements. Selecting all curves at once and meshing them with separate rod element properties for each weld type was significantly more efficient in this case. When using the method of selecting rod elements by property, all the elements of that property are selected. These are then used for the automatic selection of adjacent plate elements and the orientation of the material coordinate system of them. The FAT values were set according to the description in table 7.1. The output of this process were therefore two groups of plate elements belonging to the respective weld types, with assigned FAT values and residual stress identificator in the titles and correctly oriented material coordinate systems.

7.8 Weld fatigue analysis

The fatigue analysis was performed based on the six calculated fatigue load cases and the two groups of elements obtained in the previous step. The overview of the inputs that required selection in the respective dialog windows can be seen together in fig. 7.7. The selected Output Sets correspond to the results of the individual fatigue load cases. The selected Groups correspond to the two groups created in the previous step.

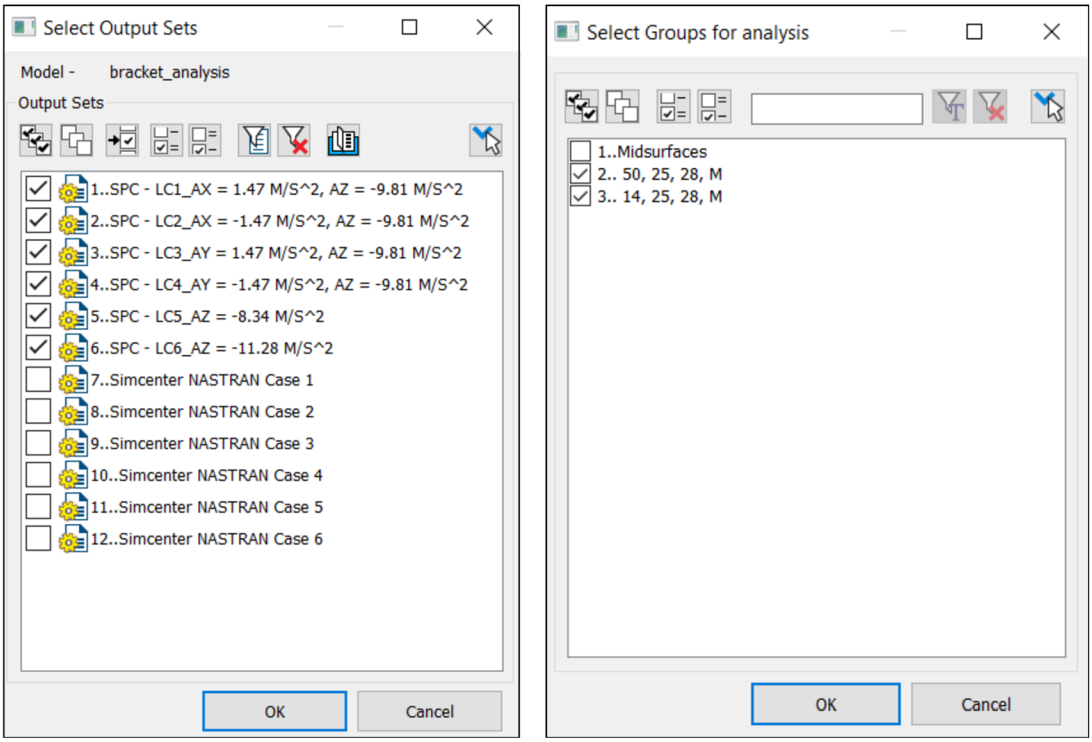

Fig. 7.7: Input selection in the respective dialog windows of the API program

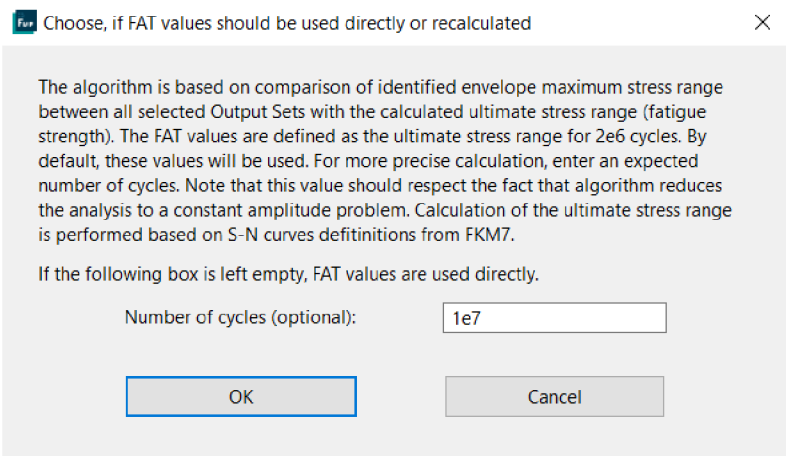

Fig. 7.8: Dialog window with entered number of cycles for analysis

In the dialog window, asking for the number of cycles, $1 \cdot 10^7$ was entered (as can be seen in fig. 7.8). This choice complies with the endurance limit approach of ČSN EN 12663-1 [1] for the applied S-N curves. The S-N curve for normal stresses follows the requirement of having an endurance limit defined for $1 \cdot 10^7$ cycles or less, as it has the knee point $N_D = 5 \cdot 10^6$ cycles.

However, the S-N curve for shear stresses has a knee point at $N_D = 1 \cdot 10^8$ cycles. As it is permissible to consider fatigue strength as a value at $1 \cdot 10^7$ cycles by ČSN EN 12663-1 [1], it was considered here for simplicity.

The alternative would be to consider a conservative value for the number of cycles instead. This could be, for example, $3 \cdot 10^7$ cycles. This choice would mean that the original load spectrum consisting of a total of $3 \cdot 10^7$ would be conservatively replaced by a constant-amplitude spectrum with the highest stress range identified. In the context of this example, this would only influence the utilization in shear.

The output was a new Output Set with all the Output Vectors as previously presented in fig. 6.36. After successfully running the full procedure, the API program switched to the elemental contour of the combined DoU as a double-sided vector (the results corresponding to the top and bottom are plotted for the respective element sides). The contour was plotted by default only on the elements analyzed, and no element averaging was applied. This result vector can be seen in fig. 7.9. The results were calculated almost instantly. Based on visual observation of the elemental contour of the approximate combined DoU, the critical location was outright visible, as it showed the highest value.

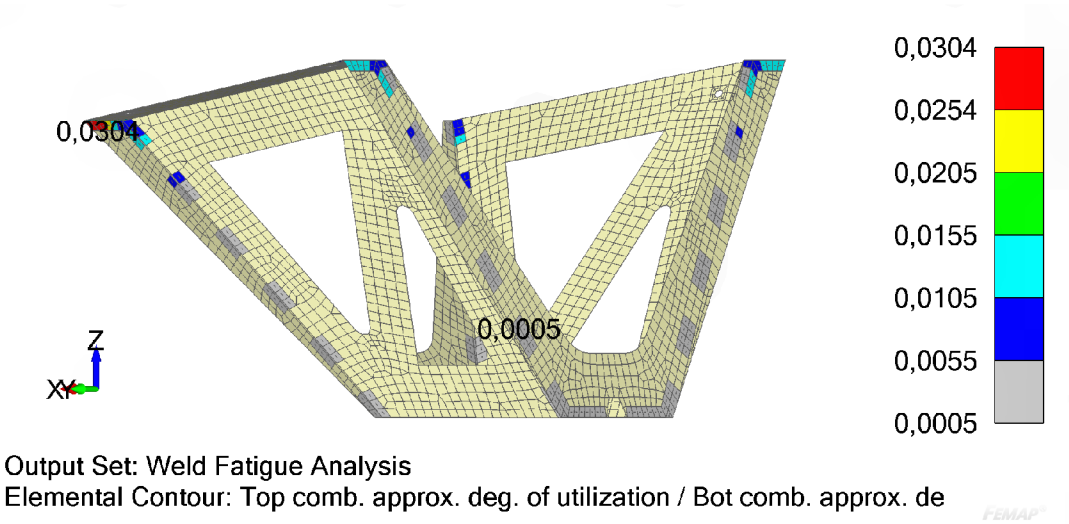

Fig. 7.9: Overall view of the analyzed component with results of combined approximate DoU on the weld elements, results dimensionless

The critical location was located on the upper part of the bracket. This means that intermittent welds pose a lesser danger, even when considering the most critical condition for the parallel FAT class. This means that they did not have to be further reanalyzed.

The overall results of utilization were very low, even for the critical location, as the stresses were also low. This is why the results are shown here using four decimal places to address the accuracy of the results.

7.9 Detailed analysis of the critical location

Detailed analysis of the critical location was performed using the combined use of the final API program and the MS Excel worksheet developed by the cooperating company. The inputs of the worksheet in terms of characteristic stresses were extracted by the API program from the element corresponding to the critical location. As can be seen in fig. 7.10, the corresponding element side is bottom. The fig. also shows the rest of the extraction procedure in practice.

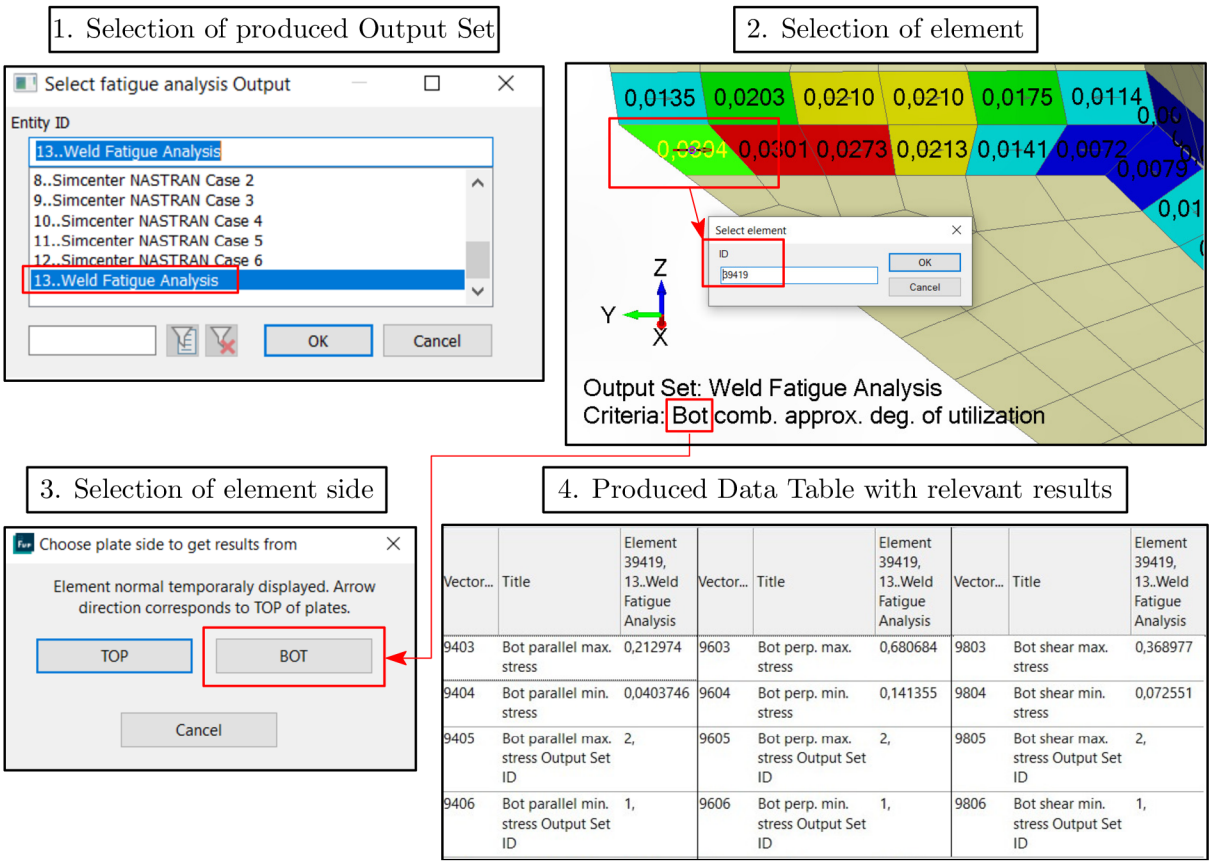

Fig. 7.10: Scheme of extraction of the relevant stress data for detailed analysis

As can be seen from the Data Table in fig. 7.10, the load cases responsible for the envelope maxima and minima are the same (2 and 1) for all three stress components. No further optimization of the results would therefore be possible in this case, as the analysis results of utilization correspond to the actual worst assumed case. MS Excel worksheet was then used for detailed analysis and to include factors that were not part of the API program analysis, which can slightly change the final result. The preview of the full tables can be found in external Appendix C of this thesis, only a final snippet of the result is shown in fig. 7.11. As can be seen, the result is only slightly higher compared to the result produced in the API program.

Assesment of combined types of stresses - Chapter 4.6.2.1				
Degree of utilization - normal perpendicular	aBK, T	0.0275	-	
Degree of utilization - normal parallel	aBK, II	0.0044	-	
Degree of utilization - shear	aBK, Tau	0.0146	-	
Degree of utilization - combined	aBK,Sv	**0.0346**	< 1.00	(4.6.13 + 14) case of same signs
Assesment		COMPLY		

Fig. 7.11: Results of DoU from the MS Excel worksheet

As the critical location identified using conservative assumptions showed the combined DoU far below the allowed value of 1.00, welds on the component could be concluded to comply with the demands of the FKM Guideline and consequently also ČSN EN 12663-1. Considering the margin of safety, detailed analysis of the critical location using a denser mesh and potentially more accurate method such as the hot-spot stress approach was not necessary.

8 RESULTS

New FEMAP API programs were developed to enhance the weld fatigue analysis procedure. As has been demonstrated, the developed API programs significantly reduce the time required to identify the critical location. This is done by automating several steps that allow a conservative, simplified fatigue calculation to be run on all weld-belonging elements. The user can then extract the key stress parameters in the critical location to use them in a detailed calculation using the MS Excel worksheet that had already been part of the work procedure. In this way, the developed API programs fit perfectly into the previously established work procedure in the cooperating company and together create an improved weld fatigue calculation procedure where time and work efficiency were severely increased.

In addition, to address the correct functionality of the API programs, steps were taken to verify the results obtained. These are included in the following subsections. To prove the correctness of the functionalities using a non-trivial example, the demonstrated industry-inspired component was used for verification.

8.1 Verification of functionality of the API programs

There are three basic factors that can be checked for the first program used to assign elements to FAT groups. These are:

- Elements expected to be in the created group are actually present in the group.
- The group title format corresponds to the user choice in the dialog window.
- The material orientation of the elements is set as expected by the user choice.

All of these factors can be visually checked using the basic functionalities of FEMAP and were found to be functional correctly.

To address the correctness of the functionality of the remaining two programs, the results of the following two procedures were compared:

- results of approximate combined cyclic DoU produced as result vectors for top and bottom of the elements by the API program,
- results of combined cyclic DoU produced by manual extraction of all input stresses transformed into the material coordinate system for top and bottom of the elements and analyzed using the MS Excel worksheet.

In this way, two independently produced sets of results could be directly compared. The second approach mimics the procedure of the API program, but does not use the API programs at all (except for the orientation of the material coordinate system, which can be checked visually). This comparison was performed for 10 randomly selected elements and for their respective top and bottom results separately. Fig. 8.1 shows the comparison of the ranked results together with API-produced results adjusted by the factors excluded from the API analysis. These are namely the thickness factor $f_t = 1.1$ and the material safety factor $j_F = 1.25$ [3]. For this specific component, these factors are the same throughout all the welds; therefore, the increase is constant $^{1.25}/_{1.1} \doteq 1.136$. As the increase is constant, the additional consideration does not influence the selection of the critical location. Other excluded factors of the calculation procedure according to the FKM Guideline [3] do not contribute to the final result. Using this comparison, the agreement between the results produced by the API program and the previously used MS Excel worksheet was confirmed, since the results produced by the API program adjusted by multiplying with the factor 1.136 perfectly matched the independently calculated results.

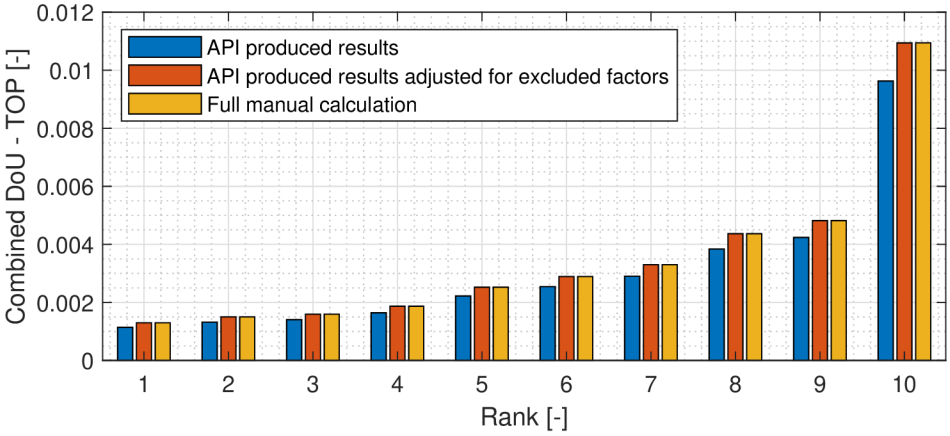

a)

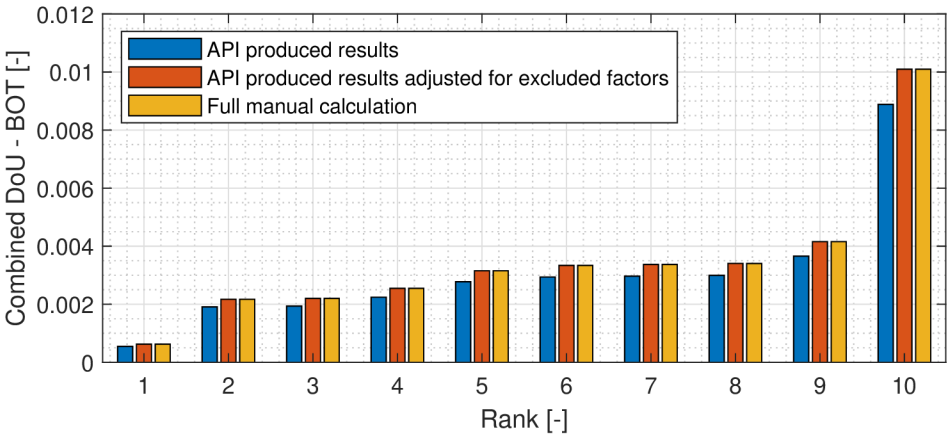

b)

Fig. 8.1: Ranked comparison of the combined DoU for 10 randomly selected elements for a) top side and b) bottom side of elements

8.2 Verification of results with SDC Verifier

To additionally verify the analysis procedure in terms of results and the correct identification of critical location, the results of the industry-inspired example presented were verified using one of the commercially available programs, SDC Verifier. The choice of the two previously presented programs was made based on the greater similarity of the choices used for the local nominal stress assessment of weld fatigue. These significant similarities include:

- assigning FAT values directly to elements,
- possibility of constant amplitude fatigue check using envelope of results,
- possibility of assessment using stresses in centroids.

When these choices were applied, it was possible to compare the results obtained in a similar way. The critical location identified by the SDC Verifier was found to be the same as the one found by the API program. The similarity of the FE criteria plots (showing results on the faces of the elements) of the combined utilization on the bottom side in the critical location can be observed in fig. 8.2. As mentioned previously, the provided version of SDC Verifier had implemented only the version of FKM 6th edition [31]. This edition did not include the different slopes of the fatigue S-N curves based on thickness for the welded components presented previously in fig. 6.33 and described in 3.1.4. Instead, it had a uniform slope of $k = 3.0$ for normal stresses and $k = 5.0$ for shear stresses.

SDC Verifier result with FKM 6th edition standard check	Developed API program result

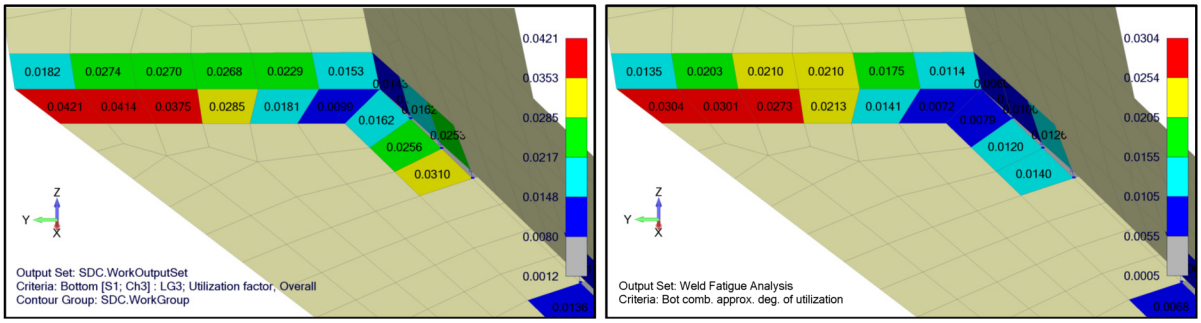

Fig. 8.2: Comparison of the results of combined DoU from SDC Verifier using FKM 6th edition check and the developed API program, results dimensionless

This means that the results difference visible in fig. 8.2 should be attributed to:

- differently defined S-N curves,
- factors excluded in the API program analysis.

However, this was not confirmed to be the case. After a deeper analysis of the anatomy of the SDC Verifier, a different implementation of the combined utilization formula was found compared to the actual formula in the standard. This formula has been presented as (6.5) and it is the same in the 7th edition of FKM [3] and the 6th edition [31]. After a discussion with the support of SDC Verifier, this was confirmed to be a mistake on their side. Fig. 8.3 shows the results in the critical location using a custom modification of the standard implemented in the SDC Verifier. This was recommended as a solution by the support team to bypass the default implementation. To also address the different definitions of S-N curves, their slopes were also altered in the custom standard.

SDC Verifier result with custom standard check	Developed API program result

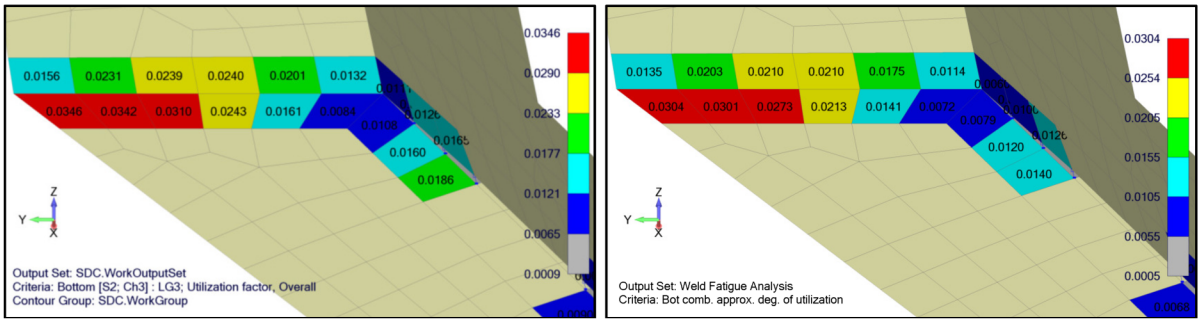

Fig. 8.3: Comparison of the results of combined DoU from SDC Verifier custom standard check and the developed API program, results dimensionless

As can be seen, the result obtained using custom modifications matches the result in the critical location calculated by the combination of the API result and the MS Excel worksheet presented in section 7.9 (that is 0.0346). This is also true for the rest of the continuous weld. The results do not show such a precise agreement in terms of the expected constant increase of 13.6 % for the displayed area of intermittent weld. This was found to be caused by a slight alteration of the weld orientation in SDC Verifier due to the present gap in the model and a slight inclination of the elements.

8.3 Perpendicular stress component effect in the area of the critical location

To address the potential flaw of using the coarse mesh with a lower-order element in terms of possibly not capturing the perpendicular stress gradient, an additional analysis was conducted. To quantify the difference in terms of different identified envelope stress ranges, an analysis was performed using the structural stress assessment method, using hot-spot stress. This was done only around the critical location area. As the presence of the critical location was mainly caused by perpendicular stress, it was a suitable area for a more detailed analysis.

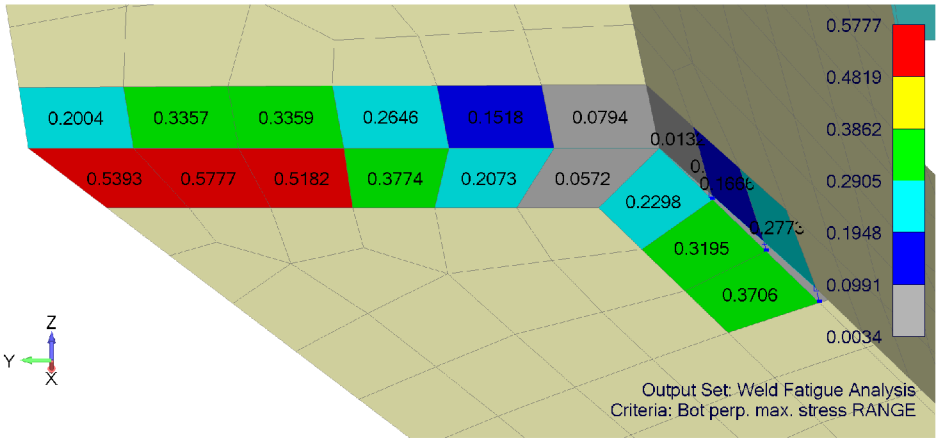

Fig. 8.4: Maximum perpendicular stress range from the API program in the critical location area as criteria plot, results in MPa

Fig. 8.4 shows the values of only the perpendicular stress range on bottom side of elements that entered the calculation of DoU. This is one of the results produced by the API program. Because the two compared stress assessment methods use differently meshed FE models, it was not directly possible to compare just two values outright. To address this, multiple perpendicular paths leading up to the node line corresponding to the weld location were analyzed. These were located near the critical location area, as can be seen in fig. 8.5, local coordinate x_1 is marked in the figure for plotting purposes.

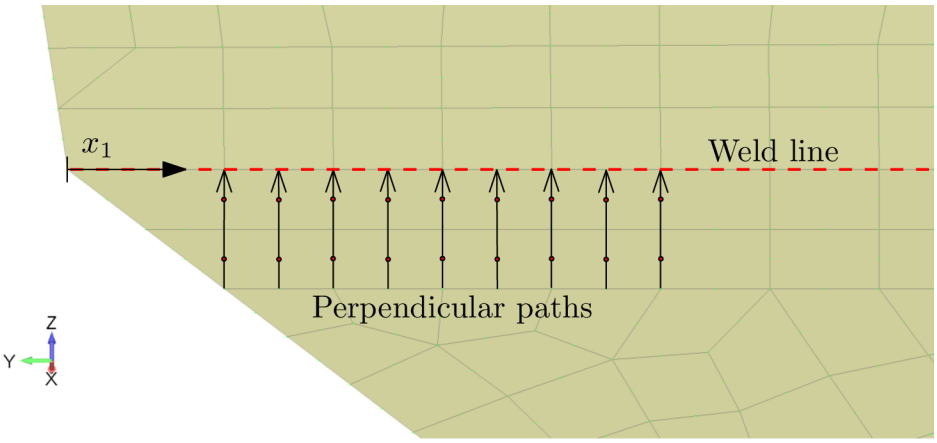

Fig. 8.5: Perpendicular paths used leading up to the weld line used for stress extraction, local coordinate x_1 marked for clarity

To correctly assess the hot-spot stresses, the original model had to be remeshed with finer mesh and higher order elements corresponding to the demands of IIW Recommendations [8]

for hot-spot of type "a" using relatively coarse mesh (see also fig. 5.6). This corresponds to an element size of 5 mm, which is half of the size used in the original model previously described. As stress extraction could be performed using both the mid-side nodes and element centroids, paths using both were used.

Based on observation of the distribution of perpendicular stress in fig. 8.6a), the values of the hot-spot stresses were higher than those obtained using the local nominal stress approach. However, because of the significantly higher FAT class, the resulting DoU is lower for the hot-spot stresses, as can be seen in fig. 8.6b). The same load case couple was found to be responsible for the maximum stress range in the area using both methods.

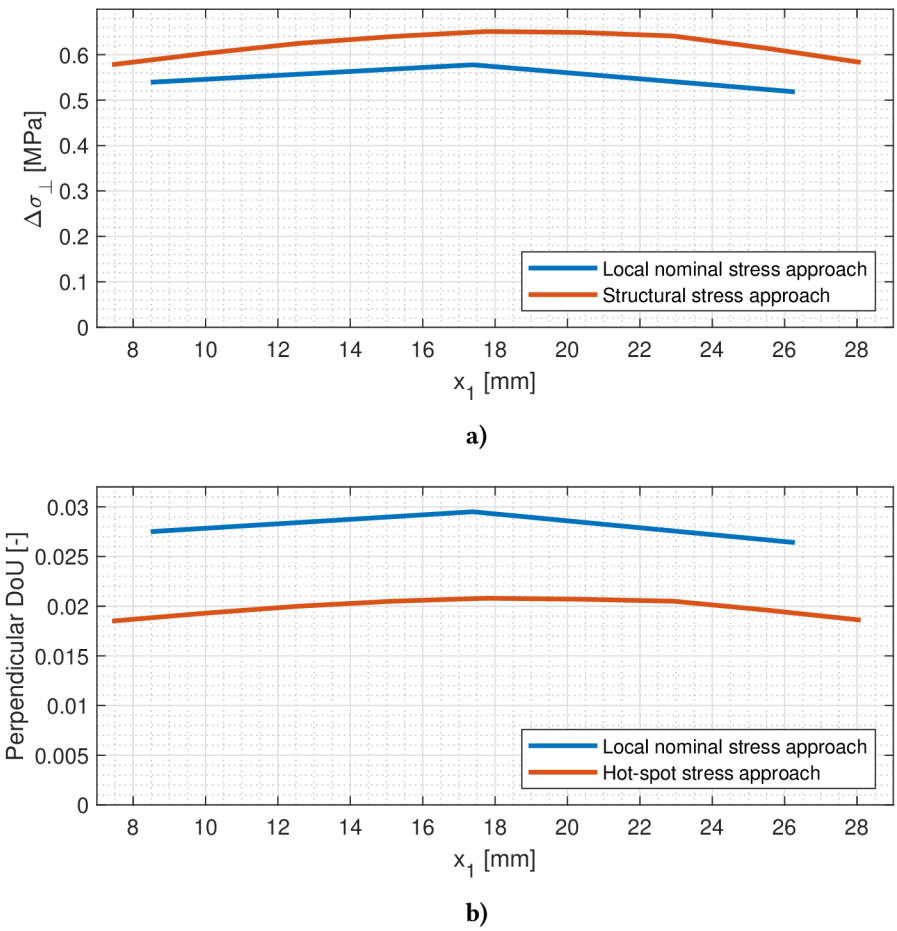

Fig. 8.6: Comparison of the results of a) maximum perpendicular stress range, b) perpendicular DoU as a function of local coordinate x_1 obtained using local nominal stress approach and hot-spot stress approach in the critical location area

For the location with the highest stress range, this was quantified in table 8.1. The corresponding FAT class for the hot-spot stress was established to be FAT 40 based on structural detail no. 2 in table 5.4.3 in the FKM Guideline [3].

Table 8.1: Comparison of the key parameters and results in terms of perpendicular DoU for the highest identified perpendicular stress range

Method	$\Delta\sigma_\perp$ [MPa]	FAT class	Perp. DoU [-]
Local nominal	0.578	25	0.0295
Stuctural	0.651	40	0.0208
% Difference	12.63 %	60.00 %	−29.49 %

As the structural stress assessment using hot-spot value showed a lower perpendicular DoU, the original established method of relatively coarse mesh using lower-order elements was found to be on the conservative side in comparison. However, this observation cannot be generalized based on a singular observation. It was mainly performed here to analyze a potentially non-conservative result in the critical location. This was not found to be the case.

9 DISCUSSION

As can be seen in chapter 7, the methodology developed successfully achieves the main goal of the thesis. Using FEMAP API programs, the user can perform weld fatigue analysis in an efficient, reliable, and timely manner. These API programs enable swift identification of the critical location. However, as previously mentioned and presented, the implemented algorithm considers only the fatigue resistance parameters of:

- FAT values for the three stress components,
- number of cycles the structure should withstand,
- mean stress effect,
- level of residual stress.

There are other factors that additionally modify fatigue resistance, according to the FKM Guideline [3]. These include the thickness factor, the surface treatment factor, the material safety factor, and the limitation of the maximum fatigue strength with respect to the plastic behavior of the material. These factors were intentionally not considered for multiple reasons.

Since fatigue resistance parameters are stored in the titles of the created groups, including more parameters in a manner in which the title would remain understandable for the user after the group was created would be very difficult. Identifying and collecting all the parameters is also very inefficient, since a vast majority of them do not significantly influence the result for the purpose of finding the critical location, and it severely slows down the whole procedure. This was clearly illuminated when testing the commercial programs. However, all of these factors are considered during the detailed analysis of the critical location using the MS Excel worksheets.

The original idea was not even to consider the mean stress effect. However, since it can shift the result between elements by a serious margin, it was additionally implemented. Because the effects of mean stress are dependent on the residual stress level, this effect also had to be implemented. If the user wishes not to consider the mean stress and residual stress level, selection of "High" residual stresses neglects both.

As could be observed in chapter 8, for the industry-inspired example, the shift between API results and the final results was constant for all elements. Therefore, it did not influence the selection of the critical location. Situations similar to this are expected to occur in the majority of cases. Arguably, extreme cases could be envisioned in which excluded factors could shift the critical location to a different place. Therefore, special care should be taken when using the algorithm in extreme cases where these factors (e.g., plate thickness, surface treatment) would be largely different between potentially critical locations. If this is expected, it can be indirectly factored into the algorithm by adjusting the FAT values before running the analysis.

The API algorithm is also, strictly speaking, a constant-amplitude approach of fatigue analysis. The fatigue life of the welded attachments to the rolling stock according to the standards studied [1; 2] can be approached as a constant-amplitude by considering conservative choices. For the industry-inspired example demonstrated, it was possible to use the endurance limit approach considering fatigue strength at $1 \cdot 10^7$ cycles, as allowed by the standard ČSN EN 12663-1 [1]. For the endurance limit approach, the calculation procedure of the FKM Guideline [3] reduces to the constant amplitude problem using the largest amplitude identified in the spectrum. This means that for applications of fatigue analysis on welded attachments for ČSN EN 12663-1 [1], the algorithm is sufficient in this way.

However, it would also be possible to apply the definition of S-N curves according to the FKM Guideline without this modification and replace the loading stress spectrum by the maximum identified stress range with $3 \cdot 10^7$ cycles. The goal of this would be to replace the

spectrum with the worst identified cycle using the total number of cycles in the whole spectrum. This would reduce the problem to constant-amplitude fatigue again in a conservative way. This would be the recommended step for applying the algorithm to the other standard studied, ČSN EN 13749 [2]. It is also worth mentioning that in cases of both standards [1; 2], this would only affect the S-N curve of the shear stress. The S-N curves of normal stresses have a knee point at $5 \cdot 10^6$ cycles, and therefore there is no difference in the result of DoU between any value of the number of cycles beyond that. The curve is considered flat according to the definition in the FKM Guideline [3].

Additionally, the algorithm is also applicable for any general case of constant-amplitude loading of welds or variable-amplitude loading where one block of the stress spectrum plays a dominant role. Of course, it is also possible to generalize the conservative replacements of spectra by the largest stress range and the total number of cycles in the spectrum, similarly to the case described above.

Admittedly, the choices taken for the implementation of the local nominal stress method in combination with FEM are the main points of discussion. To remind the reader, the procedure introduced extracts the stress components from face centroids of shell type of elements. The recommended mesh size is 2.0 – 3.0 times plate thickness, and the recommended element type is a quadrilateral linear element. The choices that led to these decisions were mentioned throughout the thesis. To sum them up once again together, they include:

- literature recommendations of relatively simple and coarse mesh for local nominal stress approach [4; 5; 8],
- practical example of using plate coarse mesh lower-order elements for eliminating influence of singularities [22] (also demonstrated in subsection 6.1.1),
- reliable stress extraction location using stresses in centroids of quadrilateral elements in FEMAP,
- stress extraction distance of 1.0 – 1.5 times distance from the weld toe for perpendicular stresses established in DVS 1612 [23],
- cooperating company preference for linear quadrilateral elements.

Furthermore, when cetroidal stresses without averaging are used, the stresses remain constant on the whole element face. Considering all of these factors together should point out the mentioned mesh choices. As mentioned in [22], this may not always be perfectly reliable for capturing the perpendicular stress gradient. However, all the API programs developed are independent of element order and mesh size. Therefore, using denser mesh or quadratic elements is perfectly possible to address this. However, in such cases, the effect of eliminating the possible influence of singularities may deteriorate. This can potentially lead to an overestimation of the stress level for locations such as the rib endings.

A comparison of results has been demonstrated using the mesh of choice for the local nominal stress and the structural stress, which has a methodological source for the mesh and stress extraction. The result based on the methodology established in this thesis was on the conservative side compared to the hot-spot stress assessment. However, this was performed only for one location on the component; therefore, these results cannot be absolutely generalized.

The objective of establishing an absolutely reliable mesh type and size in relation to the developed API programs was not further studied due to time restrictions. So far, there are at least some methodological sources that support the choices implemented. However, it could be a potential objective for future research. Furthermore, it would also be possible to establish and code a more sophisticated method of stress extraction compared to simply extracting stresses from element centroids. This possibility was also neglected, considering the time constraints.

The use of the local nominal stress assessment method was chosen as practically the only one that could be efficiently automated. However, the use of the method is generally limited by the available selection of similar structural details. If no comparable detail is available, the effects of the welds are not well quantified. In such a case, either the most conservative value of FAT should be used or another method of evaluation should be performed.

10 CONCLUSION

A methodology for calculating the fatigue strength of welded joints for thin-walled metal structures has been presented. This methodology has foundations in the analysis procedure established previously in the cooperating company that proposed the thesis topic. The enhanced methodology uses entirely new FEMAP API programs developed as part of this thesis for the analysis of welds on shell FE models. The use of these programs significantly reduces the time and effort required for the entire analysis, as it reduces the process of identifying the critical location to an absolute minimum by automating the necessary steps. The development of the FEMAP API programs can be considered a substantial contribution in this very specialized field of programming.

The developed API programs allow for a simplified conservative analysis of weld joints according to the fatigue analysis procedure using local nominal stresses according to the FKM Guideline [3]. With correctly applied choices when using these programs, it is possible to perform a weld fatigue analysis that also complies with the standard studied related to rolling stock. This has been demonstrated in an industry-inspired example of a welded bracket attached to the train vehicle analyzed according to ČSN EN 12663-1 [1]. Although the original thesis goal was to analyze multiple components, it was decided that the previewed example was sufficiently demonstrative, and performing more would be largely repetitive. As the demands of the other standard of studied rolling stock specifically related to bogie frames ČSN EN 13749 [2] have practically the same characteristics, the analysis would be performed in the same manner with only alterations of the parameters.

Although the development and application of the API programs were tailored to fit the established work procedures in the cooperating company, they are perfectly applicable to anyone. Generally speaking, the API programs developed represent an alternative to commercially developed programs when considering the single functionality of weld fatigue analysis. This, of course, applies only if the potential drawbacks in terms of API program simplifications are not a significant concern to the interested party. The developed API programs are directly available in the external appendices of this thesis. They can be used by anyone with a functional license of Siemens FEMAP, including the student version, with version 2020.1 and later. The use of the programs does not imply additional financial costs. Installation is straightforward, and the use of API programs integrates into other FEMAP functionalities. This may be very beneficial, as the user can work with a known and understandable interface. Therefore, an everyday user of FEMAP may easily be able to understand all the functionalities in just minutes of first using the developed tools. Since the API program codes are open source, they may be further developed or improved to specific needs by anyone with knowledge of FEMAP API programming.

The API programs fit directly into the work procedure of the cooperating company. They fulfill all the preferences and requirements of the company stated in the thesis assignment. Therefore, they already see a practical application in the company's work procedure with satisfaction. In cases where the fatigue analysis of welds would take even hours, mainly because of the identification of critical location process, time was reduced to the order of minutes. Not only is this an improvement compared to the previous state of things, but the calculation process is also practically instant compared to using commercial programs and running the analysis on the same FE models. The practical methodology applied for programming introduced in this thesis could also be implemented for other FEM software packages, where options similar to the FEMAP API would be possible.

The methodology described using the API programs is limited to the analysis of FEM stresses in the base material. Therefore, it is applicable for cases where these stresses are

relevant in contrast to the weld type: fully penetrated fillet welds and butt welds. Cases of fillet welds not fully penetrated, where root cracking is possible, cannot be addressed using this analysis. This is not a concern for the cooperating company, as the possibility of root cracking is usually taken care of during the design phase of the produced parts, and customers are generally discouraged from such weld types. This explains why the cooperating company did not anticipate this feature when assigning the thesis topic. One of the commercial programs, SDC Verifier, cannot perform an analysis of stress in the weld throats of fillet welds as well.

To be able to develop automated tools that would optimize the weld fatigue analysis process in the cooperating company in a restricted amount of time, certain simplifications were needed. Therefore, only the most crucial factors on the fatigue resistance side of the calculation material were identified and considered. In this way, critical locations should be identified by running the automated API program, which does not take into account the other factors that should only shift the overall results if all welds are similar. However, there may be cases where this may not be true. In such situations, it is possible to modify the fatigue resistance data in terms of FAT values to address this. However, factors not considered in the API program analysis are always considered in the end by performing analysis using MS Excel worksheets for detailed analysis of the identified critical location. These worksheets were developed before the work on this thesis in the cooperating company.

Similarly to the simplifications on the material side of the calculation, conservative simplifications on the loading side were also taken. These are considering the highest stress ranges for each stress component and then also combining them as if acting simultaneously. Therefore, it simplifies a spectrum into a constant-amplitude problem. In certain situations, this may be sufficient. One such example is the welded attachments to rolling stock studied in this thesis. In some cases, the conservative assumptions made, can lead to overestimated results. Then it is up to the user to analyze the results and possibly modify them.

Since there are no established methodological instructions on the mesh specifications for the local nominal stress approach using FEM, a compromise was established based on research and consultation with the cooperating company. For now, this compromise serves as the mesh recommendations for the analysis procedure. However, the generality of using this mesh size and element order together with analyzing the elemental (= centroidal) results in all possible cases remains unclear and could be a topic of future research. Together with the simplified stress extractions from only the centroids of the elements, this remains the most disputable point of this thesis. Therefore, it could be worked on in the future by further studying the mutual relevance of mesh size, element order, and stress extraction location on the element.

Despite the shortcomings mentioned , the developed programs are still applicable in practice, and together with the rest of the methodology, they fulfill all the original goals of the thesis.

REFERENCES

[1] ÚŘAD PRO TECHNICKOU NORMALIZACI, METROLOGII A STÁTNÍ ZKUŠEBNICTVÍ. ČSN EN 12663-1+A1, *Železniční aplikace – Pevnostní požadavky na konstrukce skříní kolejových vozidel – Část 1: Lokomotivy a vozidla osobní dopravy (a alternativní metoda pro nákladní vozy).* Prague, 2015.

[2] ÚŘAD PRO TECHNICKOU NORMALIZACI, METROLOGII A STÁTNÍ ZKUŠEBNICTVÍ. ČSN EN 13749, *Železniční aplikace – Dvojkolí a podvozky - Metoda specifikování pevnostních požadavků na rámy podvozků.* Prague: Česká agentura pro standardizaci, 2022.

[3] *Analytical Strength Assessment of Components, FKM Guideline.* 7th Edition. VDMA Verlag, 2020. ISBN 978-3-8163-0745-7.

[4] JIA, Junbo. *Essentials of Applied Dynamic Analysis.* Risk Engineering. Heidelberg: Springer Berlin, 2014. ISBN 978-3-642-37003-8. Available at: https://doi.org/10.1007/978-3-642-37003-8. [cit. 2024-02-01].

[5] FRICKE, Wolfgang. IIW guideline for the assessment of weld root fatigue. Online. *Welding in the World.* 2013, vol. 57, iss. 6, p. 753-791. ISSN 0043-2288. Available at: https://doi.org/10.1007/s40194-013-0066-y. [cit. 2024-01-31].

[6] WELDING ANSWERS. *Troubleshooting Weld Cracking – The importance of crack location.* Online. WELDING ANSWERS. 2023. Available at: https://weldinganswers.com/troubleshooting-weld-cracking-the-importance-of-crack-location/. [cit. 2024-03-20].

[7] COMSOL. *Material Fatigue Definition.* Online. Multiphysics Cyclopedia. 2016, Last modified: February 21, 2017. Available at: https://www.comsol.com/multiphysics/material-fatigue. [cit. 2024-01-31].

[8] HOBBACHER, A. F. *Recommendations for Fatigue Design of Welded Joints and Components.* 2nd ed. Springer Cham, 2016. ISBN 978-3-319-23757-2. Available at: https://doi.org/10.1007/978-3-319-23757-2. [cit. 2024-02-01].

[9] DEPALE, Bruno; BENNEBACH, Mohamed a ARQUIS, Eric. Residual life of steel structures and equipment: problems and application to cranes. Online. *Mechanics and Industry.* 2019, vol. 20, iss. 8. ISSN 2257-7777. Available at: https://doi.org/10.1051/meca/2019047. [cit. 2024-02-01].

[10] PEDERSEN, Mikkel Melters. *Introduction to Metal Fatigue.* Online. Department of Engineering, Aarhus University, 2018. Available at: https://doi.org/10.13140/RG.2.2.25216.28163. [cit. 2024-01-31].

[11] LEE, Yung-Li; BARKEY, Mark E. a KANG, Hong-Tae. *Metal fatigue analysis handbook: practical problem-solving techniques for computer-aided engineering.* Waltham: Butterworth-Heinemann, c2012. ISBN 978-0-12-385204-5. Available at: https://doi.org/10.1016/C2010-0-66376-0. [cit. 2024-02-01].

[12] LEARNEASY: LIVE AND LEARN. *Properties.* Online. LEARN easy. Available at: https://www.mem50212.com/MDME/MEMmods/MEM30007A/properties/Properties.html. [cit. 2024-05-12].

[13] FAN, J. L.; GUO, X. L.; WU, C. W. a ZHAO, Y. G. Research on fatigue behavior evaluation and fatigue fracture mechanisms of cruciform welded joints. Online. *Materials Science and Engineering: A.* 2011, vol. 528, iss. 29-30, p. 8417-8427. ISSN 09215093. Available at: https://doi.org/10.1016/j.msea.2011.08.037. [cit. 2024-01-31].

[14] PÖRTNER, Hartwig. *Multi-axial Fatigue Models for Composite Lightweight Structures.* Online, Master's Thesis. Göteborg: Chalmers University of Technology, 2013. Available at: https://publications.lib.chalmers.se/records/fulltext/195134/195134.pdf. [cit. 2024-01-31].

[15] MITCALC. *Design and strength check of welded connections.* Online. Available at: https://www.mitcalc.com/doc/welding/help/en/welding.htm. [cit. 2024-01-31].

[16] STEELCONSTRUCTION.INFO. *Welding.* Online. Available at: https://www.steelconstruction.info/Welding. [cit. 2024-01-31].

[17] JONSSON, Bertil; DOBMANN, G.; HOBBACHER, A. F.; KASSNER, M. a MARQUIS, G. *IIW Guidelines on Weld Quality in Relationship to Fatigue Strength.* Online. Springer Clam, 2016. ISBN 978-3-319-19198-0. Available at: https://doi.org/10.1007/978-3-319-19198-0. [cit. 2024-01-31].

[18] WERMAC ORG. *Types of Welding Joints - The 5 Different Types Of Welding Joints.* Online. c2008 - 2024. Available at: https://www.wermac.org/others/welding_basic-welding-joints_butt-weld_fillet-weld.html. [cit. 2024-01-31].

[19] WCWELDING.COM. *Parts Of A Weld.* Online. Available at: https://www.wcwelding.com/parts-of-a-weld.html. [cit. 2024-01-31].

[20] PEDERSEN, Mikkel Melters. *Improving the Fatigue and Control Performance of Loader Cranes.* Online, PhD Thesis. Aalborg: Aalborg University, 2011. Available at: https://vbn.aau.dk/ws/files/549475683/MMP_PhD_Thesis.pdf. [cit. 2024-01-31].

[21] THE RAILWAY TECHNICAL. *Bogies.* Online. c2019. Available at: http://www.railway-technical.com/trains/rolling-stock-index-l/bogies.html. [cit. 2024-01-31].

[22] CAE SIMULATION & SOLUTIONS. *Overview of Weld Assessment with LIMIT: LIMIT 2023.* PDF. 2023. Unpublished work, provided with installation of the software.

[23] DEUTSCHER VERBAND FÜR SCHWEISSEN UND VERWANDTE VERFAHREN E.V. DVS 1612, *Gestaltung und Dauerfestigkeits- bewertung von Schweißverbindungen mit Stählen im Schienenfahrzeugbau.* 2009.

[24] NIEMI, Erkki; FRICKE, Wolfgang a MADDOX, Stephen J. *Structural Hot-Spot Stress Approach to Fatigue Analysis of Welded Components.* Online. 2nd ed. Springer Singapore, 2017. ISBN 978-981-10-5568-3. Available at: https://doi.org/10.1007/978-981-10-5568-3. [cit. 2024-01-31].

[25] DEUTSCHER VERBAND FÜR SCHWEISSEN UND VERWANDTE VERFAHREN E. V. MERKBLATT DVS 0905, *Industrielle Anwendung des Kerbspannungskonzeptes für den Ermüdungsfestigkeitsnachweis von Schweißverbindungen.* 2017.

[26] FRICKE, Wolfgang. Guideline for the Fatigue Assessment by Notch Stress Analysis for Welded Structures. Online. *Conference: Annual Assembly of International Institute of Welding.* 2008, vol. IIW-Doc. XIII-2240r2-08/XV-1289r2-08. Available at: https://www.researchgate.net/publication/266038561_Guideline_for_the_Fatigue_Assessment_by_Notch_Stress_Analysis_for_Welded_Structures. [cit. 2024-01-31].

[27] BAUMGARTNER, J.; SCHMIDT, H.; INCE, E.; MELZ, T. a DILGER, K. Fatigue assessment of welded joints using stress averaging and critical distance approaches. Online. *Welding in the World.* 2015, vol. 59, iss. 5, p. 731-742. ISSN 0043-2288. Available at: https://doi.org/10.1007/s40194-015-0248-x. [cit. 2024-01-31].

[28] BRUDER, T.; STÖRZEL, K.; BAUMGARTNER, J. a HANSELKA, H. Evaluation of nominal and local stress based approaches for the fatigue assessment of seam welds. Online. *International Journal of Fatigue.* 2012, vol. 34, iss. 1, p. 86-102. ISSN 01421123. Available at: https://doi.org/10.1016/j.ijfatigue.2011.06.002. [cit. 2024-01-31].

[29] SIEMENS INDUSTRY SOFTWARE INC. *Simcenter Nastran Quick Reference Guide: Simcenter Nastran 2212 Series* PDF. 2022. Unpublished work, provided with installation of the software.

[30] CAE SIMULATION & SOLUTIONS. *Company.* Online. Fatigue Analysis Software | Weld Assessment | Finite Element. c2024. Available at: https://www.limit-fatigue.com/company/. [cit. 2024-03-19].

[31] *Analytical Strength Assessment of Components, FKM Guideline.* 6th revised Edition. VDMA Verlag, 2012. ISBN 978-3-8163-0649-8.

[32] *Strength Assessment According to the FKM Guideline.* Online. Version LIMIT2020. 2020. Available at: https://www.limit-fatigue.com/wp-content/uploads/2020/04/LIMIT_2020_FKM_Course_BaseWeld.pdf. [cit. 2024-03-19].

[33] SDC VERIFIER. *About SDC Verifier | SDC Verifier.* Online. SDC Verifier | Simulation and Structural Verification. C2024. Available at: https://sdcverifier.com/about/. [cit. 2024-03-20].

[34] SDC VERIFIER. *Load Group | Help | SDC Verifier for Femap.* Online. SDC Verifier | Simulation and Structural Verification. Available at: https://sdcverifier.com/software/help/load-group.html. [cit. 2024-03-20].

[35] SDC VERIFIER. *Fatigue Groups | Help | SDC Verifier for Femap.* Online. SDC Verifier | Simulation and Structural Verification. Available at: https://sdcverifier.com/software/help/fatigue-group.html. [cit. 2024-03-20].

[36] JENSEN, Adrian. *Automation and Optimization with the FEMAP API: A Beginner's Guide for FEMAP and NX Nastran Users.* Online. Rev. 0. 2019. Available at: https://www.appliedcax.com/support-and-training/technical-online-seminars/seminars/Femap-and-NX-Nastran-Technical-Seminar-A-Beginner%27s-Guide-to-the-FEMAP-API-Rev-0.pdf. [cit. 2024-03-20].

[37] ATA ENGINEERING, INC. *On-Demand Webinar: Intro to the Femap API.* Online. 2019. Available at: YouTube, https://youtu.be/BGtZZZhr4Ws?si=B9ndz_chATmRaiIa. [cit. 2024-03-20].

[38] SIEMENS INDUSTRY SOFTWARE INC. *Femap API Guide: Femap 2301 MP1.* PDF. 2023. Unpublished work, provided with installation of the software.

[39] PICH, Peter and FRICKE, Chip. *Orient Material Angle Tengent to Curve.* BAS. 2013. Unpublished work, FEMAP API code provided with installation of the program.

[40] KRIENGSIRI, Patrick. *Advanced Post-Processing with the FEMAP API.* Online. 2013. Available at: https://iberisa.wordpress.com/wp-content/uploads/2014/06/fs13-11_advancedpostprocessingapi_splm_kriengsiri.pdf. [cit. 2024-03-20].

[41] ÚŘAD PRO TECHNICKOU NORMALIZACI, METROLOGII A STÁTNÍ ZKUŠEBNICTVÍ. ČSN EN 1999-1-1, *Eurokód 9: Navrhování hliníkových konstrukcí – Část 1-1: Obecná pravidla pro konstrukce.* Prague, 2009.

[42] ÚŘAD PRO TECHNICKOU NORMALIZACI, METROLOGII A STÁTNÍ ZKUŠEBNICTVÍ. ČSN EN 1993-1-1, *Eurokód 9: Navrhování ocelových konstrukcí – Část 1-1: Obecná pravidla a pravidla pro pozemní stavby.* Prague, 2006.

[43] ÚŘAD PRO TECHNICKOU NORMALIZACI, METROLOGII A STÁTNÍ ZKUŠEBNICTVÍ. ČSN EN 1993-1-2, *Eurokód 9: Navrhování ocelových konstrukcí – Část 1-2: Obecná pravidla – Navrhování konstrukcí na účinky požáru.* Prague, 2006.

[44] FIDELIS ENGINEERING ASSOCIATES. *What Is The Difference Between A Kinematic (RBE2) And A Distributing (RBE3) Coupling In FEA?* Online. 2021. Available at: https://www.fidelisfea.com/post/what-is-the-difference-between-a-kinematic-rbe2-and-a-distributing-rbe3-coupling-in-fea. [cit. 2024-04-22].

LIST OF USED SYMBOLS AND ABBREVIATIONS

Abbreviations

Abbreviation	Description
API	Application Programming Interface
COG	Center of gravity
DOFs	Degrees of freedom
DoU	Degree of utilization
FAT	Classification reference to S-N curve
FE	Finite element
FEA	Finite element analysis
FEM	Finite element method
GUI	Graphical User Interface
HCF	High cycle fatigue
IIW	International Institute of Welding
LCF	Low cycle fatigue
MPC	Multi-point constraint
MS	Microsoft
NDT	Non-destructive testing
PWT	Post-weld treatment
UIT	Ultrasonic impact treatment
VB	Visual Basic

Latin symbols

Symbol	Description	Unit
A	Cross-section area	mm^2
A_{ele}	Factor of distance between the fatigue life curve and the S-N curve	-
a	Weld throat dimension	mm
$a_{BK,\sigma_{\parallel}}$	Cyclic degree of utilization for parallel stress	-
$a_{BK,\sigma_{\perp}}$	Cyclic degree of utilization for perpendicular stress	-
a_{BK,σ_v}	Cyclic degree of utilization for combined loading	-
$a_{BK,\tau}$	Cyclic degree of utilization for shear stress	-
a_x	Acceleration in x-coordinate direction	m/s^2
a_y	Acceleration in y-coordinate direction	m/s^2
a_z	Acceleration in z-coordinate direction	m/s^2
b	Width	mm
C	Constant in equation of S-N curve with exponent k	MPa
D	Critical damage value	-
E	Young's modulus	GPa
F	Force	N
F_{max}	Maximum force	N
F_{max}	Minimum force	N
$F_{max,1}$	Maximum force from 1st spectrum block	N
$f(R)$	FAT modification bonus factor	-
g	gravitational acceleration	m/s^2
i	Stress spectrum block counter, $i = 1, 2, ... p$, ordered from the largest amplitude	-
K_{BK}	Variable amplitude factor	-
$K_{E,\sigma}$	Residual stress factor for normal stress	-
$K_{E,\tau}$	Residual stress factor for shear stress	-
$K_{t,\perp}$	Notch factor	-
k	S-N curve slope	-
M_σ	Mean stress sensitivity for normal stress	-
M_τ	Mean stress sensitivity for shear stress	-
m	Mass	kg
N	Number of cycles to failure	-
N_D	Number of cycles at the knee point of the S-N curve	-
N_i	Number of cycles to failure for the i-th spectrum block	-

Symbol	Description	Unit
n_i	Expected number of cycles for the i-th spectrum block	-
N_f	Number of cycles for a specific fatigue strength	-
P_s	Probability of survival	%
p	Total number of blocks in the stress spectrum	-
R	Stress ratio	-
r_{ref}	Notch reference radius	mm
S	Nominal normal stress	mm
$S_{a,\parallel,i}$	Nominal normal perpendicular stress amplitude, i-th stress spectrum block	MPa
$S_{a,\perp,i}$	Nominal normal perpendicular stress amplitude, i-th stress spectrum block	MPa
$S_{m,\parallel,i}$	Nominal normal perpendicular mean stress, i-th stress spectrum block	MPa
$S_{m,\perp,i}$	Nominal normal perpendicular mean stress, i-th stress spectrum block	MPa
T	Nominal shear stress	MPa
$T_{a,i}$	Nominal shear stress amplitude, i-th stress spectrum block	MPa
$T_{m,i}$	Nominal shear mean stress, i-th stress spectrum block	MPa
t	Thickness	mm
x_1	Local coordinate	mm
y_{eff}	Effective stress extraction distance	mm

Greek symbols

Symbol	Description	Unit
$\Delta\sigma$	Stress range	MPa
$\Delta\sigma_\parallel$	Parallel (normal) stress range	MPa
$\Delta\sigma_\perp$	Perpendicular (normal) stress range	MPa
$\Delta\tau$	Shear stress range	MPa
μ	Poisson's ratio	-
σ	Normal stress	MPa
$\sigma_{0.5t}$	Stress in distance 0.5 times thickness from the weld	MPa
$\sigma_{1.5t}$	Stress in distance 1.5 times thickness the weld	MPa
$\sigma_\parallel$	Parallel (local normal) stress	MPa
$\sigma_\perp$	Perpendicular (local normal) stress	MPa
$\sigma_{\perp,max,1}$	Maximum perpendicular stress from the 1st stress spectrum block	MPa
σ_a	Stress amplitude	MPa
$\sigma_{a,\parallel}$	Parallel (normal) stress amplitude	MPa
$\sigma_{a,\parallel,i}$	Local normal parallel stress amplitude, i-th stress spectrum block	MPa
$\sigma_{a,\perp}$	Perpendicular (normal) stress amplitude	MPa
$\sigma_{a,\perp,i}$	Local normal parallel stress amplitude, i-th stress spectrum block	MPa
$\sigma_{a,1}$	Stress amplitude from the 1st stress spectrum block	MPa
σ_e	Endurance limit (also called fatigue limit)	MPa
σ_{hs}	Hot-spot stress	MPa
σ_K	Notch stress	MPa
$\sigma_{K,eff}$	Effective stress	MPa
σ_m	Mean stress	MPa
$\sigma_{m,\parallel}$	Parallel (normal) mean stress	MPa
$\sigma_{m,\parallel,i}$	Local normal parallel mean stress, i-th stress spectrum block	MPa
$\sigma_{m,\perp}$	Perpendicular (normal) mean stress	MPa
$\sigma_{m,\perp,i}$	Local normal parallel mean stress, i-th stress spectrum block	MPa
$\sigma_{m,1}$	Mean stress from the 1st stress spectrum block	MPa
σ_{max}	Maximum stress	MPa
σ_{min}	Minimum stress	MPa
σ_{nom}	Local nominal stress	MPa
σ_y	Yield stress	MPa
τ	Shear stress	MPa
τ_a	Shear stress amplitude	MPa
$\tau_{a,i}$	Local shear stress amplitude, i-th spectrum block	MPa
τ_m	Shear mean stress	MPa
$\tau_{m,i}$	Local shear mean stress, i-th spectrum block	MPa

LIST OF FIGURES

3.1 Examples of weld cracks originating from a) the weld toe [5] and b) the weld root [6] of a fillet weld . . . 14
3.2 Sinusoidal stress cycle with denoted parameters [7] . . . 15
3.3 Example of complex stress history as successive maxima and minima [8] . . . 16
3.4 Examples of visual representations of the stress history as a) histogram of stress parameters based on the rainflow counting algorithm [7] and b) stress range spectrum [9] . . . 16
3.5 Examples of S-N curves with (curve A) and without (curve B) endurance limit [12] . . . 18
3.6 S-N curve based on experimental data points with probability of survival P_s of 50 and 97.7 % [13] . . . 19
3.7 FAT class definition marked in the S-N graph [8] . . . 19
3.8 Example of FAT class from the table of structural details from [8] . . . 20
3.9 FAT classes S-N curves for steel loaded in normal stress, standard applications [8] . . . 20
3.10 Influence of tensile residual stress on the actual mean stress in the weld toe [20] 22
3.11 Bonus factor $f(R)$ applicable for modification of FAT in certain cases [8] . . . 22
3.12 Constant-amplitude S-N curve with graphical representation of the different damage hypotheses [14] . . . 24
3.13 Typical examples of butt weld and fillet weld with basic terminology [16] . . . 24
3.14 Examples of butt welds with partial penetration [18] . . . 25
3.15 Terms used to describe weld geometry on a fillet and butt weld [19] . . . 26
3.16 Crack initiation locations on cruciform fillet weld joint [5] . . . 27
3.17 The main types of improvement of welded joints and their effect [20] . . . 27
3.18 Post-weld treatment techniques overview [20] . . . 28
4.1 Vehicle body coordinate system according to [1] . . . 30
4.2 Schematic of a suspension system showing the general arrangement with bogie frame [21] . . . 32
4.3 Coordinate system of the bogie according to [2] . . . 33
4.4 Procedure of fatigue strength assessment using a) maximal stress amplitude b) equivalent stress amplitude, redrawn based on [3] . . . 35
5.1 Comparison of local nominal (green), structural (red) and notch (blue) stress approaches [10] . . . 39
5.2 Examples of macro-geometric effects on local nominal stress σ_{nom}, stress concentrations at a) cut-outs, b) curved beams, c) wide plates [8] . . . 39
5.3 Local nominal stress σ_{nom} distribution in a beam-like body [8] . . . 40
5.4 Stress linearization with two reference points leading up to the hot-spot [8] . 42
5.5 Examples of relative coarse meshing, including stress evaluation points and extrapolation paths: a) welded component showing potential hot-spots of types "a" and "b"; b) solid element model with extrapolation points in the center points of the elements; c) shell element model with extrapolation points for the weld ends located at the mid-side nodes and for the transverse welds at the center points of the elements [24] . . . 42
5.6 Prescribed mesh sizes and extraction points a) and b) as options for type "a" hot-spot and c) and d) for type "b" hot-spot [8] . . . 43
5.7 Fictitious rounding of notches using the reference radius r_{ref} = 1 mm on weld geometry [8] . . . 44

5.8 Recommended reference radii size depending on plate thickness, originally from [25] . . . 44
5.9 Stress concentration factor stresses for mild notch, originally from [26] 45
5.10 Effective normal stress $\sigma_{K,eff}$ in the distance y_{eff} for weld root (left) and toe (right) [3] . . . 46
6.1 Example configuration with marked main dimensions in millimeters 47
6.2 Nominal FAT classes relevant for the direction of loading, values originally from [8] . . . 48
6.3 Transformed centroidal stresses perpendicular to welds, yellow arrow marking orientation x-axis of the material coordinate system, results in MPa 50
6.4 Transformed stresses perpendicular to welds, no averaging between elements applied, results in MPa . . . 51
6.5 Stress in direction perpendicular to the weld with marked value in distance of 1.5 times thickness of the plate . . . 52
6.6 Structural FAT classes relevant for the direction of loading, values originally from [8] . . . 53
6.7 Perpendicular stress as function of distance from the weld on the shell element model, the stress extraction distances for hot-spot stress calculation marked . 53
6.8 FE model of a quarter of the example component with stresses in direction of the loading force, results in MPa . . . 54
6.9 Perpendicular stress as a function of distance from the weld on the solid element model, the stress extraction distances for hot-spot stress calculation marked 55
6.10 Stress results with respect to the global x-axis of the quarter model, results in MPa . . . 56
6.11 Plane strain submodel using sufficiently dense mesh with results displaying the notch stress as maximum in the toe area, results in MPa 57
6.12 Detail of the notch stress in the root area, results in MPa 57
6.13 First principal stress result in the plane strain submodel with the highlighted nodes used for results extraction as prescribed for the effective stress method . 58
6.14 Perpendicular stress as function of distance from the peak notch stress to the depth, with marked stress extraction distance 58
6.15 Interface of LIMIT® with identified welds marked in red based on different property IDs in FE model containing numerous welds 63
6.16 Assessment points on the double-sided fillet T weld in LIMIT® [32] 64
6.17 Stress extraction points in prescribed distance on an element marked in green as applied in LIMIT®, nodes marked in red, coordinate system aligned to the weld is displayed in the points [32] 64
6.18 Load Manager used for operations with FE results in LIMIT® 65
6.19 Job setup of a fatigue analysis on defined "Setups" and "Loads" in LIMIT® . . . 65
6.20 Detail of a contour result of elemental DoU displayed on elements belonging to the welds (element edges not displayed for clarity) in LIMIT® 66
6.21 User interface of SDC Verifier directly within the interface of FEMAP during weld analysis . . . 67
6.22 "Weld Finder" settings in SDC Verifier 67
6.23 "Standard details" to be filled in by the user in SDC Verifier 68
6.24 Overall utilization factor on weld elements produced by SDC Verifier in FEMAP 69
6.25 Scheme of interaction between the VB code and FEMAP as database via the API 71
6.26 Display of the API programming environment in a running FEMAP session . . 72

6.27 Custom Tools menu based directly on the corresponding folder where FEMAP was installed . . . 73
6.28 Outlined work procedure scheme with the implemented FEMAP API programs highlighted in green . . . 74
6.29 Example of curved geometry where the black highlighted offset curves allow creation of elements with consistent elements size (centroids approximately represented by arrows of material coordinate system) . . . 76
6.30 User dialog menu for selecting the method of creating FAT groups of elements 77
6.31 User dialog menu for entering FAT values and residual stress for a group of elements . . . 78
6.32 Simple example of plate type of elements that are assigned the material coordinate system based on shared edge with the rod element . . . 79
6.33 Proportion of the FAT value based on the number of cycles to failure as defined in [3] for a) normal and b) shear stress depending on plate thickness . . . 80
6.34 Fatigue analysis program functional scheme running in parallel on each element, only evaluation for top shown for clarity . . . 81
6.35 Comparison of results of the equation for combined cyclic DoU for cases of the same signs and different signs (plotted for $a_{BK,\tau} = 0.5$) . . . 84
6.36 List of Output Vectors with their IDs produced by the API program as displayable results . . . 84
7.1 The welded bracket and other significant parts of the assembly considered in analysis, main approximate dimensions marked in millimeters . . . 87
7.2 The three welded plates separated by color and proposed welds . . . 88
7.3 Surface splits in locations of welds that enable the creation of quadrilateral elements . . . 89
7.4 FE model of the bracket with details on special non-shell elements . . . 90
7.5 Imposed boundary condition of fixing all DOFs on the center line of the frame flanges . . . 91
7.6 Creation of a single weld element group using the automated method with prepared rod element property as weld type identifier . . . 92
7.7 Input selection in the respective dialog windows of the API program . . . 93
7.8 Dialog window with entered number of cycles for analysis . . . 93
7.9 Overall view of the analyzed component with results of combined approximate DoU on the weld elements, results dimensionless . . . 94
7.10 Scheme of extraction of the relevant stress data for detailed analysis . . . 95
7.11 Results of DoU from the MS Excel worksheet . . . 95
8.1 Ranked comparison of the combined DoU for 10 randomly selected elements for a) top side and b) bottom side of elements . . . 97
8.2 Comparison of the results of combined DoU from SDC Verifier using FKM 6th edition check and the developed API program, results dimensionless . . . 98
8.3 Comparison of the results of combined DoU from SDC Verifier custom standard check and the developed API program, results dimensionless . . . 98
8.4 Maximum perpendicular stress range from the API program in the critical location area as criteria plot, results in MPa . . . 99
8.5 Perpendicular paths used leading up to the weld line used for stress extraction, local coordinate x_1 marked for clarity . . . 99
8.6 Comparison of the results of a) maximum perpendicular stress range, b) perpendicular DoU as a function of local coordinate x_1 obtained using local nominal stress approach and hot-spot stress approach in the critical location area . 100

LIST OF TABLES

4.1 Fatigue loading accelerations in x, y and z directions as multiples of gravitational acceleration, exceptions marked by * [1] 31
4.2 Fatigue loading accelerations in three perpendicular directions as multiples of gravitational acceleration for fatigue assessment [2] 33
6.1 Parameters of the load spectrum 48
6.2 Comparison of results using different stress assessment methods 59
6.3 Overview of results pushed into Data Table 86
7.1 FAT parameters derived for the weld geometries; values and detail numbers originally from [8] 88
7.2 Material parameters used for FE linear elastic models of materials [3; 41; 42; 43] 89
7.3 Accelerations in fatigue load cases based on table 4.1 for P-II type of passenger rolling stock 91
8.1 Comparison of the key parameters and results in terms of perpendicular DoU for the highest identified perpendicular stress range 100

LIST OF EXTERNAL APPENDICES

thesis_appendices.zip

- **Appendix A:** Preview of Excel worksheets from the demonstration example analysis
  - demo_example_excel_previews.pdf
- **Appendix B:** Folder with developed FEMAP API programs files
  - Weld Fatigue
    - Create FAT Groups.BAS
    - Fatigue Analysis.BAS
    - Stress Parameters Extraction.BAS
- **Appendix C:** Preview of Excel worksheets from the welded bracket analysis
  - bracket_analysis_excel_previews.pdf